UCLA
UCLA Electronic Theses and Dissertations

Title

Causes and consequences of competition in spatially variable environments for plant coexistence and distributions: a study with California annual plants

Permalink

https://escholarship.org/uc/item/8zf0b26n

Author

Hayashi, Kenji Thomas

Publication Date

2025

Peer reviewed|Thesis/dissertation

eScholarship.org Powered by the California Digital Library
University of California

UNIVERSITY OF CALIFORNIA

Los Angeles

Causes and consequences of competition in spatially variable environments for plant coexistence and distributions: a study with California annual plants

A dissertation submitted in partial satisfaction of the
requirements for the degree Doctor of Philosophy
in Biology

by

Kenji Thomas Hayashi

2025

© Copyright by

Kenji Thomas Hayashi

2025

ABSTRACT OF THE DISSERTATION

Causes and consequences of competition in spatially variable environments for plant coexistence and distributions: a study with California annual plants

by

Kenji Thomas Hayashi
Doctor of Philosophy in Biology
University of California, Los Angeles, 2025
Professor Nathan Kraft, Chair

Spatial variation in the environment and associated changes in species composition are ubiquitous features of ecological communities. Ecologists have long sought to understand how such joint variation in the abiotic and biotic environment shapes species populations and communities. This endeavor has taken on renewed importance as environmental change increasingly threatens to disrupt species interactions. However, characterizing the causes and consequences of species interactions across disparate environments remains a major empirical challenge. Here, I leverage an experimentally tractable California annual grassland system to study how spatial variation in the environment and competition shapes plant coexistence and distributions.

In Chapter 1, I ask how spatially variable competition drives mismatches between plant fitness and occurrence along environmental gradients. By experimentally quantifying the demography of eight annual plant species along edaphic gradients in a serpentine grassland, either with or without competitors, I demonstrate that competitors can modify species' demographic responses to environmental gradients. Crucially, observed occurrence patterns were often poorly related to these demographic responses. These findings caution against assuming that variation in occurrence implies variation in fitness, or vice versa.

In Chapter 2, I turn my attention to how spatial heterogeneity promotes species coexistence via the spatial storage effect. I studied 24 annual plant species in the grassland from Chapter 1 and found that they exhibit variable responses to spatial variation in the environment and competition that depend on their functional traits. Additionally, these trait-based demographic responses contributed to elevated competition at otherwise favorable sites. These results are consistent with the storage effect and demonstrate how functional traits can modulate coexistence in spatially variable environments.

In Chapter 3, I conducted a greenhouse experiment to characterize competition between an annual grass and forb under watering treatments emulating range-wide rainfall variation. I found that although per capita competition was strongest in arid conditions, community-wide competition was stronger in moister environments where fitness asymmetries were large. These contrasting results emphasize the importance of distinguishing between competition at the individual and community level. Together, this dissertation combines experiments with modern coexistence theory to offer an integrative account of plant coexistence and distributions in a spatially variable world.

The dissertation of Kenji Thomas Hayashi is approved.

Amy Angert

Colin Kremer

Elsa Ordway

Morgan Winn Tingley

Nathan Kraft, Committee Chair

University of California, Los Angeles

2025

Table of contents

List of figures

List of tables

Acknowledgments

Ever since discovering my passion for ecology as an undergraduate student, much of my life has been defined by the pursuit of a Ph.D. in ecology and an aspiration to contribute to a deeper understanding of the natural world. However, that is not to say that this journey has been an easy one. In fact, this dissertation would not have been possible without endless support from my family, friends, mentors, and colleagues. I will forever cherish the relationships and interactions that helped me persevere throughout the six years I spent at UCLA. I would like to use this space to express my gratitude toward the many people who helped me grow into the scientist and person that I am today.

I would like to start by thanking Nathan Kraft for being a tremendously inspiring and supportive advisor. It is no exaggeration to say that Nathan's work is a large part of what inspired me to pursue a Ph.D. in ecology in the first place. But more importantly, Nathan has taught me so much about what it means to be an ecologist, including how to develop, answer, and communicate exciting research questions. I am grateful for his patience and generous support that helped me translate my broad research interests into tractable projects. He also allowed me the freedom to take several brief (or sometimes extended) forays into various areas of ecology, statistics, computing, and teaching that collectively enriched my time as a Ph.D. student and helped shape my identity as a scientist. I am grateful for how Nathan always respected my somewhat slow and cautious approach to scientific inquiry, encouraged me when I was doubting myself, and pushed me forward when I was feeling stuck. I am incredibly fortunate to have Nathan as a mentor, and I look forward to continued collaborations in years to come.

I would also like to thank my doctoral committee members, Amy Angert, Colin Kremer, Elsa Ordway, and Morgan Tingley, for insightful discussions and feedback that greatly improved my dissertation research. Amy's pioneering work on plant coexistence and distributions is foundational for several of my dissertation chapters, and I am very grateful to her for generously agreeing to join my committee when I contacted her out of the blue. I am thankful to Colin for being someone that I could always count on to root for me, both at UCLA and beyond. I've had the pleasure of interacting with Colin in both research and classroom settings, and I learned a lot from him about functional traits and acclimation. I want to thank Elsa Ordway for always making time to chat about my research interests and for helping me ground my dissertation research in the broader context of California ecosystems. I am grateful to Morgan Tingley for critically engaging with my manuscripts, providing invaluable feedback on statistical analyses, and offering encouragement as I looked toward next steps in my career. I also want to thank my guidance committee members, Priyanga Amarasekare and Lawren Sack, for helping me find my footing as I started to pursue research at UCLA. I am especially grateful to Priyanga for inviting me to her lab meetings and inspiring me to do my best possible research. Thank you all for your support over the years, be it in person or on Zoom.

This dissertation also benefited greatly from the help of many others. I want to thank Sedgwick Reserve staff, especially Kate McCurdy and Lyza Johnsen, for assistance during my many visits to the reserve for fieldwork for Chapter 1. I am grateful to Gaurav Kandlikar, Andy Kleinhesselink, Oscar Godoy, and Jonathan Levine for their contributions that made Chapter 2 possible. I thank Weimin Deng and staff at the UCLA Plant Growth Center for help during the countless hours that I spent watering and measuring plants in the greenhouse for Chapter 3. Throughout all this work, I greatly enjoyed working with many undergraduate students, including Tim Foster, Soline Grimbert, Jinsuh Jung-Aum, Fidel Negrete, and Julie Yang.

My friends and colleagues in the Department of Ecology and Evolutionary Biology, especially in the Kraft Lab, made my time at UCLA truly special. Gaurav Kandlikar, Marcel Caritá Vaz, Mary Van Dyke, Andy Kleinhesselink, and Ian McFadden warmly welcomed me into the lab and immediately made me feel at home. Gaurav and Marcel were amazing role models that I continue to look up to; they showed me how curiosity, deep thinking, and collegiality can enable great science. Mary showed me how to do exciting research at Sedgwick and was a dependable companion in the lab over many years. In later years, Lauren Glevanik, Jordan Yanowitz, Samantha Catella, Hannah Carroll, Haylee Oyler, Alex Cisneros Carey, Maya Sagarin, Kami Schneider, and Zhenfei Li made the lab a fun and vibrant place. I also want to thank my cohort mates for being there with me through the highs and lows of graduate school. I am grateful to have shared many laughs and struggles with Marissa Ochoa and Aidan Howenstine. I am also grateful to Maddi Cowen and Rosa McGuire for being great friends that constantly inspired me to become a better scientist and person. Working through *Statistical Rethinking* with Maddi and Rosa was a highlight of my learning in graduate school and ended up becoming an important foundation for several analyses in my dissertation. I thank many others who shared time and space with me at UCLA, including Nick Russo, Ashlyn Ford, Erick Zerecero, Gabby Najm, Oshiomah Oyageshio, Chris Kyriazis, Marvin Browne, Ioana Anghel, Berenice Badillo, Alayna Mead, Kaija Gahm, Rachel Turba, Rachel Potter, Evan Doughty, Christian Henry, Leila Fletcher, Camila Medeiros, Alec Baird, Carissa DeRanek, Nidhi Vinod, Anna Ongjoco, and Hannah Stouter.

Another pillar of my time at UCLA came in the form of teaching. I am especially glad to have taught several quarters of Plant Ecology with Nathan. Serving as a teaching assistant for this class helped me grow as a teacher and reinforced my knowledge as a plant ecologist. I also learned a great deal from teaching with Lawren Sack, Felipe Zapata, Jonathan Marcot, Anthony Baniaga, Leryn Gorlitsky, and Emily Curd. I want to thank K. Supriya, Katie Dixie, and the CIRTL@UCLA community for creating a welcoming and productive space for me (and many others) to pursue evidence-based teaching practices. Relatedly, I am very proud to have worked on developing EcoEvoApps with so many amazing friends and colleagues: Gaurav Kandlikar, Rosa McGuire, Xinyi Yan, Marcel Caritá Vaz, Damla Cinoğlu, Maddi Cowen, Alejandra Martínez-Blancas, Lauren Sullivan, and Sheila Vazquez-Morales.

Of course, my journey in ecology began well before I started at UCLA. I had many extraordinary professors and mentors at Brown University and beyond, but I want to start by thanking Jon Witman for introducing me to the study of ecology and to the possibility of a career as an ecologist—something I had never even considered until I took his Principles of Ecology class. I would also like to thank Dov Sax, Brian Enquist, John Wiens, and Stephen Matter for taking me into their labs as I explored my research interests in ecology and evolutionary biology. I am immensely grateful to Dov for creating a lab where I found some incredible friends and role models. I especially want to thank Emily Hollenbeck and Donny Perret for their contagious positivity and passion for ecology that made me feel like I too could pursue a Ph.D. in this field. I also want to thank Liz Miller and Lorah Patterson for their mentorship as they led me through various stages of their research projects. I am grateful to Sohini Ramachandran for introducing me to the R programming language, which quickly became an indispensable tool and a source of much enjoyment in my everyday work. I would not be where I am today had it not been for these (and many other) formative experiences.

Finally, words cannot express how grateful I am to my family for their love and support over the years. I want to thank my mother (Donna) and father (Takahiko) for giving me the upbringing and courage that made it possible for me to pursue my dreams. I also want to thank my brother (Michio) for venturing into adulthood with me and visiting me in LA. Many thanks to my grandparents, aunts, uncles, and cousins who cheered me on through life and graduate school. Last but not least, I am so grateful to my partner, Elizabeth Purington, for uplifting me and sharing this journey with me, including helping me out in the field and greenhouse. This dissertation was a team effort. Much of my time in graduate school was quite literally plagued by the COVID-19 pandemic, which made it difficult to see those that are dearest to me. But it was especially in times like this that I felt so lucky to have you all in my life. Thank you for being there for me until now and in the future.

Chapter 1 has been submitted for publication as Hayashi, K. T., and N. J. B. Kraft. Spatially variable competition contributes to mismatched responses of plant fitness and occurrence to environmental gradients. KTH and NJBK conceptualized the study and developed the methodology. KTH led investigation, data curation, and formal analysis with input from NJBK. KTH led writing of the original draft of the manuscript with substantial input from NJBK. KTH and NJBK contributed to review and editing of the manuscript.

Chapter 2 is in preparation for submission as Hayashi, K. T., G. S. Kandlikar, A. R. Kleinhesselink, O. Godoy, J. M. Levine, and N. J. B. Kraft. Functional traits mediate demographic responses of California annual plants to spatial variation in the environment and competition: implications for the spatial storage effect. NJBK, OG, and JML conceptualized and designed the experiments. NJBK, OG, and JML implemented the 2013 experiment. GSK, NJBK, and JML deployed the 2015 experiment. GSK, NJBK, and ARK collected data for the 2015 experiment. KTH, NJBK, JML, and GSK designed the research questions for this manuscript. KTH, GSK, and NJBK conducted data curation and analysis. KTH wrote the original draft of the manuscript with input from NJBK.

Chapter 3 is in preparation for submission as Hayashi, K. T., and N. J. B. Kraft. Water supply shapes fitness asymmetries and competitive coexistence of California annual plants. KTH and NJBK conceptualized the study and designed the experiment. KTH led data collection, validation, analysis, and visualization with input from NJBK. KTH wrote the original draft of the manuscript with input from NJBK. KTH and NJBK contributed to review and editing of the manuscript.

My dissertation research was performed in part at the University of California Natural Reserve System Sedgwick Reserve. This work was supported in part by a Mildred E. Mathias Graduate Student Research Grant from the University of California Natural Reserve System. The research in this dissertation was also supported by U.S. National Science Foundation grants DEB 1644641 and DEB 2022810. I thank UCLA Graduate Division and the Department of Ecology and Evolutionary Biology for several fellowships and grants that also supported this work.

Curriculum vitae

Kenji Thomas Hayashi

Education

B.S. in Biology, Brown University 2014–2018

Publications

2. McGuire, R. M.*, **K. T. Hayashi***, X. Yan*, M. Caritá Vaz, D. Cinoğlu, M. C. Cowen, A. Martínez-Blancas, L. L. Sullivan, S. Vazquez-Morales, and G. S. Kandlikar. 2022. EcoEvoApps: Interactive apps for theoretical models in ecology and evolutionary biology. Ecology and Evolution 12:e9556. * indicates equal contribution.
1. Miller, E. C., **K. T. Hayashi**, D. Song, and J. J. Wiens. 2018. Explaining the ocean's richest biodiversity hotspot and global patterns of fish diversity. Proceedings of the Royal Society B: Biological Sciences 285:20181314.

Presentations

7. **Hayashi, K. T.**, and N. J. B. Kraft. 2023. Competition along a water supply gradient: towards scaling competition to species distributions with California annual plants. Ecological Society of America, Portland, OR, USA.
6. **Hayashi, K. T.**, and N. J. B. Kraft. 2021. Spatially-variable competitive interactions shape the performance and distributions of annual plant species in a California grassland. Ecological Society of America (virtual).
5. **Hayashi, K. T.** 2021. Understanding the distributions of annual plant species in a California grassland. University of California, Santa Barbara, Sedgwick Reserve, Lunch & Learn Seminar (virtual).
4. **Hayashi, K. T.** 2020. Community assembly and species distributions in a California grassland: insights from population dynamics and functional traits. University of Texas at Austin, Department of Integrative Biology, EcoLunch Seminar (virtual).
3. **Hayashi, K. T.**, M. N. Van Dyke, G. S. Kandlikar, and N. J. B. Kraft. 2020. How does functional composition of the species pool impact plant performance locally? Ecological Society of America (virtual).

2. **Hayashi, K. T.** 2018. Functional traits, elevation, and the assembly of Rocky Mountain meadow communities. Brown University, Department of Ecology and Evolutionary Biology, Undergraduate Thesis Talks, Providence, RI, USA.
1. **Hayashi, K. T.** 2017. Assessing plant community assembly along an elevational gradient: a functional trait hypervolume approach. Rocky Mountain Biological Laboratory, Undergraduate Research Symposium, Gothic, CO, USA.

Grants & fellowships

Departmental Conference Grant, UCLA	2023
Halde Quarter Fellowship, UCLA	2022
Departmental Research Grant, UCLA	2019–2020, 2022
Vavra Fellowship, UCLA	2018–2022
Summer Mentored Research Fellowship, UCLA	2021
Mildred E. Mathias Graduate Student Research Grant, UC Natural Reserve System	2020
Palevsky Fellowship, UCLA	2018
Barclay Scholarship, Rocky Mountain Biological Laboratory	2017
BrownConnect LINK Award, Brown University	2016

Honors & awards

Member of winning group, ESIIL Environmental MosAIc Hackathon	2023
Departmental Graduate Teaching Award, UCLA	2023
Honorable Mention, NSF Graduate Research Fellowship	2020
Honors in the Biological Sciences, Brown University	2018

Teaching

Teaching Assistant (Plant Ecology; Plant Physiology; Natural History Collections in the Biological Sciences; Tropical Ecology; Plant Diversity and Evolution; Community Ecology; Genetics, Evolution, and Ecology), UCLA	2019–2025
Software Carpentry workshops (R for Reproducible Scientific Analysis; Version Control with Git; The Unix Shell), UCLA	2021–2022
Teaching Assistant (Evolutionary Biology; Conservation Biology; Intermediate Japanese), Brown University	2015–2017

Teaching certifications

- *Instructor*, The Carpentries 2022
- *Associate*, Center for the Integration of Research, Teaching, and Learning at UCLA 2021

Service

Research mentor to five undergraduate students at UCLA (2020–2023)
Committee member for departmental co-working space “Hacky Hours” at UCLA (2019–2023)
Peer reviewer for The American Naturalist, Functional Ecology, Plant Ecology

Chapter 1

Spatially variable competition contributes to mismatched responses of plant fitness and occurrence to environmental gradients

This chapter has been submitted for publication as Hayashi, K. T., and N. J. B. Kraft. Spatially variable competition contributes to mismatched responses of plant fitness and occurrence to environmental gradients. KTH and NJBK conceptualized the study and developed the methodology. KTH led investigation, data curation, and formal analysis with input from NJBK. KTH led writing of the original draft of the manuscript with substantial input from NJBK. KTH and NJBK contributed to review and editing of the manuscript.

1.1 Abstract

1. Species distributions have long been understood to depend on the complex interplay between the abiotic environment and biotic interactions. Empirical work in ecological communities has increasingly revealed how competition can mediate species' demographic responses to environmental variation, but understanding how the demographic consequences of spatially variable competition manifest in observed distribution patterns remains an important challenge.

2. Here, we describe a conceptual framework for characterizing competition-driven mismatches between responses of fitness and occurrence to environmental gradients. We then explore these mismatches for eight annual plant species in an edaphically variable California grassland landscape.

3. We experimentally quantified how species' demographic rates (germination rate, fecundity) and fitness respond to spatial variation in the soil environment, either in the presence or absence of naturally occurring neighbors. We also surveyed species' occurrence to characterize their distributions across the study landscape. Combining these demographic and occurrence data, we asked whether observed occurrence patterns are congruent with responses of intrinsic fitness (i.e., fitness in the absence of competitors) to soil gradients.

4. We found that competition altered responses of fitness to the primary soil gradient (soil texture) for many (4/8) species. In turn, occurrence patterns were often poorly or even inversely related to responses of intrinsic fitness to this environmental axis. In contrast, we found that competition had relatively little effect on responses of fitness and occurrence to a secondary

soil gradient (soil Ca:Mg).

5. *Synthesis*. We demonstrate that spatially variable competition can contribute to mismatched responses of fitness and occurrence to environmental variation. Importantly, these quantitative mismatches depend on the species and environmental gradient in question. Our results caution against assuming that variation in occurrence implies variation in intrinsic fitness (or vice versa) without first disentangling how the abiotic environment and competition impact the demographic processes that underlie species distributions.

Keywords: competition, demography, neighbor removal experiment, plant population and community dynamics, serpentine grassland, species distributions, spatial heterogeneity, stress gradient

1.2 Introduction

Understanding how the abiotic environment and biotic interactions jointly shape species distributions is a long-standing challenge in ecology and biogeography (Dobzhansky 1950, MacArthur 1972, Louthan et al. 2015). In particular, establishing the extent to which species' current distributions reflect their direct demographic responses to the environment, or rather are modified by complex biotic interactions, is a critical step in predicting species' future distributions (Davis et al. 1998, Pearson and Dawson 2003). Although there is widespread theoretical (e.g., Price and Kirkpatrick 2009, Svenning et al. 2014, Godsoe et al. 2017, Usinowicz and Levine 2018) and empirical (e.g., Wisz et al. 2013, Armitage and Jones 2020, Legault et al. 2020, Usinowicz and Levine 2021) evidence that biotic interactions such as competition can limit where species are found, quantifying the effects of competition on demography and distributions along real-world environmental gradients is often logistically challenging (but see e.g., Stanton-Geddes et al. 2012, Lyu and Alexander 2022, Craig et al. 2023). Thus, as environmental change drives shifts in the abundance and distributions of species both within and across ecological communities (e.g., Parmesan and Yohe 2003, Kelly and Goulden 2008, Chen et al. 2011, Bowler et al. 2017, Feeley et al. 2020, Rosenblad et al. 2023), competition remains a critical source of uncertainty in forecasting the future of biodiversity (Gilman et al. 2010, HilleRisLambers et al. 2013, Alexander et al. 2016).

The first principles of population dynamics dictate that species persist in environments where they have a positive population growth rate (fitness) when rare (Hutchinson 1978, Grainger et al. 2019b). Environmentally driven variation in fitness in the absence of biotic interactions (intrinsic fitness) is the foundation for species distributions (Holt 2009, Schurr et al. 2012, Ehrlén and Morris 2015), but other processes can create mismatches between intrinsic fitness and observed distributions (Pulliam 2000). For example, competition can prevent species from establishing or persisting in certain environments by reducing fitness in the presence of competitors (realized fitness) to below self-replacement levels (MacArthur and Levins 1967, Chesson 2000b). More subtly, competition can create discrepancies between how intrinsic and realized fitness vary in response to environmental gradients if the identity, density, or per capita effects of competitors depend on the environment (Louthan et al. 2015). Notably, recent experimental work has demonstrated not only that the outcomes of competition depend on environmental context (e.g., Germain et al. 2018, Wainwright et al. 2019, Van Dyke et al. 2022, Cervantes-Loreto et al. 2023), but also that competition can mediate species' responses to environmental change (e.g., Liancourt et al. 2013, Esch et al. 2018). These findings imply that species' current or future distributions may be incongruent with their intrinsic demographic responses to the environment (Figure 1.1), which limits our ability to predict species' responses to environmental change (e.g., Davis et al. 1998, Alexander et al. 2015). Progress on this topic requires a better understanding of how spatially variable competition shapes species distributions along real-world environmental gradients.

A common prediction is that species experience more intense competition in environments where they exhibit higher intrinsic fitness. This idea is foundational for the study of plant strategies (e.g., CSR model, Grime 1977) and species coexistence (Chesson 2000a) in spatially variable environments. Similarly, the stress-gradient hypothesis posits that competition increases in frequency or strength in more benign abiotic environments (Bertness and Callaway 1994, Maestre et al. 2009). Such co-variation between intrinsic fitness and competition can emerge if species share functional traits or evolutionary histories that promote similar responses to environmental variation (Mayfield and Levine 2010, Adler et al. 2013). While the importance of competition for species distributions has long been hypothesized to depend on environmental context (Dobzhansky 1950, MacArthur 1972, Louthan et al. 2015), the consequences of co-variation between intrinsic fitness and competition are rarely studied in the context of species distributions (but see e.g., Armitage and Jones 2020, Usinowicz and Levine 2021). Perhaps counterintuitively, species might be more likely to occur in more competitive environments if competition only weakly dampens demographic responses to the environment, such that occurrence approximately tracks intrinsic fitness (Figure 1.1b). However, with stronger competition in intrinsically favorable environments, competition can reverse demographic responses to the environment (Figure 1.1c). Even in the absence of intrinsic responses, variation in competition can drive realized demographic responses to the environment (Figure 1.1d). Importantly, these last two scenarios (Figure 1.1c, d) both create incongruence between trends in observed occurrence and intrinsic fitness along environmental

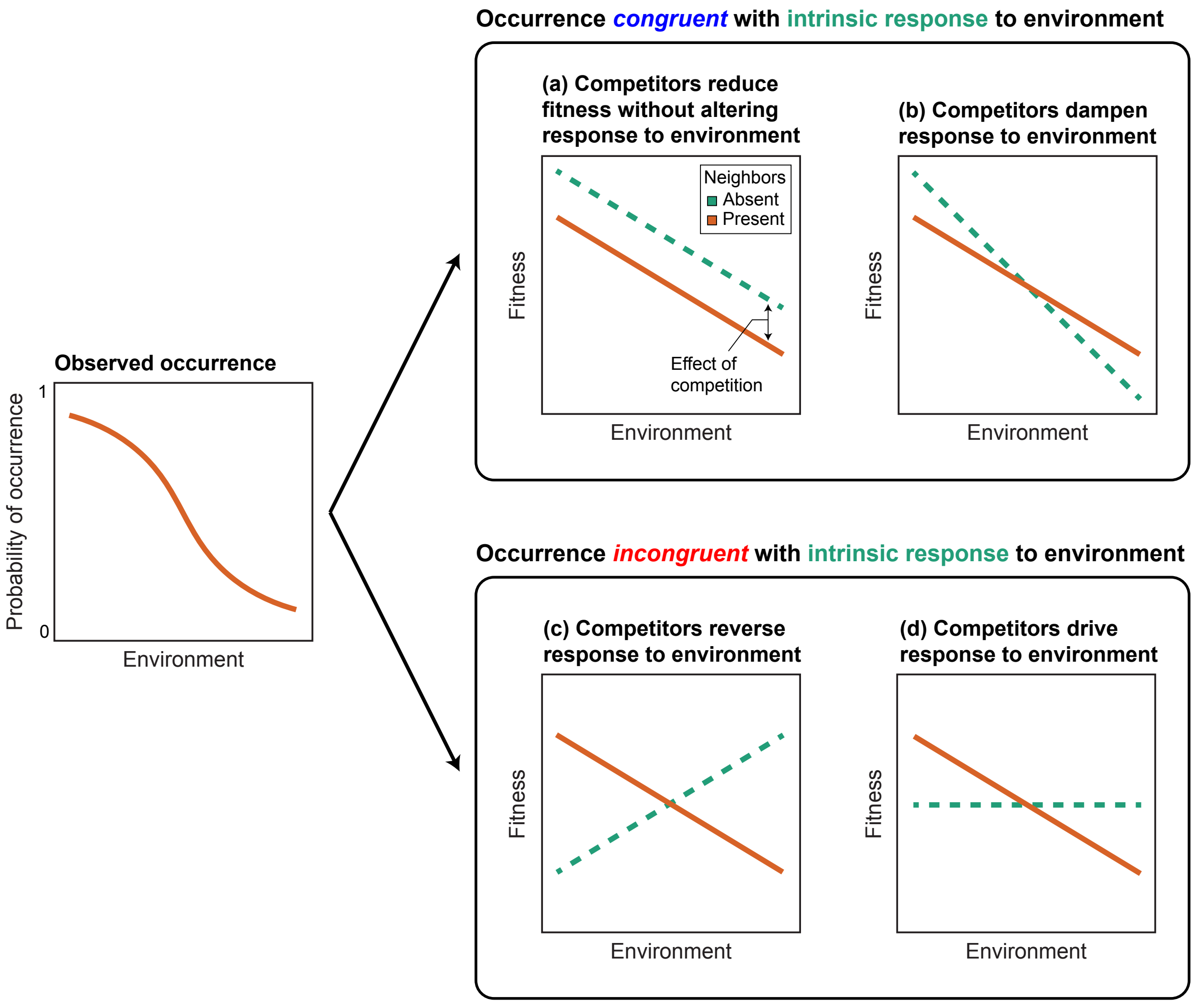

Figure 1.1: Conceptual framework for identifying competition-driven mismatches between responses of occurrence and fitness to environmental gradients. Observed occurrence patterns (leftmost panel) may be expected to reflect species' realized demographic responses to the environment (i.e., demographic responses in the presence of competitors; solid orange lines, identical in panels a–d). However, the extent to which observed occurrence patterns track species' intrinsic demographic responses to the environment (i.e., demographic responses in the absence of biotic interactions; dashed green lines) is often unclear. If competitors (a) uniformly reduce fitness or (b) merely dampen demographic responses, occurrence can be approximately congruent with species' intrinsic responses to the environment. However, if demographic responses are (c) reversed or (d) even driven by spatially variable competition, occurrence patterns will be incongruent with species' intrinsic responses to the environment. Note that positive effects of neighbors (i.e., facilitation) are allowed here for graphical simplicity, but are not necessary for these scenarios to play out within a given range of environmental conditions.

gradients. Beyond the well-established understanding that the absence of a species from an area does not necessarily reflect the suitability of the abiotic environment (Davis et al. 1998, Pearson and Dawson 2003), the complexities of these scenarios highlight the need to critically evaluate the practical assumption that species' distributions approximate their intrinsic demographic responses to environmental variation.

Here, we build up an understanding of how the abiotic environment and competition interact to shape the demography and distributions of species in an experimentally tractable natural landscape. Specifically, we conducted a spatially distributed demographic experiment to evaluate the consequences of spatially variable competition for plant demography and distributions in an edaphically heterogeneous California annual grassland. We experimentally quantified how the demography and fitness of eight annual plant species respond to variation in the abiotic environment, either in the presence or absence of naturally occurring competitors. We asked: (1) What are species' intrinsic demographic responses to the abiotic environment? (2) How does competition modify these intrinsic responses? Then, combining these demographic results with occurrence surveys, we asked: (3) Are observed occurrence patterns congruent with intrinsic or realized demographic responses to the environment? Our results reveal complex and variable relationships between fitness, competition, and occurrence depending on the species and environmental gradient under consideration. Critically, we find that occurrence patterns are often poorly related to—or even in opposition to—species' intrinsic demographic responses to environmental gradients, highlighting the complex role of spatially variable competition in shaping species distributions.

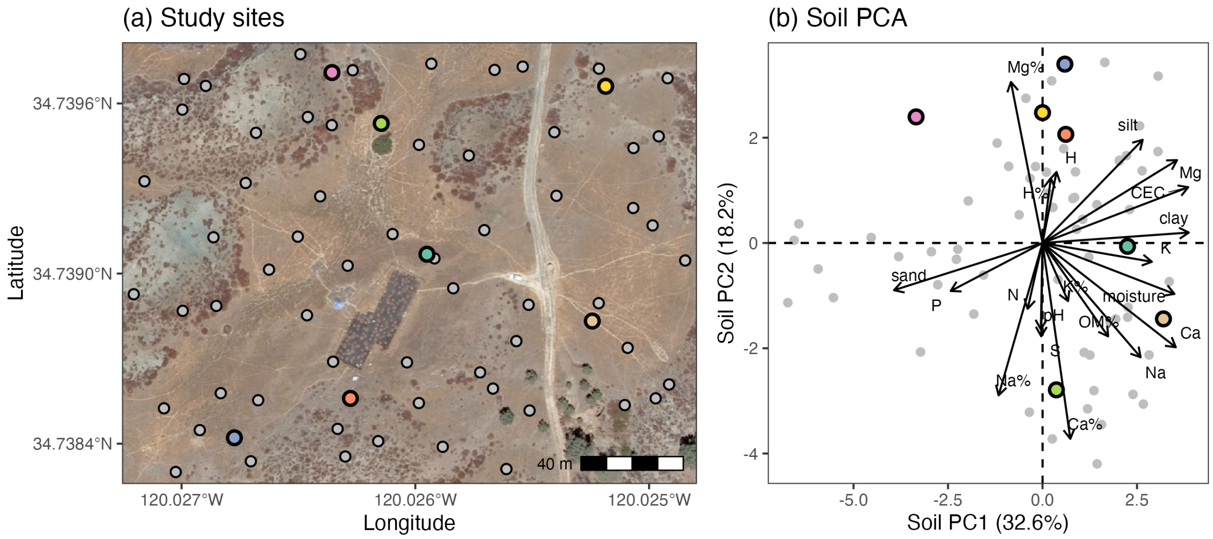

Figure 1.2: Locations and soil environments of study sites. Colored points represent experimental sites. Gray points represent survey sites. (a) Map of study sites. High resolution orthoimagery courtesy of the U.S. Geological Survey. (b) Principal component analysis (PCA) of soil variables at study sites. Arrows represent the loadings of individual soil variables with respect to PC1 and PC2. The percentage of variance explained by each axis is given in parentheses.

1.3 Materials and methods

1.3.1 Study system

We conducted our study at the University of California Natural Reserve System Sedgwick Reserve in Santa Barbara County, California, USA. This region experiences a Mediterranean climate with hot, dry summers and cool, wet winters. We focused on a ~4-ha area of the reserve characterized by serpentine-derived hummocks interspersed among a grassland matrix (Figure 1.2a, Figure A.1). The hummocks host many native annual forbs, whereas the matrix is dominated by invasive annual grasses (e.g., *Avena* spp., *Bromus* spp.) (Gram et al. 2004). The abiotic and biotic heterogeneity of this landscape, coupled with the dominance of experimentally tractable annual plants, makes this system well-suited for addressing our research questions.

1.3.2 Demographic experiment

To quantify the demographic responses of annual plant species to spatial variation in the environment and competition, we grew eight native annual plant species (Table 1.1) at seven sites distributed across the study area (Figure 1.2a). These experimental sites represent a subset of sites previously selected to capture environmental variation across this area (Kandlikar et al. 2022). Each site (~4 m × ~4 m) was comprised of twenty 0.5 m × 0.5 m plots, evenly divided among two neighborhood treatments in which the resident community was either removed or left intact prior to planting. Each plot contained eight 15 cm × 15 cm subplots, each of which was seeded at its center with a fixed number of seeds (24 to 40 depending on the species) of one of the eight focal species in November 2019. Seeds were collected and aggregated from across the study area in 2016–2018.

Table 1.1: Plant species used in this study.

Code	**Species**	**Family**
ACWR	*Acmispon wrangelianus*	Fabaceae
CHGL	*Chaenactis glabriuscula*	Asteraceae
FEMI	*Festuca microstachys*	Poaceae
HECO	*Hemizonia congesta*	Asteraceae
LACA	*Lasthenia californica*	Asteraceae
PLER	*Plantago erecta*	Plantaginaceae
SACO	*Salvia columbariae*	Lamiaceae
URLI	*Uropappus lindleyi*	Asteraceae

In January–February 2020, we recorded germination rate (g) in each subplot by counting the number of germinants found in the seeded locations, then thinned these germinants down to a single focal individual. We marked focal individuals with toothpicks and tracked them for the duration of the growing season (January–July). Due to below-average early-season rainfall in January–February (2020 = 0.67 in, mean = 8.62 in, County of Santa Barbara 2025b), we added ~0.6 in of water to all plots following germination, equivalent to a typical storm at this time of year. In April–July 2020, as focal individuals started to show signs of senescence, we estimated the lifetime fecundity (F) of each individual. See Appendix S2 for detailed methods for estimating fecundity. In total, we recorded germination rate in 1,078 subplots and estimated fecundity for 708 focal individuals. We maintained the neighborhood removal treatment by weeding out any background germinants throughout the experiment.

1.3.3 Occurrence surveys

To characterize our focal species' distributions across the study landscape, we revisited all experimental sites (colored points in Figure 1.2) in April–May 2021 and surveyed the occurrence of each focal species in each of 68 uncleared experimental plot. We also surveyed occurrence at 61 additional sites distributed across the study area (gray points in Figure 1.2). We selected these survey sites by overlaying on the study area a 7 × 9 grid of 25 m × 25 m cells and randomly generating a point within each grid cell using QGIS (QGIS Development Team 2020). Each survey site was comprised of a single 0.5 m × 0.5 m plot, equivalent to one experimental plot.

1.3.4 Soil sampling

To characterize the soil environment at our study sites, we collected soil samples at all sites (seven experimental sites + 61 survey sites) alongside occurrence surveys. We collected soil from ~5–10 cm below the soil surface at three locations within each site (one near the center and two along the edges of the site). We aggregated soil samples for each site and submitted them to A&L Western Laboratories in Modesto, California, USA for chemical and physical analysis. We similarly collected soil samples following a rainfall event and estimated soil moisture as gravimetric water content. See Table A.1 for descriptions of all soil variables used in this study.

1.3.5 Statistical analyses

To describe the soil environment at our study sites, we performed a principal component analysis (PCA) of the 20 soil variables in Table A.1 (Figure 1.2b, Figure A.2, Figure A.3). All soil variables were centered and scaled to unit variance prior to performing the PCA. Based on results of parallel analysis (Horn 1965, Dinno 2024), we retained the first four axes (adjusted eigenvalues > 1) for all subsequent analyses. These axes correspond to 77% of cumulative variance explained (PC1 = 32.6%, PC2 = 18.2%, PC3 = 16.9%, PC4 = 9.3%).

We used Bayesian hierarchical models to estimate the demographic responses of our focal species to the soil environment in the presence or absence of naturally occurring neighbors. For germination rate, we modeled the number of germinants as following a beta-binomial distribution with an expected probability of germination, μ, and precision, ϕ. We specified a linear model for μ with a logit link function as:

$$\text{logit}\left(\mu\right) = \alpha_{\text{sp,trt}} + \sum_{j=1}^{4} \beta_{j,\text{sp,trt}} \times \text{PC}_j + \gamma_{\text{sp,trt,site}} \tag{1.1}$$

where α is an intercept and β_j is a slope for soil principal component axis $j = 1, \dots, 4$ for each species ($\text{sp} = 1, \dots, 8$) and neighborhood treatment ($\text{trt} = 1$ is with neighbors present; $\text{trt} = 2$ is with neighbors absent). For clarity, we hereafter refer to the slope coefficients in the presence or absence of neighbors as β_{present} and β_{absent}, respectively. We also apply this convention to other quantities estimated in the presence or absence of neighbors. γ is a random intercept for each species and treatment at each site $= 1, \dots, 7$. γ was hierarchically modeled as:

$$\gamma_{\text{sp,trt,site}} \sim \text{Normal}\left(0, \sigma\right) \tag{1.2}$$

where σ is the standard deviation that describes variation in γ. Next, we modeled fecundity as following a zero-inflated negative binomial distribution, which combines (i) a negative binomial distribution with an expected fecundity, μ, and shape, ϕ, with (ii) an expected probability of zero-inflation, θ. We specified linear models for μ and θ in the same form as the right-hand side of Equation 1.1, using a log link function for μ and a logit link function for θ. For both models, we allowed ϕ to differ by species. See Appendix S3 for a full account of these models.

To estimate the response of fitness to the soil environment and competition, we implemented a joint model of the germination and fecundity models described above. We then used the joint posterior distribution for the germination and fecundity sub-models to compute fitness as the finite rate of increase (r) in the functional form of a model of seed banking annual plants (MacDonald and Watkinson 1981, Chesson 1990):

$$\frac{N_{t+1}}{N_t} = (1-g)s + gF \tag{1.3}$$

$$r = \ln\left(\frac{N_{t+1}}{N_t}\right) \tag{1.4}$$

where N_t is the number of seeds in year t and s is the annual rate of seed survival in the seed bank. We used species-specific estimates of s compiled from previous work in this study area (Levine and HilleRisLambers 2009, Godoy et al. 2014, 2017), assuming s to be constant across sites. We employed this joint modeling approach, rather than directly modeling fitness, because excess zeros in our fecundity data contributed to biomdalities in fitness estimates computed from our experimental data. We used this joint fitness model for all demographic analyses. In the context of our demographic experiment, we refer to fitness estimated in the presence or absence of neighbors as realized fitness (r_{present}) and intrinsic fitness (r_{absent}), respectively.

We used a Bayesian generalized linear model to quantify the occurrence patterns of our focal species along soil gradients. To align the scope of this analysis with our demographic experiment, we focused on occurrence data for sites within the range of soil PC1–PC4 captured by experimental sites, corresponding to 92 plots at 31 sites. We modeled occurrence as following a beta-binomial distribution with an expected probability of occurrence, μ, and precision, ϕ. We specified a linear model for μ following Equation 1.1, but excluding the random intercept term (γ) and without indexing other terms by neighborhood treatment (trt) as these components were not applicable here. We allowed ϕ to differ by species. See Appendix S4 for a full account of this model. Then, to evaluate the congruence between occurrence and fitness along soil gradients, we computed the posterior probability that the slopes (β_j) for occurrence and fitness in response to each of soil PC1–PC4 have the same sign. That is, for each posterior sample, we asked whether the slopes for occurrence and fitness (in the presence or absence of neighbors) along a given soil axis were both positive or both negative, then calculated the proportion of posterior samples that satisfied this criterion. Note that the expected response of fitness to soil PC1–PC4 was nonlinear, so we computed an axis-wide slope (β_j^*) by taking the difference in expected fitness at maximum ($\max(\text{PC}_j)$) and minimum values of the axis ($\min(\text{PC}_j)$) and dividing this difference by $\Delta\text{PC}_j = |\max(\text{PC}_j) - \min(\text{PC}_j)|$.

We implemented Bayesian statistical models using Stan (Stan Development Team 2024) via `cmdstanr` (Gabry et al. 2024). For all models, we used weakly informative priors (see Appendices S3 and S4) that were intended to keep parameters within plausible ranges given nonlinear link functions (Wesner and Pomeranz 2021) and prior work in our study system (Godoy et al. 2014, Kraft et al. 2015b, Kandlikar et al. 2022, Van Dyke et al. 2022). We confirmed model convergence by inspecting diagnostic quantities ($\widehat{R} < 1.01$, $N_{\text{eff}}/N > 0.1$) and trace plots. We report posterior support for statistical effects as the probability of direction (i.e., the probability of a positive or negative effect, $[0.5,\ 1]$) where applicable. We also report credible intervals as 95% highest-density continuous intervals (HDCIs) unless stated otherwise. See Appendices S3 and S4 for details of our statistical modeling approach. We conducted analyses using R version 4.4.1 (R Core Team 2024).

1.4 Results

1.4.1 Soil environment

Soil PC1 was characterized by a gradient in soil texture, with clay content loading positively and sand content loading negatively along the axis (Figure 1.2b). Cation exchange capacity (CEC), cation content, and soil moisture positively co-varied with clay content along soil PC1. As such, this axis also captures important differences in soil fertility. Soil PC2 was characterized by a gradient in cation composition, with Mg saturation loading positively and Ca saturation loading negatively along the axis (Figure 1.2b). All sites exhibited an excess of Mg relative to Ca (Ca:Mg < 1) characteristic of serpentine soils (Brady et al. 2005, Fernandez-Going et al. 2012). Taken together, our study sites capture continuous variation in the canonical physical and chemical properties of serpentine soils (Walker 1954, Gram et al. 2004). Therefore, we focus on results for soil PC1 and PC2 below. Soil PC3 and PC4 appeared to reflect variation in pH and organic matter content, respectively (Figure A.2).

1.4.2 Demographic responses to environment and competition

Our focal species tended to exhibit higher intrinsic demographic performance (i.e., demographic performance in the absence of neighbors) in more fine-textured soils with higher Mg saturation. In the absence of neighbors, germination rate increased with soil PC1 or PC2 for 3/8 species ($\Pr(\beta_{\text{absent}} > 0) \geq 0.975$; Figure A.8, Figure A.9, Table A.4). Responses of fecundity to soil PC1 and PC2 were less clear (two species with $\Pr(\text{direction}) \geq 0.95$; Figure A.10, Figure A.11, Table A.7). Combining these demographic rates, fitness increased with soil PC1 or PC2 for 5/8 species ($\Pr(\beta^*_{\text{absent}} > 0) \geq 0.975$; Figure 1.3, Figure A.12, Table A.10).

Neighbors had variable effects on fitness across environments. On average, neighbors decreased the fitness of all but one of our focal species ($\Pr(\Delta r < 0) \geq 0.975$, where $\Delta r = r_{\text{present}} - r_{\text{absent}}$; Figure A.7, Table A.3). Additionally, we found evidence that neighbors alter the response of fitness to soil PC1 (i.e., there is an interaction effect between neighborhood treat-

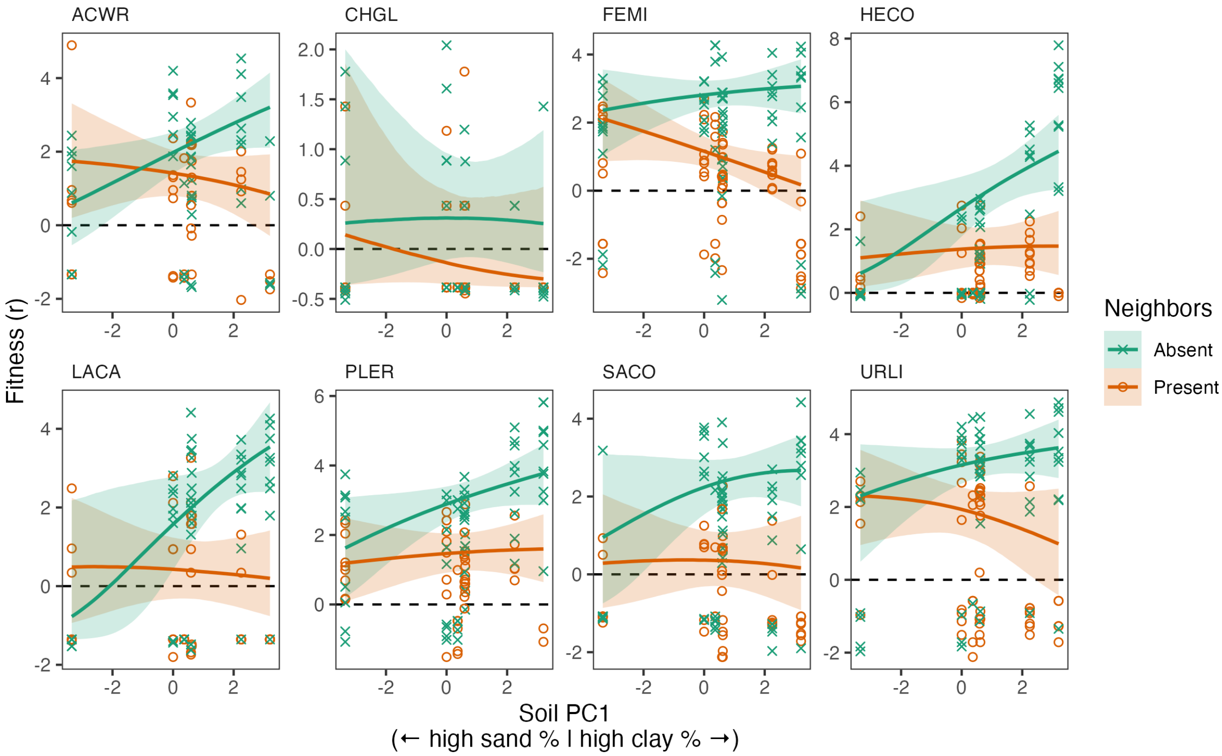

Figure 1.3: Response of fitness (r) to soil PC1 in the presence or absence of neighbors. Posterior expectations are shown for each species with soil PC2–PC4 held at average conditions across experimental sites. Solid lines represent medians. Shaded areas represent 95% quantile intervals.

ment and soil PC1, $\Delta\beta^* = \beta^*_{\text{present}} - \beta^*_{\text{absent}}$). Specifically, neighbors reduced the slope for fitness in response to soil PC1 for 4/8 species: ACWR and LACA ($\Pr(\Delta\beta^* < 0) \geq 0.975$), as well as FEMI and HECO with marginally less support ($\Pr(\Delta\beta^* < 0) > 0.972$; 95% HDCIs do not overlap 0) (Figure 1.3, Table A.12). For ACWR, HECO, and LACA, neighbors flattened the response of fitness to soil PC1, wherein positive intrinsic responses to this axis were largely negated by the presence of neighbors (Table A.10; Table A.11). Notably, for FEMI, neighbors appeared to largely drive the realized response of fitness to soil PC1 (Table A.10; Table A.11), consistent with Figure 1.1d. In contrast, we did not find clear evidence that neighbors alter the response of fitness to soil PC2 ($\Pr(\text{direction}) < 0.884$ for all species; Figure A.12, Table A.12). Overall, we found contrasting roles of competition in mediating demographic responses to the soil environment, with competition altering responses of fitness to a soil texture gradient (PC1) while having relatively minimal effect on responses of fitness to a soil nutrient (Ca:Mg) gradient (PC2). Results for germination rate and fecundity are shown in Appendix S3.

1.4.3 Congruence between occurrence and fitness

In accordance with our demographic results, the degree of congruence between trends in occurrence and fitness along soil gradients was highly variable depending on the species and soil axis under consideration. Occurrence was negatively associated with higher clay and cation content for 5/8 species ($\Pr(\beta < 0) \geq 0.975$ for soil PC1; Figure 1.4, Table A.15) and positively associated with lower Ca:Mg for one species ($\Pr(\beta > 0) \geq 0.975$ for soil PC2; Figure A.15, Table A.15). Strikingly, for all but two species, the responses of occurrence and intrinsic fitness to soil PC1 were more likely than not to be in opposite directions (Figure 1.5; mean probability of congruence = 0.27,

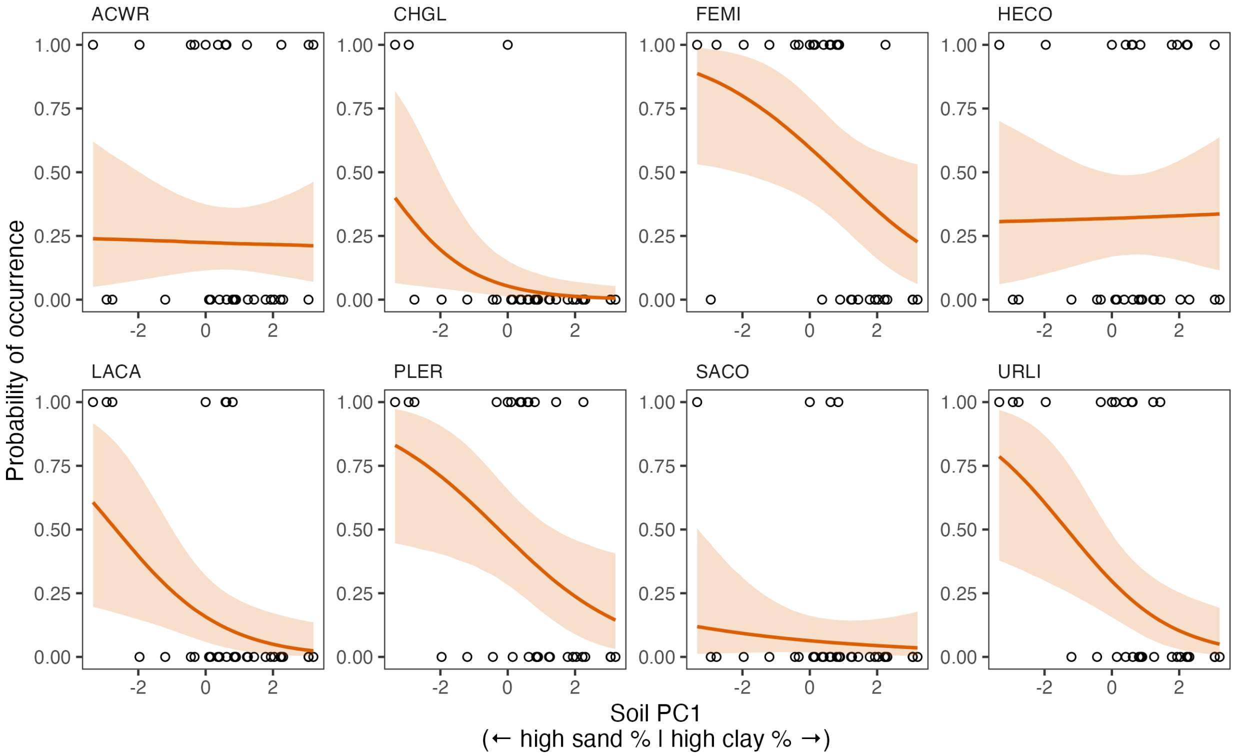

Figure 1.4: Observed patterns of occurrence along soil PC1. Posterior expectations are shown for each species with soil PC2–PC4 held at average conditions across sites. Solid lines represent medians. Shaded areas represent 95% quantile intervals.

SE = 0.074). For instance, LACA is expected to exhibit a positive intrinsic response to soil PC1 (Figure 1.3), yet its probability of occurrence is expected to decrease along this axis (Figure 1.4), resulting in a probability of congruence of 0.021. In contrast, the responses of occurrence and intrinsic fitness to soil PC2 tended more toward being congruent with one another (Figure A.16; mean probability of congruence = 0.60, SE = 0.094). Accounting for the effects of neighbors on fitness tended to improve congruence between occurrence and fitness, especially with respect to soil PC1 (Figure 1.5; mean probability of congruence = 0.64, SE = 0.075). These results provide empirical support for spatially variable competition as an important but complex driver of mismatches between occurrence and fitness along environmental gradients.

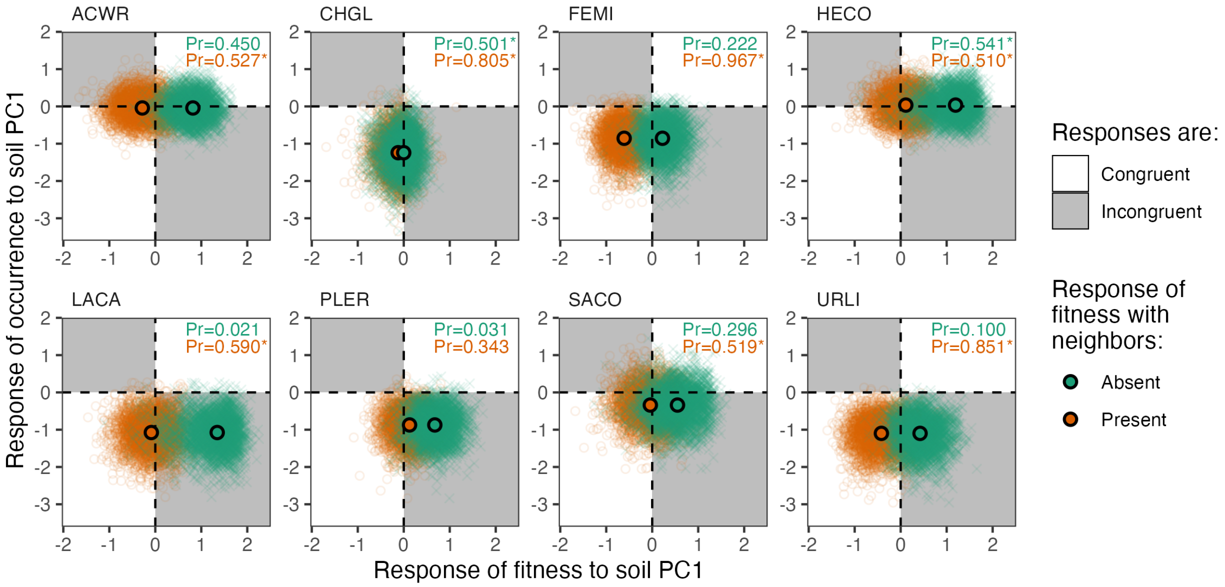

Figure 1.5: Congruence between responses of occurrence and fitness to soil PC1. For each species, the slope of occurrence in response to soil PC1 ($\beta_{j=1}$ for the occurrence model) is plotted against the axis-wide slope of fitness in response to soil PC1 ($\beta^*_{j=1}$ for the fitness model), the latter of which is computed in the presence (orange) or absence (green) of neighbors. Point clouds are posterior samples (thinned to 4,000 samples for visualization) and center points are medians. White regions denote congruent responses (i.e., slopes are both positive or both negative) and gray regions denote incongruent responses (i.e., one slope is positive while the other slope is negative). The total probability of congruence (i.e., the proportion of posterior samples that fall in the white regions) is shown in the top-right corner of each panel. Asterisks indicate that responses are more likely to be congruent that not (i.e., Pr(congruence) > 0.5); note that these are not results of statistical significance tests.

1.5 Discussion

Competitive interactions have long been understood to contribute to species distributions (Wisz et al. 2013), from the zoning of barnacles in the rocky intertidal (Connell 1961) to the migration of plant species in response to climate change (Alexander et al. 2015). While empirical work in ecological communities has increasingly revealed how competition can mediate species' demographic responses to environmental variation (e.g., Liancourt et al. 2013, Germain et al. 2018, Esch et al. 2018, Wainwright et al. 2019, Van Dyke et al. 2022, Cervantes-Loreto et al. 2023), understanding how the demographic consequences of competition manifest in observed distribution patterns remains challenging. Disentangling the contributions of intrinsic fitness (i.e., fitness in the absence of biotic interactions) and competition to species distributions in natural landscapes is an important step toward more accurately predicting species distributions (Davis et al. 1998), especially as environmental change threatens to modify biotic interactions in ecological communities (Gilman et al. 2010, HilleRisLambers et al. 2013, Alexander et al. 2016). Here, we combined a spatially distributed demographic experiment with occurrence surveys to evaluate the consequences of competition for plant species' demography and distributions in a California annual grassland. We found evidence that competition can alter the response of fitness to environmental gradients, effectively decoupling realized fitness (i.e., fitness in the presence of neighbors) from intrinsic fitness. Furthermore, we found that competition often contributes to incongruence between occurrence and fitness, such that observed occurrence patterns can be poorly or even inversely related to species' intrinsic responses to environmental variation. Notably, competition had contrasting effects on fitness and occurrence depending on the species and environmental gradient under consideration. Our findings illustrate the importance of accounting for spatially variable competition in the study of species distributions and caution against the practical but simplifying assumption that species' distributions track their intrinsic demographic responses to environmental variation.

Competition is most often described as limiting species distributions by excluding species from intrinsically suitable environments (e.g., Connell 1961, Bertness and Ellison 1987, Bullock et al. 2000). Accordingly, much research has focused on the role of competition in setting discrete distributional limits at the edges of species' ranges (e.g., Price and Kirkpatrick 2009, Stanton-Geddes et al. 2012, Ettinger and HilleRisLambers 2013, Louthan et al. 2015, Anderegg and HilleRisLambers 2019, Lyu and Alexander 2022). However, much of the ecological world is not well described by discrete transitions. Species often exhibit continuous variation in demographic performance in response to continuous variation in the abiotic and biotic environment. Therefore, understanding how competition drives quantitative variation in occurrence (or abundance) is critical to disentangling the processes shaping species' current and future distributions. In particular, an important way that competition can influence distribution patterns is by altering the response of fitness to the abiotic environment (Figure 1.1).

In our experiment, we found that competitors altered several (4/8) species' fitness responses to a soil texture gradient (PC1; Figure 1.3). In turn, we found that observed occurrence patterns often failed to track responses of intrinsic fitness to this axis (Figure 1.5). In fact, most (6/8) species were more likely than not to exhibit an increased probability of occurrence in less intrinsically favorable conditions along soil PC1. Such mismatched responses of occurrence and intrinsic fitness to soil PC1 were especially prominent for LACA and PLER ($\Pr(\text{congruence}) < 0.032$), both of which are forb species often associated with the transition zone between serpentine hummocks and grassland matrix (Gram et al. 2004). In contrast, competitors had relatively little effect on species' fitness responses to a soil nutrient (Ca:Mg) gradient (PC2; Figure A.12), and observed occurrence patterns were more likely to be congruent with intrinsic responses of fitness to this axis (Figure A.16). Our results expand on previous findings that competition can alter species' demographic responses to environmental variation (e.g., Liancourt et al. 2013, Esch et al. 2018) by providing empirical evidence that such altered responses can quantitatively impact species distributions. Importantly, we show that competition can even contribute to trends in occurrence along environmental gradients that are opposite to what would be expected from demographic responses in the absence of competitors.

Our results have particularly important implications for predicting or interpreting species distributions based on observed distribution patterns. Expanding on earlier work (Davis et al. 1998, Pearson and Dawson 2003), we find that competition not only contributes to incongruence between occurrence and fitness, but also has contrasting consequences depending on the species and environmental gradient in question. This complexity cautions against extrapolating from observed distribution patterns without careful consideration of how particular species experience competition along specific environmental gradients. In the absence of detailed demographic data, widely utilized species distribution models (SDMs) can account for competition by including proxies of competitive effects (e.g., population density) as predictors (Elith and Leathwick 2009, Wisz et al. 2013). The variable effects of competition on demography and distributions observed in this study suggest that SDMs should ideally allow the effects of competition proxies to vary by species and to interact with environmental variables. These implications also extend to demographically or physiologically informed models of species' niches and distributions (e.g., Kearney and Porter 2009, Schurr et al. 2012, Merow et al. 2014, Ehrlén and Morris 2015, Benito Garzón et al. 2019), wherein inadequately accounting for variable effects of competition might yield misleading predictions in terms of how species' distributions are expected to track their intrinsic responses to environmental gradients.

Our demographic results were partially consistent with long-standing predictions of covariation between intrinsic fitness and competition across spatial environmental gradients (Figure 1.1b, c) (Grime 1977, Bertness and Callaway 1994, Chesson 2000a). In particular, 3/8 species (ACWR, HECO, LACA) displayed higher intrinsic fitness in finer-textured soils (high PC1), where they were also more limited by competition. Consequently, responses of fitness to soil PC1 for these species were largely flattened by the presence of competitors (Figure 1.3). Although evaluating the mechanisms underlying variation in competition was beyond the scope of this study, this pattern could be driven in part by an increased dominance of invasive grasses such as *Avena fatua*, *Bromus diandrus*, and *Bromus hordeaceus* in sites with finer-textured soils (Figure A.4). These invasive species have been shown to suppress native plants in California serpentine grasslands through a variety of mechanisms, including resource competition, recruitment limitation, and habitat modification (e.g., Hamilton et al. 1999, Seabloom et al. 2003a, 2003b, Chen et al. 2018, LaForgia 2021). As such, the competitive effects measured in our study may be viewed as integrating over multiple types of negative effects imposed by neighbors. While this approach has the benefit of capturing realistic, total effects of interactions, dissecting different sources of variation in competitive effects is an important next step toward a more mechanistic understanding of species distributions (see also Louthan et al. 2015).

Considering that our demographic experiment captured only a single generation of population dynamics in a system with substantial interannual rainfall variability (Levine and Rees 2004), albeit in a water year with about average total rainfall (2019–2020 = 21.57 in + 0.6 in added manually, mean = 21.52 in, County of Santa Barbara 2025b), it is notable that we were able to detect imprints of competition on observed occurrence patterns across our study landscape. However, similar to previous work that found occurrence and demographic parameters to be weakly associated (Thuiller et al. 2014), observed occurrence patterns often could not be clearly explained by experimentally estimated responses of fitness to the soil environment and competition (Figure 1.5; Figure A.16). One possibility is that interannual variation in the competitive environment introduces complexities in the population dynamics that underlie occurrence (e.g., Pitt and Heady 1978, Hobbs et al. 2007, Hallett et al. 2019). Additional processes such as dispersal limitation, source-sink dynamics, demographic stochasticity, and other biotic interactions may also contribute to observed occurrence patterns (Pulliam 2000). For example, Craig et al. (2023) found that source-sink dynamics play an integral role in decoupling annual plant occupancy from fitness in a Northern California grassland at both the species and community level. We note that, despite an abundance of sites where one or more of our focal species were absent (Figure 1.4, Figure A.15), we only found up to moderate (~80%) support for environmental filtering (i.e., absence from sites due to $r_{\text{absent}} < 0$, sensu Kraft et al. 2015b) and competitive exclusion (i.e., absence from sites due to $r_{\text{present}} < 0$ when $r_{\text{absent}} > 0$) along soil PC1 and PC2 in our experiment (Figure A.13, Figure A.14). This observation aligns with previous findings that the (re-)establishment of native plants in California grasslands is often seed-limited (Seabloom et al. 2003a, 2003b, Germain et al. 2017), but more work is needed to explore this possibility in our study landscape.

1.6 Conclusions

The complex interplay between demography and competition across abiotic environments is a critical source of uncertainty in explaining or predicting species distributions. In particular, understanding how the demographic consequences of competition translate to species distributions along real-world environmental gradients remains an important challenge. Here, we outlined a conceptual framework for identifying quantitative mismatches between fitness and occurrence along environmental gradients. We then provided experimental evidence for mismatched responses of plant fitness and occurrence to edaphic gradients in a California annual grassland. Importantly, we showed that competition can contribute to observed trends in fitness and occurrence along environmental gradients that are decoupled—or even reversed—from responses of intrinsic fitness (i.e., fitness in the absence of neighbors) to environmental variation. However, the consequences of competition for fitness and occurrence were highly dependent on the species and environmental gradient under consideration. Our results caution against assuming that observed patterns of fitness or occurrence track species' intrinsic responses to environmental variation without careful consideration of spatially variable competition. Targeted demographic studies such as ours can complement statistical species distribution models by revealing when and how observed distribution patterns reflect intrinsic fitness vs. competitive interactions.

1.7 Acknowledgments

We acknowledge the Chumash peoples as the traditional land caretakers of the area where we conducted our field study. We acknowledge the Gabrielino/Tongva peoples as the traditional land caretakers of Tovaangar (Los Angeles basin, So. Channel Islands), where UCLA is located. We thank T. Foster, G. Kandlikar, E. Purington, and M. Vaz for assistance with the field experiment. We thank Sedgwick Reserve staff, including L. Johnsen and K. McCurdy, for support at the reserve. We are grateful to A. Cisneros Carey, L. Glevanik, E. Ordway, H. Oyler, M. Sagarin, K. Schneider, M. Tingley, and J. Yanowitz for feedback on the manuscript. The manuscript also benefited from discussion with A. Angert and C. Kremer. This work was performed at the University of California Natural Reserve System Sedgwick Reserve (https://doi.org/10.21973/N3C08R) and supported by a Mildred E. Mathias Graduate Student Research Grant from the University of California Natural Reserve System. This work was supported by National Science Foundation grants DEB 1644641 and DEB 2022810.

1.8 Data availability statement

Original data and code for analyses are archived on Zenodo at https://doi.org/10.5281/zenodo.12978683 (Hayashi and Kraft 2024a).

Chapter 2

Functional traits mediate demographic responses of California annual plants to spatial variation in the environment and competition: implications for the spatial storage effect

This chapter is in preparation for submission as Hayashi, K. T., G. S. Kandlikar, A. R. Kleinhesselink, O. Godoy, J. M. Levine, and N. J. B. Kraft. Functional traits mediate demographic responses of California annual plants to spatial variation in the environment and competition: implications for the spatial storage effect. NJBK, OG, and JML conceptualized and designed the experiments. NJBK, OG, and JML implemented the 2013 experiment. GSK, NJBK, and JML deployed the 2015 experiment. GSK, NJBK, and ARK collected data for the 2015 experiment. KTH, NJBK, JML, and GSK designed the research questions for this manuscript. KTH, GSK, and NJBK conducted data curation and analysis. KTH wrote the original draft of the manuscript with input from NJBK.

2.1 Abstract

Spatial variation in the abiotic and biotic environment is a ubiquitous feature of ecological communities, with theory showing that this spatial heterogeneity is important for species coexistence and biodiversity maintenance. One such mechanism of species coexistence in spatially variable environments is the spatial storage effect, which can promote coexistence provided that species exhibit distinct demographic responses to the abiotic environment that covary with the strength of competition across space. However, empirical tests of the spatial storage effect are scarce, and our understanding of what drives variation in the strength of this mechanism remains limited. Here, using an edaphically heterogeneous California annual grassland, we asked how plant functional traits mediate the demographic responses of species to spatial variation in the environment and competition that underlie the spatial storage effect. We experimentally quantified how the lifetime fecundity of 24 annual plant species responds to variation in the environment and competition by growing species in the presence or absence of competitors at 16 sites across two different growing seasons. We found that species were only partially correlated in their responses to spatial variation in the environment or competition, and that several species experienced greater competition at more favorable sites, consistent with the requirements of the spatial storage effect. We also found that nine leaf, root, seed, and whole-plant functional traits each mediated fecundity responses to the environment and competition in different ways. Notably, individual traits that explained fecundity responses to environmental gradients (Ca:Mg, sand %, soil depth) were typically different from those that explained responses to variation in competition. Additionally, we found that trait-based demographic responses to the environment and competition differed between years. Our results demonstrate that functional traits can contribute to the spatial storage effect by modulating spatial patterns of demography that underlie the mechanism, but that interactions between the environment, competition, and traits are complex and variable.

Keywords: competition, fecundity, modern coexistence theory, serpentine grassland, spatial heterogeneity, trait-environment interactions

2.2 Introduction

The mechanisms of species coexistence have long fascinated ecologists (Hutchinson 1961, MacArthur and Levins 1967, Chesson 2000b, 2018, Levine et al. 2017, Simha et al. 2022). Simultaneously, centuries of observations have shown that environmental gradients drive turnover in the species and functional composition of ecological communities (von Humboldt and Bonpland 1805, Schimper 1903, Whittaker 1975, Wright et al. 2005, Wieczynski et al. 2019). In accordance with these observations, theory suggests that spatial variation in the environment plays an integral role in promoting species coexistence (Chesson 2000a, Amarasekare 2003, Leibold et al. 2004, Snyder 2008, Hart et al. 2017). Recent empirical work has underscored that species diversity observed in natural communities often cannot be supported in a homogeneous environment (e.g., Kraft et al. 2015b, Hallett et al. 2019, Wainwright et al. 2019, Van Dyke et al. 2022), further pointing to the importance of environmental fluctuations for biodiversity maintenance. However, empirical tests of fluctuation-dependent coexistence mechanisms remain scarce relative to theoretical developments (Amarasekare 2003, Siepielski and McPeek 2010, but see e.g., Adler et al. 2006, Angert et al. 2009, Letten et al. 2018, Hallett et al. 2019), especially in a spatial context (e.g., Sears and Chesson 2007, Harrison et al. 2010, Towers et al. 2020). Understanding how spatial environmental variation promotes species coexistence is particularly important now as global environmental change threatens to alter the interplay between the abiotic environment and biotic interactions across spatial scales (Gilman et al. 2010, Blois et al. 2013, Valladares et al. 2015, Alexander et al. 2016, Godoy 2019, Hallett et al. 2023).

The spatial storage effect is a general mechanism of species coexistence in spatially variable environments (Chesson 2000a). In essence, this mechanism describes how spatial variation in both the abiotic environment and competition interact to promote species coexistence at spatial scales that encompass said variation. Three main ingredients tend to promote species coexistence via the storage effect (Chesson 2000a, Johnson and Hastings 2022). The first is *species-specific responses to the environment*, such that species are differentially favored at different sites. The second is *covariance between responses to the environment and competition*, or "EC covariance" for short. That is, species should be more limited by competition in more favorable environments, for example as a result of increased competitor density. In particular, a greater EC covariance when a species is common, and conversely a weaker EC covariance when it is rare, is expected to stabilize coexistence by concentrating intraspecific competition relative to interspecific competition (Chesson 2000b, Kuang and Chesson 2009). The third is *buffered population growth* in which the negative effects of competition are dampened in unfavorable environments. Such buffering effects can arise through spatial population structure that allows poor performance in unfavorable sites to be offset by good performance "stored" in favorable sites (Chesson 2000a, Johnson et al. 2023). When combined, these ingredients can help rare species increase in abundance, thereby promoting species coexistence (Turelli 1978, Grainger et al. 2019b). Despite the theoretical significance of the spatial storage effect, pioneering field studies have found mixed evidence for it in empirical systems (e.g., Sears and Chesson 2007, Towers et al. 2020). Thus, examining ecological causes of variation in the spatial storage effect will shed further light on when and how environmental variation promotes species coexistence.

Functional traits—morphological, physiological, or phenological traits that impact fitness (Violle et al. 2007)—can provide mechanistic insights into species' responses to the abiotic environment and competition (McGill et al. 2006, Funk et al. 2017), with implications for species coexistence (Adler et al. 2013, Levine 2016). Functional traits have been shown to predict plant species' demographic responses to environmental gradients (e.g., Kandlikar et al. 2022, Siefert and Laughlin 2023). They have also been found to explain niche and fitness differences that determine the outcomes of competition between species (Kraft et al. 2015b, Pérez-Ramos et al. 2019, Van Dyke et al. 2022). One way that functional traits can contribute to species coexistence via the storage effect is by mediating species-specific responses to the environment (Snyder 2008, Adler et al. 2013). If species with different traits exhibit different demographic responses to environmental gradients, as indicated by a statistical trait-environment interaction (Laughlin et al. 2018), species' responses to the environment should be at least partially uncorrelated. Notably, Angert et al. (2009) demonstrated that a functional trade-off between growth and resource use in Sonoran desert annual plants contributes to a temporal storage effect by decoupling species' responses to environmental (e.g., precipitation) fluctuations. Another way that functional traits can contribute to the storage effect is by mediating demographic responses to spatial variation in competition. In particular, EC covariance may be influenced by traits whose roles in competition depend on the environment (i.e., there is a statistical interaction between the environment, competition, and traits). However, although recent years have seen significant advances in characterizing trait-based demographic responses to environmental variation (Chalmandrier et al. 2021, Siefert and Laughlin 2023), identifying how traits mediate responses to competition across disparate environments remains challenging (but see Kunstler et al. 2016).

Here, we evaluate how plant functional traits contribute to species coexistence in a spatially variable California grassland landscape by testing for ingredients of the spatial storage effect. We experimentally quantified the fecundity responses of 24 annual plant species to spatial variation in the abiotic environment and competition. We then asked: (1) Are species' demographic responses to the environment partially uncorrelated? This would correspond to species-specific responses to the environment. (2) Are species more limited by competition in more favorable environments? This would correspond to a positive EC covariance, which could enable a coexistence-promoting storage effect. Next, using nine functional traits related to plant population dynamics in this system, we asked: (3) How do functional traits mediate species' responses to the environment and competition? More specifically: (3.1) How do traits influence species' responses to environmental gradients? (3.2) How do traits influence species' responses to spatial variation in competition? Finally, in light of substantial interannual rainfall variability in this system, we asked: (4) How do the above spatial patterns of demography compare between different years? Our results reveal that trait-based demographic responses to the environment and competition are complex and that functional traits can play a role in species coexistence by modulating spatial patterns of demography that underlie the spatial storage effect.

2.3 Methods

We experimentally characterized annual plant species' demographic responses to spatial variation in the abiotic environment and competition at the University of California Natural Reserve System Sedgwick Reserve. To explore interannual variation in spatial patterns of demography, we analyzed two iterations of this experiment conducted in the 2013–2014 and 2015–2016 growing seasons. The two experiments (hereafter "2013 experiment" and "2015 experiment") followed the same methodology but differed in study species due to differences in seed availability. Of 24 total species, 19 and 17 species were used in the 2013 and 2015 experiments, respectively, with 12 species shared across the two experimental years (Table 2.1). While rainfall in this area in the 2015–2016 water year (454 mm) was just under average (64-year mean = 547 mm), the 2013–2014 water year (230 mm) was among one of the driest years on record since 1960 (County of Santa Barbara 2025b). Due to poor germination and establishment in the drier 2013 experiment and a resulting sparsity of fecundity data, we primarily present methods and results for the 2015 experiment and draw contrasts with the 2013 experiment when possible.

2.3.1 Field experiment

We conducted our field experiment in a ~4-ha grassland landscape comprised of serpentine hummocks interspersed among a grassland matrix in the northeastern corner of Sedgwick Reserve. Serpentine soils, typically shallow with low Ca:Mg and high sand content (Walker 1954, Fernandez-Going et al. 2012), present strong edaphic gradients over relatively small spatial scales (e.g., several meters, Gram et al. 2004), making this an experimentally tractable system for addressing our research questions. Additionally, California grasslands are characterized by a Mediterranean climate with hot, dry summers, and cool, wet winters that experience substantial interannual variation in rainfall (Pitt and Heady 1978, Hobbs et al. 2007).

To estimate plant responses to the environment, 17 functionally variable annual plant species were grown in the absence of competitors at 16 sites distributed across the study landscape in 2015–2016 (Table 2.1). Methods for this experiment are detailed in Kandlikar et al. (2022). Briefly, seeds of each species were planted in five replicate plots at each site in November 2015. Germinated seeds were thinned down to a single focal individual per species per plot in February 2016. All neighbors within a 15 cm radius of focal individuals were weeded out, thereby minimizing plant-plant interactions. The lifetime fecundity of focal individuals was estimated in April–June 2016 as a metric of species' demographic responses to the environment at each site. Additionally, soil samples were collected at each site and analyzed for physical and chemical properties. We retrieved a publicly archived version of these demographic and environmental data for use in the present study (Kandlikar 2021).

Concurrent with the above experiment, we also grew species in the presence of competitors in order to estimate their responses to competition. At each site, we established a 2.4 m × 3 m plot that was cleared of natural vegetation and seeded homogeneously with a mixture of the 17 study species. This seed mixture had a similar number of seeds per species and was added to plots at a total seed density of ~16 g m^{-2} (approximately double the average seed density of annual plants in this area, Levine and HilleRisLambers 2009). Each plot was divided into twenty 0.6 m × 0.6 m subplots, each of which was assigned to one of the study species (three subplots were unused in the 2015 experiment). Within each subplot, we identified about five focal individuals with at least

7.5 cm between one another and estimated their fecundity as described in Kandlikar et al. (2022). Collectively, 2,815 focal individuals (including those that failed to reproduce) were tracked for fecundity either in the presence or absence of competitors.

Table 2.1: Plant species used in this study. Species are marked with plus signs (+) for the year(s) in which they were used in the field experiment. Taxonomy follows Baldwin et al. (2012).

Code	**Species**	**Family**	**2013**	**2015**
ACAM	*Acmispon americanus*	Fabaceae	+	
ACWR	*Acmispon wrangelianus*	Fabaceae	+	+
AMME	*Amsinckia menziesii*	Boraginaceae	+	+
BRMA	*Bromus madritensis*	Poaceae		+
CEME	*Centaurea melitensis*	Asteraceae	+	+
CHGL	*Chaenactis glabriuscula*	Asteraceae		+
CLBO	*Clarkia bottae*	Onagraceae	+	+
CLPU	*Clarkia purpurea*	Onagraceae	+	+
ERBO	*Erodium botrys*	Geraniaceae	+	
ERCI	*Erodium cicutarium*	Geraniaceae	+	
EUSP	*Euphorbia spathulata*	Euphorbiaceae	+	+
FEMI	*Festuca microstachys*	Poaceae		+
GECA	*Geranium carolinianum*	Geraniaceae	+	
HECO	*Hemizonia congesta*	Asteraceae	+	+
HOMU	*Hordeum murinum*	Poaceae		+
LACA	*Lasthenia californica*	Asteraceae	+	+
MEPO	*Medicago polymorpha*	Fabaceae	+	+
MICA	*Micropus californicus*	Asteraceae		+
MIDO	*Microseris douglasii*	Asteraceae	+	
NAAT	*Navarretia atractyloides*	Polemoniaceae	+	
PLER	*Plantago erecta*	Plantaginaceae	+	+
SACO	*Salvia columbariae*	Lamiaceae	+	+
SIGA	*Silene gallica*	Caryophyllaceae	+	
URLI	*Uropappus lindleyi*	Asteraceae	+	+

2.3.2 Functional traits

With the aim of evaluating how functional traits mediate species' demographic responses to the environment and competition, we examined nine leaf, root, seed, and whole-plant functional traits (Table B.1) that were previously measured and linked to plant population dynamics in our study system (Kraft et al. 2015b, Kandlikar et al. 2022, Van Dyke et al. 2022). An overview of these traits is provided here: Leaf nitrogen content (foliar N), leaf dry matter content (LDMC), and specific leaf area (SLA) represent the leaf economics spectrum that spans resource-acquisitive to conservative strategies (Wilson et al. 1999, Wright et al. 2004). LDMC also has consequences for leaf longevity and palatability (Ryser 1996, Blumenthal et al. 2020). Leaf size plays a key role in plant energy and water balance (Parkhurst and Loucks 1972, Wright et al. 2017). Specific root length (SRL) relates to belowground resource strategies (i.e., a root or whole-plant economics spectrum, Freschet et al. 2010, Kramer-Walter et al. 2016). Maximum height and seed mass represent investment in growth and resource provisioning to offspring, respectively, with direct implications for competition (Westoby 1998, Díaz et al. 2016). Phenology controls the timing of competition in annual plant communities (Levine et al. 2022). Carbon isotope discrimination (δ^{13}C) is a measure of integrated water use efficiency (Seibt et al. 2008). Trait data were obtained from Kraft et al. (2015b) and Kandlikar et al. (2022), with detailed methods for trait measurements provided therein. Additionally, we conducted a principal component analysis (PCA) to summarize variation in functional traits across all 24 study species (Figure B.1, Figure B.2). All traits were centered and scaled to unit variance prior to performing the PCA. We retained the first two axes (PC1, PC2) for subsequent analyses in accordance with results of parallel analysis (adjusted eigenvalues > 1, Horn 1965, Dinno 2024).

2.3.3 Statistical analyses

We used a series of Bayesian hierarchical models to analyze variation in fecundity in the context of each of our research questions (1–3). We implemented all Bayesian statistical models using Stan (Stan Development Team 2024) via `cmdstanr` (Gabry et al. 2024) in R version 4.4.1 (R Core Team 2024). We analyzed the two experimental years (2013, 2015) separately given their different species lists (Table 2.1). Below, we describe our procedure for analyzing the 2015 experiment, which generally applied to the 2013 experiment as well.

(1) Are species' demographic responses to the environment partially uncorrelated?

To estimate the correlation between species in responses to the environment or competition, we first modeled fecundity for species i at site k as following a zero-inflated negative binomial distribution with a species-specific probability of zero-inflation, θ_i. We specified a linear model for the negative binomial mean, μ, as:

$$\log(\mu) = \gamma_{E,i,k} - \gamma_{C,i,k} C \tag{2.1}$$

where C denotes the presence ($C = 1$) or absence ($C = 0$) of competitors. Here, γ_E is the log-transformed fecundity expected in the absence of competitors, representing a species' response to the environment at a given site. γ_C then describes the species' response to competition at this site. Following Chesson (2000a), the competition term is explicitly written as negative so that a larger value of γ_C corresponds to a greater (more negative) impact of competition on fecundity. We allowed the negative binomial shape, ϕ, to differ by species.

We hierarchically modeled the response to environment, γ_E, as a species-level correlated varying effect:

$$\gamma_{E,i,k} = \overline{\gamma_E} + \delta_{E,i,k} \tag{2.2}$$

$$\begin{bmatrix} \delta_{E,1,k} \\ \vdots \\ \delta_{E,n,k} \end{bmatrix} \sim \text{MVNormal}\left(\begin{bmatrix} 0 \\ \vdots \\ 0 \end{bmatrix}, \mathbf{S_E} \right) \tag{2.3}$$

where $\overline{\gamma_E}$ is the mean response to the environment and $\delta_{E,i,k}$ is the deviation from this mean for species $i = 1, \ldots, n$ at site k. We modeled δ_E as drawn from a zero-centered multivariate normal distribution with an $n \times n$ covariance matrix, $\mathbf{S_E}$. This covariance matrix was further decomposed into an $n \times n$ correlation matrix, $\mathbf{R_E}$, and a vector of n standard deviations, σ_E. Each element of this correlation matrix is a model-based estimate of the correlation between species in their fecundity responses to the environment across sites (with the mean response factored out) and is analogous to Pearson's correlation coefficient. We also employed an analogous hierarchical structure for the response to competition, γ_C, with a corresponding correlation matrix, $\mathbf{R_C}$, that describes the correlation between species in their fecundity responses to competition across sites. For this analysis, we excluded four species (AMME, CLBO, CLPU, MICA) that made model fitting difficult due to a severe lack of fecundity data across sites (e.g., the species only reproduced at 3/16 sites), leaving n = 13 species or 78 species pairs. For the 2013 experiment, we similarly excluded seven species (AMME, CLBO, CLPU, ERBO, ERCI, GECA, SIGA).

(2) Are species more limited by competition in more favorable environments?

Next, to estimate the within-species correlation between responses to the environment and competition, we modeled fecundity for each species separately by simplifying Equation 2.1 as:

$$\log(\mu) = \gamma_{E,k} - \gamma_{C,k} C \tag{2.4}$$

We hierarchically modeled the response to environment, γ_E, and the response to competition, γ_C, as site-level correlated varying effects:

$$\gamma_E = \overline{\gamma_E} + \delta_{E,k} \tag{2.5}$$

$$\gamma_C = \overline{\gamma_C} + \delta_{C,k} \tag{2.6}$$

$$\begin{bmatrix} \delta_{E,k} \\ \delta_{C,k} \end{bmatrix} \sim \text{MVNormal}\left(\begin{bmatrix} 0 \\ 0 \end{bmatrix}, \mathbf{S} \right) \tag{2.7}$$

Here, we modeled the pair of deviations from the species' mean responses to the environment and competition, $[\delta_E, \delta_C]$, as drawn from a zero-centered multivariate normal distribution with a 2×2 covariance matrix, **S**. From this covariance matrix, we obtained the correlation matrix, **R**, which describes the correlation in fecundity responses to the environment and competition across sites (with the mean response factored out). Although covariance is of direct interest to the storage effect, we focus on correlation here to facilitate interpretation and comparison between species. We fit this model for each of the study species using only sites at which at least one focal individual reproduced. For this analysis, we excluded four species (AMME, CLBO, CLPU, MICA) that failed to reproduce at more than 8/16 sites, as responses to the environment and competition could not be readily identified at these sites. Additionally, we dropped one species (FEMI) for which the fitted model failed to satisfy the diagnostic criteria described below. For the 2013 experiment, we similarly excluded seven species (AMME, CLBO, CLPU, ERBO, ERCI, GECA, SIGA) and dropped three more species (CEME, LACA, MEPO) with unsatisfactory model diagnostics.

(3) How do functional traits mediate species' responses to the environment and competition?

Finally, we modeled responses of fecundity to environmental gradients (Ca:Mg, sand %, soil depth) as mediated by functional traits. To this end, we expanded the linear model for the negative binomial mean fecundity (Equation 2.1) as:

$$\log(\mu) = \gamma_I + \gamma_E E - \gamma_C C + \gamma_{EC} EC + \gamma_{\text{species}} + \gamma_{\text{site}} \tag{2.8}$$

where γ_I is the intercept, γ_E is the slope for an environmental variable, E, γ_C is the response to competition as described above, and γ_{EC} is the statistical interaction between responses to the environment and competition. γ_{species} and γ_{site} are random intercepts for species and site, respectively, each modeled as drawn from a zero-centered normal distribution with a standard deviation of σ_{species} or σ_{site}. We then allowed each main effect to vary as a function of a trait, x:

$$\gamma_I = \alpha_I + \beta_I x \tag{2.9}$$

$$\gamma_E = \alpha_E + \beta_E x \tag{2.10}$$

$$\gamma_C = \alpha_C + \beta_C x \tag{2.11}$$

$$\gamma_{EC} = \alpha_{EC} + \beta_{EC} x \tag{2.12}$$

where α is the intercept and β is the slope for the trait in each linear model. Note that Equations 2.9–2.12 effectively introduce interactions between the trait and the predictor terms in Equation 2.8. The environmental variable and trait values were both centered and scaled to unit variance for model fitting. Thus, α_I can be interpreted as the log-transformed fecundity expected in the absence of competitors under an average environmental condition with an average trait value. We fit this model separately for each combination of one of three environmental variables and one of 11 traits (9 traits + 2 PCA axes). We retained all species and sites for this analysis.

We fit all models by running four chains of Stan's main Markov chain Monte Carlo (MCMC) algorithm with default initial values and the control parameter `adapt_delta` = 0.99. For analyses (1) and (2), we ran 1,000 warmup and 5,000 sampling iterations per chain, resulting in N = 20,000 posterior samples. For analysis (3), we ran 1,000 warmup and 1,000 sampling iterations per chain, resulting in N = 4,000 posterior samples. We evaluated model convergence by confirming that there were no divergent transitions, the $\hat{R}$ convergence diagnostic < 1.01, the effective sample size (N_{eff}) > 400, and the ratio N_{eff}/N > 0.1 for all parameters (Vehtari et al. 2021, Stan Development Team 2022). Models that failed to satisfy any of these diagnostic criteria were excluded from results, including the model for analysis (1) for the 2013 experiment. Note that hierarchical models were coded using a non-centered parameterization to facilitate MCMC sampling. We used weakly regularizing priors (Lemoine 2019, Banner et al. 2020, Wesner and Pomeranz 2021) that were informed in part by prior work in this study system (Kraft et al. 2015b, Van Dyke et al. 2022): e.g., $\gamma_E \sim \text{Normal}(5,\ 2.5)$, $\gamma_C \sim \text{Normal}(0,\ 5)$, $\beta \sim \text{Normal}(0,\ 1)$, $\mathbf{R} \sim \text{LKJcorr}(2)$, $\sigma \sim \text{Exponential}(1)$. We present results based on $\geq$ 97.5% posterior support (Makowski et al. 2019), unless explicitly stated otherwise.

2.4 Results

We found mixed evidence for correlated responses of species to environmental variation across sites (Figure 2.1a). Median correlation between species in responses of fecundity to the environment ranged from -0.45 to 0.58 with a mean of 0.14. Thirteen of 78 species pairs (16.7%) exhibited positive correlations in responses to the environment. These positive correlations were observed both within and between grasses and forbs. Overall, while some species had similar site preferences, responses of fecundity to site-level environmental variation were variable across species and far from perfectly correlated. In fact, two species pairs (2.6%) exhibited negative correlations in responses to the environment.

In contrast to responses to the environment, we found limited evidence for correlated responses of species to variation in competition across sites (Figure 2.1b). Median correlation between species in responses of fecundity to competition ranged from -0.45 to 0.35 with a mean of 0.00. Only one species pair (BRMA-CEME) exhibited a moderate, negative correlation between responses to competition. That is, BRMA was less impacted by competition at sites where CEME was more impacted by competition, and vice versa, despite these species being positively correlated in their responses to spatial environmental variation (Figure 2.1a).

Within species, responses of fecundity to the environment often positively covaried with responses of fecundity to competition (Figure 2.2). We found a positive correlation between responses of fecundity to the environment and competition for seven of 12 species (58.3%). Only

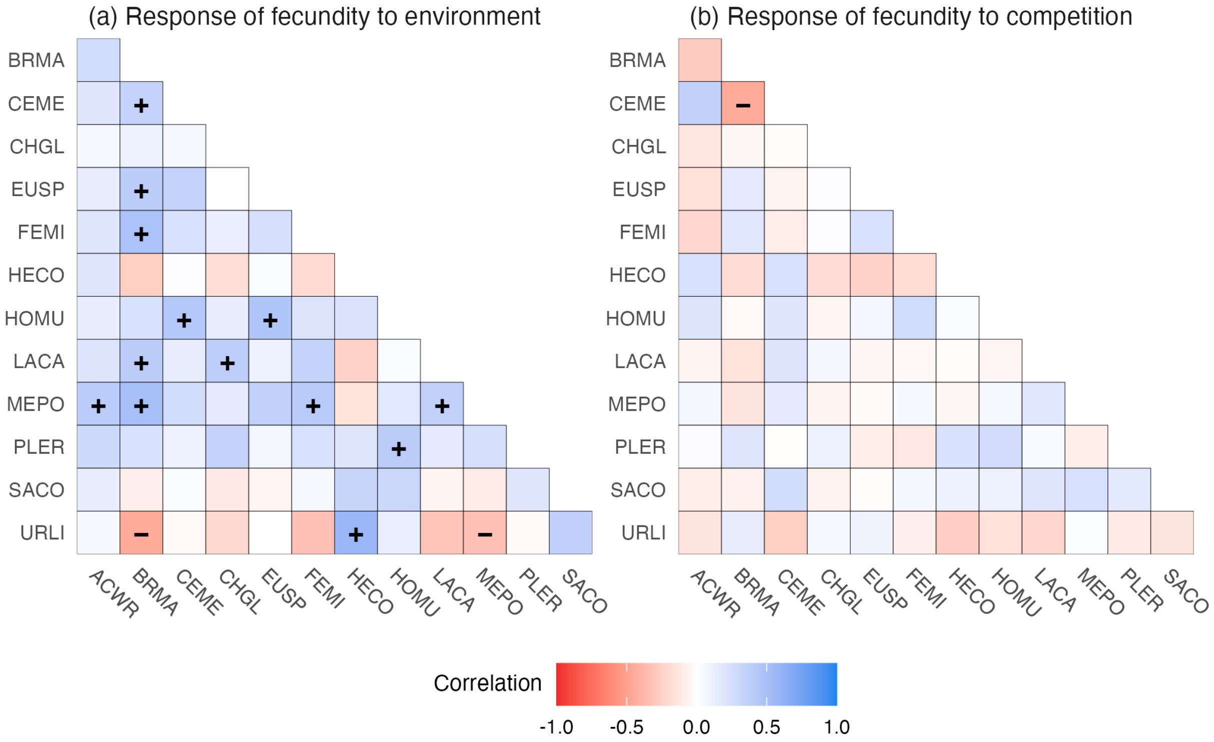

Figure 2.1: Correlation between responses of fecundity to (a) environment or (b) competition for each species pair in the 2015 experiment. Cells are colored by median correlation. Species pairs with Pr(correlation $>$ 0) $\geq$ 0.975 are indicated with plus signs (+), whereas species pairs with Pr(correlation $<$ 0) $\geq$ 0.975 are indicated with minus signs (−).

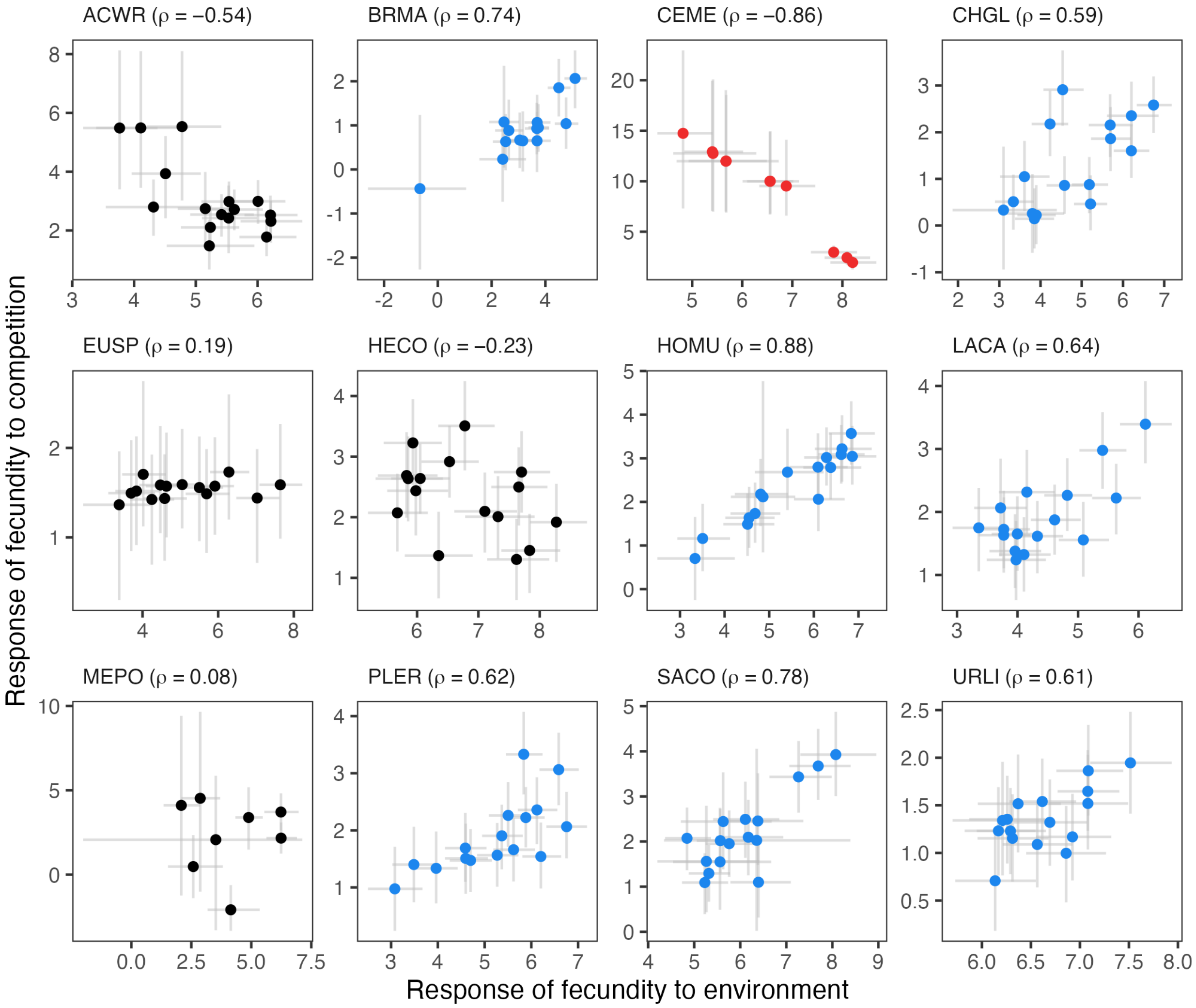

Figure 2.2: Correlation (ρ) between responses of fecundity to environment and competition for each species in the 2015 experiment. Median correlations are given in panel labels. Species with $\Pr(\rho > 0) \geq 0.975$ are indicated with blue points, whereas species with $\Pr(\rho < 0) \geq 0.975$ are indicated with red points. Points represent posterior medians. Gray lines represent 95% credible intervals.

one species (CEME) displayed a negative correlation between responses of fecundity to the environment and competition. Taken together, several species were more limited by competition at sites where they achieved higher fecundity in the absence of competitors.

Several functional traits explained variation in both fecundity without competitors and the response of fecundity to competition. Under mean environmental conditions, species with low LDMC, large leaves, or tall maximum height had increased fecundity (Figure 2.3c). The primary trait PCA axis (PC1), which corresponded strongly to variation in these three traits and foliar N (Figure B.1, Figure B.2), also explained variation in fecundity. Competition reduced fecundity on average by over a factor of 1.5 (Figure 2.3b). Notably, the same traits that conferred increased fecundity also resulted in elevated impacts of competition on fecundity (Figure 2.3d). Species with high foliar N, late phenology, or large seed mass were also more limited by competition.

We found evidence for trait-environment interactions in which functional traits mediated responses of fecundity to environmental gradients. Fecundity was on average higher in soils with greater Ca:Mg or depth (Figure 2.4a). LDMC, SLA, or the secondary trait PCA axis (PC2, largely representing variation in SLA, δ^{13}C, phenology, and seed mass; Figure B.1, Figure B.2) mediated responses of fecundity to variation in Ca:Mg (Figure 2.4c). Additionally, many of the same traits that explained variation in mean fecundity (LDMC, leaf size, maximum height) also mediated responses to variation in soil depth (Figure 2.4c), signifying the importance of these traits (or their correlates) in shaping spatial patterns of fecundity across the study landscape.

Responses of fecundity to competition also varied along environmental gradients, with elevated impacts of competition observed in soils with less sand % or greater depth (Figure 2.4b). While several traits mediated the strength of this interaction between the environment and compe-

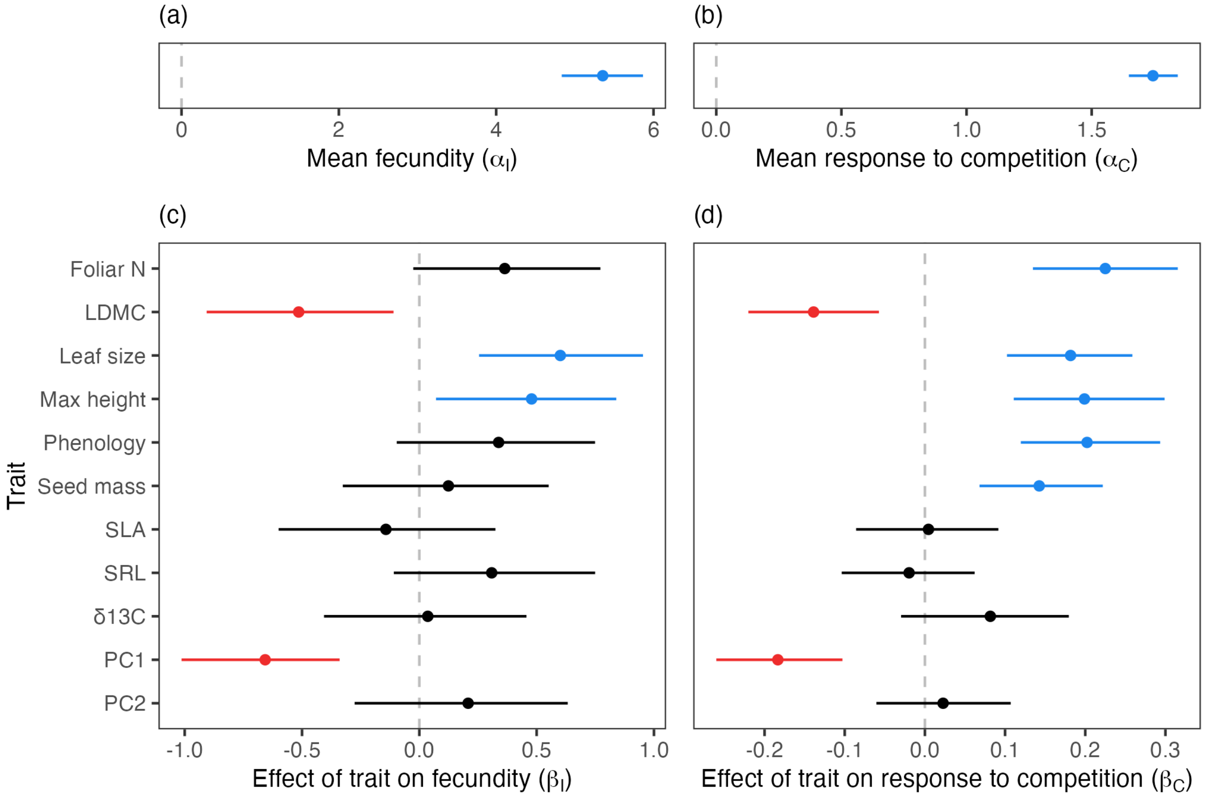

Figure 2.3: Effects of functional traits on fecundity under mean environmental conditions in the 2015 experiment. (a) Fecundity without competitors given mean environment and traits. (b) Response to competition given mean environment and traits. (c) Effects of traits on fecundity without competitors. (d) Effects of traits on response to competition. Parameter estimates with Pr(>0) $\geq$ 0.975 are shown in blue, whereas parameter estimates with Pr(<0) $\geq$ 0.975 are shown in red. Points represent posterior medians. Solid lines represent 95% credible intervals. Note that models were fit separately for each trait. Parameter estimates shown in (a, b) are summarized over all posterior samples from these separate models. Results shown here are for soil depth as the environmental variable (results are comparable with different environmental variables).

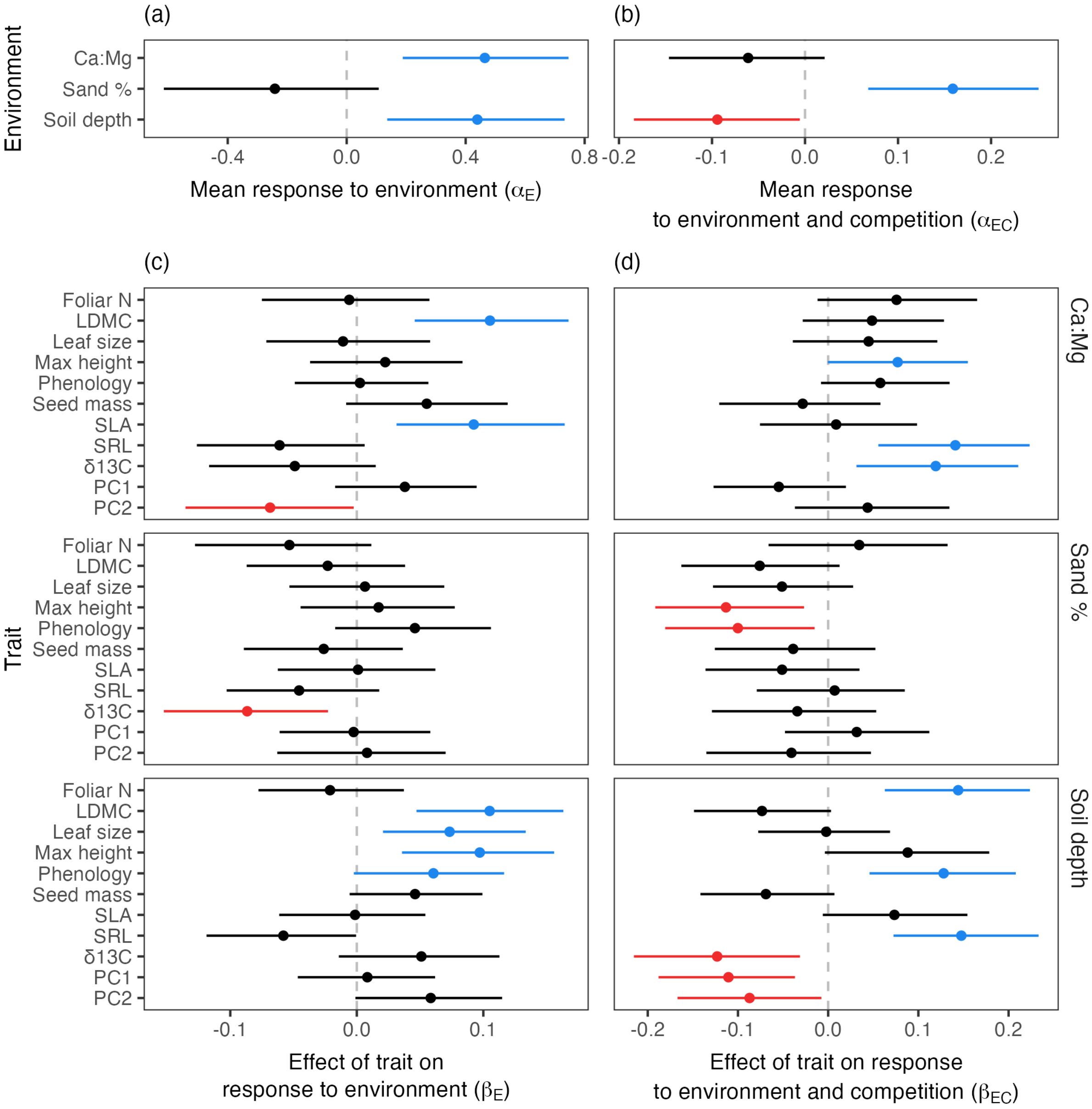

Figure 2.4: Effects of functional traits on responses to environment and competition in the 2015 experiment. (a) Response of fecundity to environment given mean traits. (b) Interaction between responses of fecundity to environment and competition given mean traits. (c) Effects of traits on response of fecundity to environment. (d) Effects of traits on interaction between responses of fecundity to environment and competition. Parameter estimates with Pr(>0) $\geq$ 0.975 are shown in blue, whereas parameter estimates with Pr(<0) $\geq$ 0.975 are shown in red. Points represent posterior medians. Solid lines represent 95% credible intervals. Note that models were fit separately for each combination of environmental variable and trait. Parameter estimates shown in (a, b) are summarized over all posterior samples from these separate models.

tition (Figure 2.4d), these traits were typically different from those that mediated direct responses to the environment (Figure 2.4b). For example, although trait PC1 had little clear relation to how fecundity responded to variation in soil depth in the absence of competitors (Figure 2.5a), species represented by larger values of trait PC1 (higher LDMC, lower leaf size, foliar N, and maximum height; Figure B.1) were more limited by competition in deeper soils (Figure 2.5b). That is, the response of fecundity to variation in soil depth depended on trait PC1, but only in the presence of competitors. In all, many functional traits explained responses of fecundity to spatial variation in the environment and competition. However, interactions between traits, environment, and competition were complex, with different traits explaining different dimensions of species' responses to the environment and competition.

We have focused on results of the 2015 experiment thus far, but the drier 2013 experiment provided a number of contrasting results. First, we did not find strong support for within-species correlation between responses of fecundity to the environment and competition (Figure B.3), although this may be due in part to data deficiency. Similarly, we did not find clear evidence for trait-mediated differences between species in mean fecundity (Figure B.4c), which suggests that fitness differences between species may have been smaller in this drier year. Second, competition reduced fecundity less on average than in the 2015 experiment (Figure B.4b), and functional traits had different effects on responses of fecundity to competition (Figure B.4d). In particular, at least three traits (foliar N, leaf size, trait PC1) had opposing effects on responses to competition between the two years. Third, functional traits also had different effects on responses of fecundity to spatial variation in the environment and competition (Figure B.5). Importantly, evidence for an interaction between the environment and competition was limited (Figure B.5b), consistent with

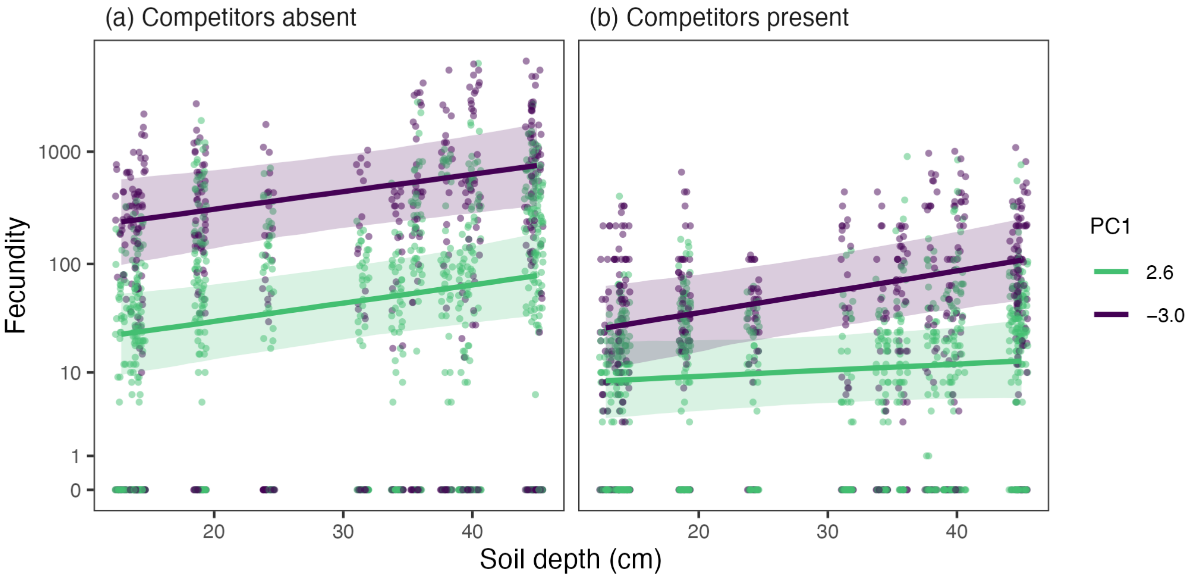

Figure 2.5: Effects of soil depth on fecundity conditional on trait PC1 and the (a) absence or (b) presence of competitors in the 2015 experiment. Predictions are computed under minimum (purple) and maximum (green) trait values in the data. Data points are colored according to whether species' trait values are below (purple) or above (green) average and are jittered horizontally for visual clarity. Solid lines represent posterior medians. Shaded areas represent 95% quantile credible intervals. Note that the y-axis is shown on the $\log(y+1)$ scale, where y is fecundity.

the aforementioned lack of correlation between responses of fecundity to the environment and competition (Figure B.3). However, there was evidence that a number of traits (e.g., foliar N, δ^{13}C, trait PC2) can mediate this interaction (Figure B.5d), albeit with opposing effects between the two years. This suggests that species may still experience covariation between responses to the environment and competition depending on their traits. Taken together, annual environmental context appeared to have a strong influence on how functional traits explain species' responses to spatial variation in the soil environment and competition.

2.5 Discussion

Spatial variation in the abiotic environment underlies many fundamental mechanisms of species coexistence in ecological communities (Chesson 2000a, Amarasekare 2003, Leibold et al. 2004). The spatial storage effect is one such mechanism, but the few empirical tests of it to date have found mixed evidence for its operation in natural communities (Sears and Chesson 2007, Towers et al. 2020). In this study, we explored how functional traits can mediate species' demographic responses to the abiotic environment and competition, and thereby modulate the spatial storage effect, in an edaphically variable California grassland landscape. We found that key ingredients of the spatial storage effect (species-specific responses to the environment, covariance between responses to the environment and competition) emerged among spatially distributed experimental plant communities, with evidence that a wide array of functional traits can explain corresponding demographic responses to the environment and competition. Our results demonstrate how functional traits can contribute to species coexistence in spatially variable environments (Adler et al. 2013), while also revealing the complexity in how different traits explain different aspects of species' responses to the environment and competition.

We found two lines of evidence in support of species-specific responses to the environment. First, fecundity responses to environmental variation across sites were only partially correlated between species (Figure 2.1a). Responses to the environment were positively correlated for 13 of 78 species pairs (16.7%), but there was overall limited evidence that species exhibit highly correlated responses to the environment. Interestingly, responses to variation in competition appeared to be even more idiosyncratic (Figure 2.1b), underscoring the difficulty of predicting species' responses to competition in variable environments.

Second, functional traits mediated species' responses to environmental gradients (Figure 2.4c). Therefore, species with different traits are expected to respond differently to environmental variation, resulting in species-specific responses to the environment. Of particular note is a positive effect of Ca:Mg on fecundity (Figure 2.4a) that is further enhanced for species with high SLA (Figure 2.4c). This pattern, also demonstrated by Kandlikar et al. (2022), is consistent with a shift toward more resource-acquisitive strategies in less abiotically stressful environments (Wright et al. 2004, Fernandez-Going et al. 2012, Hulshof et al. 2013). Notably, we extend previous work to show that this interaction between SLA and Ca:Mg was found despite no clear effect of SLA on mean fecundity (Figure 2.3c) or responses to competition (Figure 2.3d, Figure 2.4d). This exemplifies how a trait might be involved in only certain aspects of species' demographic responses to the environment and competition. In contrast, many of the same traits associated with increased fecundity without competitors and elevated impacts of competition (LDMC, leaf size, maximum height; Figure 2.3c) also mediated responses to soil depth (Figure 2.4c). Interestingly, these trait-based responses to soil depth were seemingly masked when combined in trait PC1 due to these traits loading in opposite directions along this PCA axis (Figure B.1). This suggests that alternative functional strategies can give rise to similar demographic responses to spatial environmental variation (Marks and Lechowicz 2006), possibly complicating the role of traits in mediating species-specific responses to the environment.

We found that positive correlation between fecundity responses to the environment and competition, corresponding to an EC covariance in which species are more limited by competition in more favorable environments, was common (Figure 2.2). This was reflected in species' responses to environmental gradients, especially with a positive effect of soil depth on fecundity (Figure 2.4a) that is countered by an associated increase in competition (Figure 2.4b). However, at least one functional trait was related to species' responses to each of the three focal environmental gradients (Figure 2.4c, d), indicating that the strength of EC covariance experienced by a species can depend on its traits (e.g., as illustrated in Figure 2.5). Several traits involved in resource acquisition and use (foliar N, phenology, SRL, δ^{13}C) explained responses to variation in competition across soil depths (Figure 2.4d). Importantly, such trait-mediated responses to the environment and competition can allow EC covariance to emerge even when mean responses alone do not support such patterns. For example, we can deduce from our results that a species with low SRL can be more limited by competition in favorable environments with high Ca:Mg (Figure 2.4). Such complex interactions between the abiotic environment, competition, and functional traits can contribute to variation in the strength of the spatial storage effect by creating diverse spatial patterns in species' demography.

Our results differ from those of previous work that found limited evidence for covariance between species' responses to the environment and competition (Towers et al. 2020), a key ingredient of the spatial storage effect. One possible explanation for this difference is that our experimental approach allowed us to quantify species' demographic responses at sites where they do not naturally occur at present. These sites may often be where the environment is most unfavorable or competitive pressure is highest (Kraft et al. 2015a). Processes such as priority effects or disturbances may also mask coexistence mechanisms in natural settings (Seabloom et al. 2003b, HilleRisLambers et al. 2010, Uricchio et al. 2019). Another possibility is that strong edaphic gradients characteristic of serpentine grasslands are especially conducive to satisfying ingredients of the spatial storage effect (Whittaker 1954, Gram et al. 2004, Moore and Elmendorf 2011, Hayashi and Kraft 2024b, but see

Harrison et al. 2010).

It must also be noted that a positive EC covariance alone is insufficient to promote species coexistence via the storage effect. Rather, EC covariance must be greater when a species is common in order to stabilize coexistence by concentrating intraspecific competition relative to interspecific competition (Chesson 2000b, Kuang and Chesson 2009). More work is needed to expand our experimental approach to enable comparisons between when species are common versus rare (see also Towers et al. 2020). Additionally, we found contrasting patterns of EC covariance (Figure 2.2, Figure B.3) and trait-mediated responses to the environment and competition (Figure 2.3, Figure 2.4, Figure B.4, Figure B.5) between the two experimental years. These differences were surprisingly stark, with some traits (e.g., foliar N, phenology, δ^{13}C) having entirely opposite effects on fecundity responses to the soil environment and competition in different years. These results are consistent with theoretical and empirical results that temporal variation in the abiotic environment (e.g., seasonal rainfall) is important for species coexistence, including in California grasslands (e.g., Chesson 1994, Adler et al. 2006, Angert et al. 2009, Letten et al. 2018, Hallett et al. 2019, Van Dyke et al. 2022, but see Stump and Vasseur 2023). Overall, our findings suggest that spatiotemporal variation in the environment and competition can produce complex coexistence dynamics in natural communities. Understanding how trait plasticity in spatiotemporally varying environments influences species coexistence remains an important challenge (e.g., Stomp et al. 2008, Turcotte and Levine 2016, Pérez-Ramos et al. 2019, Muthukrishnan et al. 2020).

In conclusion, we have demonstrated how functional traits that summarize species' ecological strategies can have important yet variable consequences for species coexistence in spatially variable environments. In particular, functional traits can mediate species' demographic responses to spatial variation in the environment and competition, thus modulating key ingredients of the spatial storage effect. Importantly, our results reveal a diversity of pathways by which functional traits can be linked to demography and coexistence. In light of this complexity, future trait-based studies of coexistence mechanisms should prioritize disentangling the effects of functional traits on species' responses to the environment and competition.

2.6 Acknowledgments

We acknowledge the Chumash peoples as the traditional land caretakers of the area where we conducted our field study. We acknowledge the Gabrielino/Tongva peoples as the traditional land caretakers of Tovaangar (Los Angeles basin, So. Channel Islands), where UCLA is located. We thank C. Camilleri, A. Dhaliwal, A. Galvin, J. Gregg, R. Guidon, L. Rice, M. von Rutte, M. Van Dyke, and X. Yan for help with the field experiments and associated data collection. We thank K. McCurdy and Sedgwick Reserve staff for support at the reserve. We are grateful to L. Glevanik, E. Ordway, and M. Tingley for insightful discussion and feedback on the manuscript. This work was performed at the University of California Natural Reserve System Sedgwick Reserve (https://doi.org/10.21973/N3C08R). This work was funded in part by National Science Foundation grants DEB 1644641 and DEB 2022810.

Chapter 3

Water supply shapes fitness asymmetries and competitive coexistence of California annual plants

This chapter is in preparation for submission as Hayashi, K. T., and N. J. B. Kraft. Water supply shapes fitness asymmetries and competitive coexistence of California annual plants. KTH and NJBK conceptualized the study and designed the experiment. KTH led data collection, validation, analysis, and visualization with input from NJBK. KTH wrote the original draft of the manuscript with input from NJBK. KTH and NJBK contributed to review and editing of the manuscript.

3.1 Abstract

Variation in competitive interactions along environmental gradients is important for shaping patterns of species fitness, coexistence, and distributions. However, it is often unclear how the strength of competition between individuals (per capita competition) interacts with asymmetries in species-specific demographic performance to determine the community-level impacts of competition on population persistence (total competition). Here, we disentangle how competition varies with rainfall, an especially important abiotic factor in western North America. We experimentally parameterized population dynamics models of competition between an annual grass (*Festuca microstachys*) and forb (*Plantago erecta*) under water supply treatments emulating variation in rainfall across the geographic ranges of both species. We found that per capita competition was generally strongest when water supply was limited. In contrast, the total effect of competition on population growth was greatest at intermediate to high water supply, reflecting variation in fitness differences between species. Consequently, coexistence was most likely in arid environments, despite strong per capita interspecific competition. Our results highlight that asymmetric demographic performance can decouple per capita competition from total competition exerted by a community. We emphasize the importance of distinguishing between how species interact at the individual level and impact one another at the community level in order to accurately predict the consequences of competition in variable environments.

Keywords: competition, fecundity, low-density population growth rate, modern coexistence theory, precipitation, stress gradient

3.2 Introduction

Biotic interactions such as competition are important determinants of species distributions across spatial scales (Sexton et al. 2009, Wisz et al. 2013). In particular, experimental work in ecological communities has revealed an interactive role of the abiotic environment and competition in shaping species distributions (e.g., Taniguchi and Nakano 2000, Armitage and Jones 2020, Usinowicz and Levine 2021, Hayashi and Kraft 2024b), wherein environmental context modulates competitive outcomes and population persistence (e.g., Germain et al. 2018, Matías et al. 2018, Wainwright et al. 2019, Van Dyke et al. 2022, Cervantes-Loreto et al. 2023). However, characterizing how competition varies across geographic-scale environmental gradients remains a major empirical challenge. This challenge is compounded as global environmental change modifies species composition and competitive interactions in communities (Parmesan and Yohe 2003, Bowler et al. 2017, Feeley et al. 2020). Thus, understanding the mechanisms underlying variation in competition across environments is essential for predicting future population and community dynamics, species distributions, and resulting patterns of biodiversity (Gilman et al. 2010, HilleRisLambers et al. 2013, Blois et al. 2013, Alexander et al. 2016, Aschehoug et al. 2016, Boult and Evans 2021).

A long-standing hypothesis in community ecology and biogeography is that competition more strongly limits species' performance and distributions in less abiotically stressful environments (Dobzhansky 1950, MacArthur 1972, Bertness and Callaway 1994, Maestre et al. 2009). Such variation in competition can arise from variation in per capita competitive effects, competitor density, and competitor identity, among other potential mechanisms (Louthan et al. 2015). Modern coexistence theory offers a unifying framework for these various mechanisms of competition and their consequences for the coexistence, and hence distributions, of species in variable environments (Chesson 2000a, 2000b, Godsoe et al. 2017). Within this framework, a species' response to competition is a function of both the per capita effects and densities of intra- and interspecific competitors. In particular, strong intraspecific competition relative to interspecific competition is expected to stabilize coexistence by conferring a demographic advantage to species when at low densities (MacArthur and Levins 1967, Chesson 2000b). Conversely, if stabilization is weak, competition can limit species' distributions by excluding them from otherwise suitable environments (Godsoe et al. 2017, Alexander et al. 2018).

Modern coexistence theory additionally emphasizes that asymmetries in species' demographic performance can contribute to fitness differences between species that drive competitive exclusion (Chesson 2000b). An important advantage of this perspective is that it allows the notion of abiotic stress (critiqued by Körner 2003, see also Lortie et al. 2004) to be operationalized in terms of species-specific demographic responses to environmental conditions. Generally, two species are expected to coexist if each species' response to both the environment and competition allows it to increase in abundance from low density in the presence of the resident community, expressed mathematically as mutually positive low-density population growth rates (Turelli 1978, Grainger et al. 2019b). In environments where fitness differences are large (e.g., due to different reproductive outputs or equilibrium population densities), the resident community might exert a particularly strong effect on low-density population growth rates. Importantly, this total, community-level effect of competition can be large even if per capita competitive effects are not especially strong. Thus, distinguishing between how species interact at the individual level (per capita competition) and impact one another at the community level (total competition) is crucial for developing a robust understanding of how competition varies across environments.

Despite the distinct consequences of per capita versus total competitive effects, their relative contributions to species coexistence and distributions along large-scale environmental gradients is rarely quantified (Louthan et al. 2015). For example, a latitudinal gradient in the strength of conspecific negative density dependence (including intraspecific competition) is hypothesized to play an important role in maintaining global patterns of tree species diversity (Schemske et al. 2009, LaManna et al. 2017, Hülsmann et al. 2021). Such large-scale variation in competition is also reflected in the characteristics of species distributions (e.g., range size, Morin and Chuine 2006). However, few studies have empirically quantified how species-specific demography and per capita competitive effects jointly vary in response to continuous environmental variation. Among these studies, the predominant focus has been on how temperature regulates population dynamics (e.g., Armitage and Jones 2019, McGuire 2023, Sunday et al. 2024). From a practical standpoint, per capita competitive effects may need to be estimated via long-term observation (e.g., Adler et al. 2010, Zepeda and Martorell 2019) or intensive density gradient experiments (Hart et al. 2018, Grainger et al. 2019b), whereas aggregate competitive effects may be estimated through the likes of neighbor removal experiments (Goldberg and Barton 1992) or proxies of competitive pressure (e.g., population density, Treurnicht et al. 2016). Therefore, elucidating the causes and consequences of per capita versus total competition has important theoretical and practical implications for our understanding of how competition shapes species coexistence and distributions along abiotic gradients.

One of the most important abiotic factors determining the performance and distributions of plant species globally is water, and by extension, rainfall (Whittaker 1975, Engelbrecht et al. 2007, Choat et al. 2012, Midolo and Wellstein 2020). Rainfall is particularly important for plant population, community, and range dynamics in California and the broader western United States (e.g., Levine and Rees 2004, Harsch and HilleRisLambers 2016, Hallett et al. 2019, Harrison et al. 2020, Pearse et al. 2020, Van Dyke et al. 2022). Much of this region is characterized by dry summers and wet winters with substantial geographic and interannual variation in rainfall (Haston and Michaelsen 1997, Singh et al. 2018, Beck et al. 2018). Moreover, climate change is projected to increase rainfall volatility and drought over the course of this century (Dai 2013, Yoon et al. 2015, Swain et al. 2018), which could amplify the effects of rainfall on plant communities. Water supply via rainfall approximates a resource-based abiotic gradient (sensu Maestre et al. 2009) and is commonly employed as a measure of water availability in species distribution models (Austin and Van Niel 2011, Mod et al. 2016). This opens the door to mechanistic predictions of how competition varies along this abiotic gradient (Craine and Dybzinski 2013), even if rainfall may not directly represent plant-available water (Piedallu et al. 2013, but see Sehler et al. 2019). For instance, per capita competition may be strong in arid environments where water is a severely limited resource (e.g., Ludwig et al. 2004). Alternatively, total competition may be strong in moister environments that support more biomass or higher population densities (e.g., Rees 2013). Here, we leverage experimentally tractable California annual plants that experience strong rainfall gradients across their geographic ranges to empirically explore such predictions about the mechanisms of competition in variable environments.

In this study, we evaluate how the abiotic environment influences competition and species coexistence by disentangling the individual- and community-level competitive dynamics of an annual grass (*Festuca microstachys*) and forb (*Plantago erecta*) along an experimental water supply gradient emulating geographically relevant variation in rainfall. We grew these species in a greenhouse at six levels of water supply, crossed with varying intra- and interspecific competitor densities, and estimated both per capita (individual-level) and total (community-level) effects of competition on population growth. Specifically, we tested the hypothesis that (1) per capita competition is stronger when water supply is more limited. Additionally, we tested the hypotheses that total competition is stronger when (2.1) per capita competition is stronger or (2.2) higher water supply allows for greater intrinsic demographic performance. Finally, following the hypothesis that variation in conspecific negative density dependence drives geographic patterns of biodiversity, we asked whether (3) intraspecific competition displays a greater response to water supply than does interspecific competition.

3.3 Methods

3.3.1 Study system

Our focal species, *Festuca microstachys* (small fescue, Poaceae) and *Plantago erecta* (California plantain, Plantaginaceae), are winter annual plants native to western North America. These species co-occur in serpentine grasslands of the California Floristic Province (Gram et al. 2004), a biodiversity hotspot (Baldwin 2014). This region experiences a Mediterranean climate with hot, dry summers and mild, wet winters. Accordingly, both species germinate following rainfall in early winter and achieve their lifetime reproductive output by mid- to late spring. The geographic range of *P. erecta* is largely nested within that of *F. microstachys,* with both species experiencing a similar range of rainfall conditions throughout the growing season (December–May) (Figure 3.1). The geographic range of *F. microstachys* extends farther eastward, such that a larger portion of its range experiences limited (e.g., < 300 mm) growing season rainfall. We obtained range maps from the Botanical Information and Ecology Network (BIEN) database version 4.2.8 (Enquist et al. 2016, Maitner et al. 2018) and regional rainfall data from WorldClim 2 (Fick and Hijmans 2017). We collected seeds of the focal species for this study from a serpentine grassland in University of California Natural Reserve System Sedgwick Reserve in Santa Barbara County, California, USA (34.74°N, 120.03°W, mean December–May rainfall = 456 mm, County of Santa Barbara 2025a) in 2019. While local adaptation to regional climate is important for range dynamics (Valladares et al. 2014, DeMarche et al. 2019, Bontrager et al. 2021), logistic constraints did not allow us to work with different geographic populations in this study.

3.3.2 Greenhouse experiment

To estimate how the demographic performance and competitive interactions of our focal species vary in response to a large-scale rainfall gradient, we grew each species at varying levels of water supply and competitor density in a greenhouse at the University of California, Los Angeles Plant Growth Center. We grew plants in 4.26 L (15 cm diameter, 30 cm height) tree pots (Stuewe & Sons, Inc.) filled with Plant Growth Center Soil Mix (18.75% washed plaster sand, 18.75% sandy loam, 37.5% grower grade peat moss, 12.5% horticultural grade perlite, 12.5% #2 coarse vermiculite). Each pot was seeded with a background of one of the two species at one of five seed densities (0, 2, 4, 8, or 16 g/m^2), where 16 g/m^2 is considered to be around the maximum seed density of annual plants at Sedgwick Reserve (Levine and HilleRisLambers 2009). Each pot was additionally seeded at its center with 20 seeds of one of the two species. All planted seeds were random samples of seeds aggregated from numerous parent plants. Finally, each pot was subjected to one of six

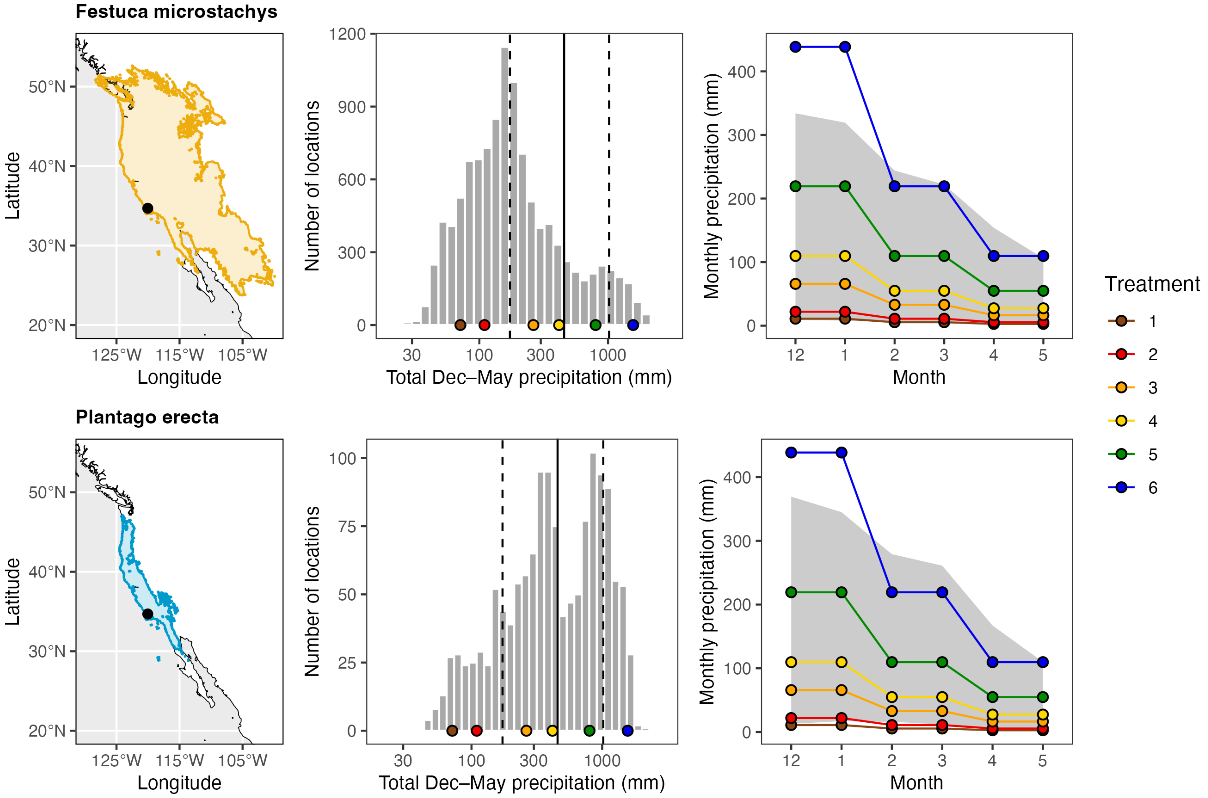

Figure 3.1: Precipitation conditions observed across the focal species' geographic ranges. Left: Range maps retrieved from BIEN (Enquist et al. 2016, Maitner et al. 2018). Black points indicate the location of Sedgwick Reserve, where seeds were collected for this study. Center: Histograms summarizing the total growing season (December–May) precipitation observed across all locations (10-arc-minute raster cells) in range maps. Solid and dashed vertical lines respectively denote the mean and 95% quantile interval of growing season precipitation observed at Sedgwick Reserve since 1960 (County of Santa Barbara 2025a). Note that x-axes are shown on the $\log_{10}$ scale. Right: Monthly precipitation during the growing season. Gray regions denote the 95% quantile intervals for monthly precipitation observed across all locations. Precipitation data were retrieved from WorldClim 2 (Fick and Hijmans 2017). Watering treatments are overlaid in terms of their respective total and monthly water supply levels (Table C.1).

watering treatments. This experimental design yielded 120 combinations of planted competitive neighborhoods and watering treatments (2 focal species $\times$ 2 background species $\times$ 5 background densities $\times$ 6 watering treatments), which were randomly assigned to the same number of pots. This design was replicated in four experimental blocks distributed across two benches, resulting in a total of 480 pots.

We designed our six watering treatments to emulate the monthly and total growing season rainfall that our focal species receive across their ranges (Figure 3.1). Each treatment was comprised of an initial two-week establishment phase (phase 0) followed by three, eight-week phases with progressively reduced water supply (phases 1–3). During phase 0, all pots received 17 mm of water per week to facilitate seed germination and seedling establishment. During phase 1, water supply per pot was 11, 22, 66, 110, 219, or 439 mm/month (divided evenly over four weeks). To minimize water loss due to over-saturating the soil, no more than 28 mm of water was added to any given pot in one day. Thus, treatments that required large water quantities were watered multiple times per week. In each subsequent phase, watering frequency was halved in all treatments to reflect the Mediterranean schedule of decreasing rainfall over the growing season. With these treatments, total water supply per pot over all phases of the experiment amounts to 71, 110, 263, 417, 800, or 1,568 mm (Table C.1), with each four-week period in phases 1–3 corresponding roughly to each month from December to May (Figure 3.1). Three of these treatments were within the 95% quantile interval of growing season rainfall observed at Sedgwick Reserve since 1960, and the other three treatments were outside this interval (Figure 3.1). This experimental design allowed us to quantify demography and competition under a wider range of water supply levels than would be possible under field conditions at Sedgwick Reserve. Note that our watering treatments are concentrated toward the arid end of the rainfall gradient, where we expected species to respond most strongly to variation in water supply, and are approximately evenly spaced on a logarithmic scale. We used EC5 Soil Moisture Smart Sensors (Onset Computer Corporation) to measure volumetric water content at 10-minute intervals in a set of soil-only pots subjected to these treatments; we confirmed that our watering treatments created a gradient in mean soil moisture over the duration of the experiment (Figure C.1). We measured out and supplied all water manually. Water was measured in milliliters and converted to millimeters supplied per unit area for reporting and analyses.

We initiated the experiment by planting seeds on November 8, 2022 and adding 28 mm of water to all pots the following day. We started phase 0 of the experiment one week later on November 16. During the first week of phase 1, we thinned down focal germinants in the center of each pot to a maximum of three individuals. We subsequently thinned these individuals down to a single focal individual per pot during the third week of phase 1. Upon the start of phase 2 on January 22, 2023, we estimated the density (number of individuals per pot, N) of species in all pots. Throughout the remaining duration of the experiment, we estimated the fecundity (F) of focal individuals as they started to show signs of senescence. When possible, we estimated fecundity for up to two additional individuals per pot; these extra individuals were located at 5 cm from the pot center in opposite directions along a randomly selected angle. To estimate fecundity, we counted the number of observed and emerging reproductive structures, then multiplied these counts by the number of seeds per structure (one seed per floret for *F. microstachys*, two seeds per flower for *P. erecta*). Note that *F. microstachys* and *P. erecta* are both capable of self-pollination (Kannenberg and Allard 1967, Bassett and Crompton 1968, Adams and Allard 1982, Espeland and Rice 2007). The pots in which no background seeds were planted were used to estimate fecundity in the absence of neighbors. After estimating fecundity in a pot, we harvested the aboveground biomass of the focal individual(s) and background neighborhood. Greenhouse conditions were maintained throughout the experiment with means ± one standard deviation as follows: temperature = 22 ± 1.7 °C, relative humidity = 41 ± 12 %, daily peak (10 am–2 pm) photosynthetically active radiation = 174 ± 145 µmol/m^2/s (Figure C.2, Figure C.3). Previous work has demonstrated that our focal species grow well under these greenhouse conditions with the same soil mix (Kandlikar et al. 2020).

3.3.3 Competition model

To characterize the competitive population dynamics of our focal species, we used the experimental data to parameterize a model of annual plant competition. We started with the following model (Cohen 1966, MacDonald and Watkinson 1981, Chesson 1990):

$$\frac{N_{i,t+1}}{N_{i,t}} = (1 - g_i)\, s_i + g_i F_i \tag{3.1}$$

$$F_i = \frac{\lambda_i}{1 + \alpha_{ii} g_i N_{i,t} + \alpha_{ij} g_j N_{j,t}} \tag{3.2}$$

where $N_{i,t}$ is population density in year t, g_i is germination rate, s_i is annual seed survival rate, and F_i is lifetime fecundity, all for species i. Equation 3.2 follows the functional form described by Beverton and Holt (1957), where λ_i is intrinsic fecundity (i.e., fecundity in the absence of density-dependence), α_{ii} is the per capita effect of species i on itself, and α_{ij} is the per capita effect of species j on species i. That is, fecundity (F_i) is reduced from λ_i according to the per capita competitive effects (α_{ii}, α_{ij}) and germinated densities ($g_i N_{i,t}$, $g_j N_{j,t}$) of intra- and interspecific competitors. This model has been shown to describe population dynamics in annual plant communities well, both phenomenologically (Levine and HilleRisLambers 2009) and mechanistically (Stouffer 2022, Van Dyke et al. 2024). As germination occurred during phase 0 of our experiment prior to initiating treatment-specific watering regimes, we focused on analyzing fecundity and its role in population dynamics using a simplified version of this model (cf. Germain et al. 2016):

$$\frac{N_{i,t+1}}{N_{i,t}} = F_i \tag{3.3}$$

$$F_i = \frac{\lambda_i}{1 + \alpha_{ii} N_{i,t} + \alpha_{ij} N_{j,t}} \tag{3.4}$$

which amounts to assuming that $g_i = 1$ (i.e., all seeds germinate each year) in Equations 3.1 and 3.2. In the right-hand side of Equation 3.4, the numerator (λ_i) is the demographic response to the environment and the denominator ($1 + \alpha_{ii} N_{i,t} + \alpha_{ij} N_{j,t}$) is the effect of competition, both in terms of fecundity.

We used Bayesian statistical models to estimate the parameters of Equation 3.4 (λ_i, α_{ii}, α_{ij}) as functions of water supply in our experiment (Figure C.4). We modeled fecundity, F, as following a negative binomial distribution:

$$F \sim \text{NegBinomial}\left(\mu, \phi\right) \tag{3.5}$$

where μ is the mean parameter that represents expected fecundity and ϕ is the shape parameter that controls overdispersion. Following Equation 3.4, we defined μ as:

$$\mu = \frac{\lambda_k}{1 + \alpha_{k1} N_1 + \alpha_{k2} N_2} \tag{3.6}$$

where N_1 and N_2 are the densities of each species ($k = 1,\ 2$). In light of evidence that plants exhibit nonlinear (e.g., unimodal) demographic (e.g., Esch et al. 2018, Tittes et al. 2019, Pearse et al. 2020) and physiological (e.g., Galmés et al. 2007, Monroe et al. 2021) responses to water availability, we modeled intrinsic fecundity, λ, for each species as a quadratic function of total water supply, w:

$$\log(\lambda) = \gamma_\lambda + \beta_{\lambda,1} w + \beta_{\lambda,2} w^2 + \gamma_{\text{block}} + \gamma_{\text{pot}} \tag{3.7}$$

where γ_λ is an intercept and $\beta_{\lambda,1}$, $\beta_{\lambda,2}$ are slope coefficients. γ_{block} and γ_{pot} are block- and pot-level random intercepts, respectively. We included random intercepts here because λ is effectively the intercept term of the nonlinear model for fecundity (Equations 3.4 and 3.6). Each random intercept was hierarchically modeled as following a zero-centered normal distribution with a standard deviation of σ_{block} or σ_{pot}:

$$\gamma_{\text{block}} \sim \text{Normal}(0, \sigma_{\text{block}}) \tag{3.8}$$

$$\gamma_{\text{pot}} \sim \text{Normal}(0, \sigma_{\text{pot}}) \tag{3.9}$$

For the purpose of model fitting, w and w^2 were the first- and second-degree terms of an orthogonal polynomial returned by the function `poly(x = W, degree = 2)` in R (R Core Team 2024), scaled by a factor of 10 so that both terms were approximately $[-0.5,\ 0.5]$, where `W` is a vector of log-transformed total water supply. Total water supply was derived for each treatment, regardless of when fecundity was estimated in each pot, in order to most closely align this predictor variable with regional rainfall data that the treatments were based on.

Next, we modeled competition coefficients, α, for each species pair as a linear function of total water supply, w:

$$\log(\alpha) = \gamma_{\alpha} + \beta_{\alpha} w \tag{3.10}$$

where γ_{α} is an intercept and β_{α} is a slope coefficient. Finally, we allowed ϕ to vary for each species as a linear function of w:

$$\log(\phi) = \gamma_{\phi} + \beta_{\phi} w \tag{3.11}$$

where γ_{ϕ} is an intercept and β_{ϕ} is a slope coefficient. Equation 3.11 allows observed fecundity to be more or less variable depending on water supply. The log link functions in Equations 3.7, 3.10, and 3.11 constrain μ and ϕ to be positive as required by the negative binomial distribution. They also constrain λ and α to be positive, where $\alpha > 0$ represents a competitive (as opposed to facilitative) effect of neighbors. The assumption of competition between *F. microstachys* and *P. erecta* is supported by previous work with these species (e.g., Van Dyke et al. 2022). We also fit models with alternative functional forms for fecundity (Equations 3.4 and 3.6) (Table C.2). These alternative models were at best equivalent to our main model in terms of predictive performance, evaluated via approximate leave-one-out cross-validation (Vehtari et al. 2017, Vehtari et al. 2024a), and did not significantly alter our results.

We implemented all Bayesian statistical models using Stan (Stan Development Team 2024) via `cmdstanr` (Gabry et al. 2024). For each model, we ran four chains of Stan's main Markov chain Monte Carlo algorithm with 10,000 iterations (5,000 warmup, 5,000 sampling) per chain, resulting in 20,000 posterior samples. We used weakly informed priors (see Appendix S1) based on previous work with our focal species (Godoy et al. 2014, Kraft et al. 2015b, Van Dyke et al. 2022) to keep parameters within plausible ranges. Additional details of our statistical models are provided in Appendix S1.

3.3.4 Invasion analysis

To evaluate the persistence and coexistence of our focal species under different levels of water supply, we used the experimentally parameterized population dynamics model to conduct invasion analyses (Chesson 2000b, Grainger et al. 2019b). We first asked whether each species is able to increase from low density in the absence of neighbors. To this end, we simulated one year of population growth starting with a single individual ($N_t = 1$), then computed the low-density population growth rate (LDGR) as $r_0 = \log(N_{t+1}/N_t)$. Here, the subscript 0 denotes that r is computed in the absence of neighbors. The invading population is expected to successfully establish and persist in the absence of neighbors if $r_0 > 0$. Next, we asked whether each species is able to invade a resident community of the other species. For example, we simulated *P. erecta* to equilibrium population density, then invaded a single individual of *F. microstachys* into this resident community and computed the LDGR (r_1, where the subscript 1 denotes the presence of neighbors). Stable coexistence is expected if $r_1 > 0$ for both species. Finally, we computed the effect of neighbors on LDGR as $\Delta r = r_0 - r_1$; this quantity represents the magnitude by which the resident community reduces LDGR (note that r is defined on the natural logarithmic scale, so this is a multiplicative effect). Thus, we take Δr to be a theoretically justified measure of the total effect of competition on population persistence. We repeated the above simulations for each species under a range of total water supply conditions. Following previous studies of plant species coexistence grounded in modern coexistence theory (e.g., Godoy and Levine 2014, Kraft et al. 2015b, Germain et al. 2018, Matías et al. 2018, Wainwright et al. 2019, Van Dyke et al. 2022), we also decomposed LDGRs into niche differences that stabilize coexistence and fitness differences that drive competitive exclusion (see Appendix S2 for details). We fully propagated uncertainty in model parameter estimates by repeating these analyses for every sample from the posterior distribution. We conducted analyses using R version 4.4.1 (R Core Team 2024).

3.4 Results

3.4.1 Fecundity without neighbors

The focal species exhibited distinct responses to water supply treatments that emulated the growing season rainfall across their geographic ranges (Figure 3.2, Table 3.1). In the absence of neighbors, fecundity of *Festuca microstachys* peaked at a total water supply of ~650 mm and decreased toward either end of the water supply gradient. In contrast, *Plantago erecta* displayed elevated fecundity under conditions of limited water supply, but exhibited little variation in fecundity across the majority of this gradient. *F. microstachys* had a higher fecundity than *P. erecta* in all but the driest conditions (< ~150 mm), with over a 10-fold difference in fecundity between species across much of the water supply gradient (> ~300 mm).

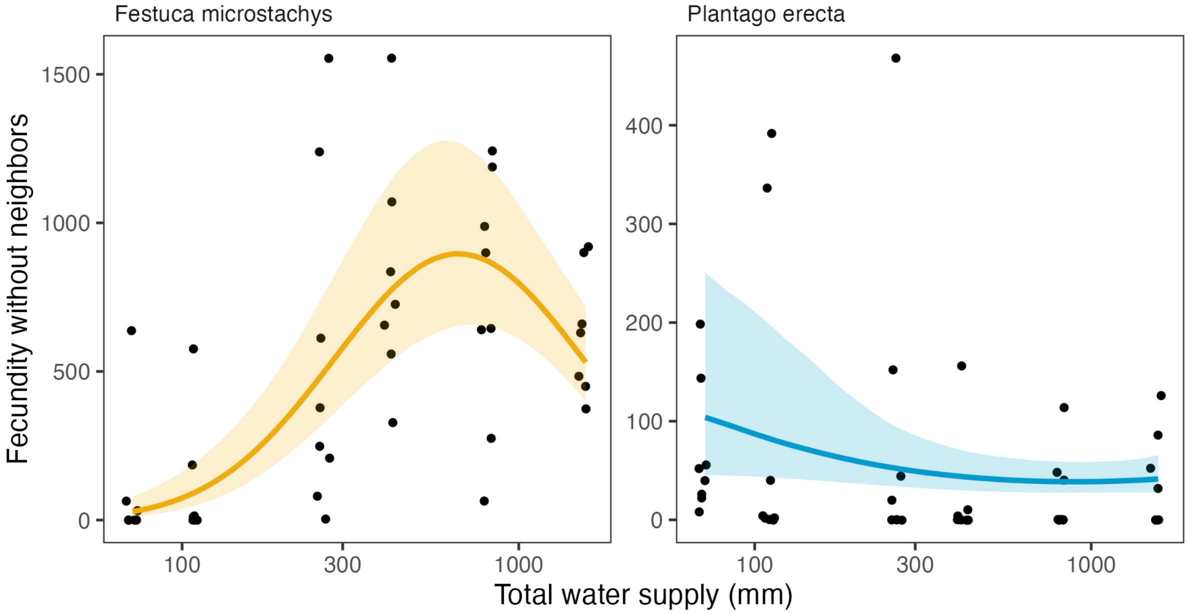

Figure 3.2: Responses of fecundity to total water supply in the absence of neighbors. Solid lines represent posterior medians of expected fecundity. Shaded areas represent 95% quantile credible intervals. Data points are jittered horizontally for visualization. Note that x-axes are shown on the $\log_{10}$ scale.

Table 3.1: Estimated predictor terms for the parameters of our main competition model as defined in Equations 3.7 and 3.10. λ_i is intrinsic fecundity, α_{ii} is the intraspecific competition coefficient, and α_{ij} is the interspecific competition coefficient for species i. Credible intervals are reported as 95% highest-density continuous intervals alongside the probability of direction (Pr, the posterior probability in $[0.5,\ 1]$ that the estimated value is in a given direction above or below 0), computed using `ggdist` (Kay 2024a, 2024b) and `bayestestR` (Makowski et al. 2019).

Species (*i*)	**Parameter**	**Term**	**Median**	**95% CI**	**Pr**
Festuca microstachys	λ_i	γ_λ	6.35	[5.58, 7.33]	1.000
		$\beta_{\lambda,1}$	2.00	[-0.22, 3.81]	0.953
		$\beta_{\lambda,2}$	-1.78	[-2.31, -1.22]	1.000
	α_{ii}	γ_α	-0.07	[-0.98, 0.95]	0.559
		β_α	-2.26	[-4.49, -0.31]	0.993
	α_{ij}	γ_α	-3.29	[-5.18, -1.68]	1.000
		β_α	-1.02	[-4.93, 3.10]	0.702
Plantago erecta	λ_i	γ_λ	4.15	[3.67, 4.78]	1.000
		$\beta_{\lambda,1}$	-1.36	[-3.24, 0.15]	0.980
		$\beta_{\lambda,2}$	0.61	[-0.10, 1.44]	0.959
	α_{ii}	γ_α	-3.52	[-4.70, -2.45]	1.000
		β_α	-5.98	[-9.63, -2.58]	1.000
	α_{ij}	γ_α	-1.19	[-1.87, -0.46]	0.996
		β_α	-3.88	[-6.30, -1.84]	1.000

3.4.2 Per capita effects of competition

Per capita competitive effects (α) tended to be strongest when water supply was more limited, although this relationship varied by species and intra- versus interspecific competition (Figure 3.3, Table 3.1). We found that the per capita effect of competition decreased with increasing water supply for three of four competition coefficients: intraspecific effects for both species and the interspecific effect of *F. microstachys* on *P. erecta* ($\Pr(\beta_\alpha < 0) > 0.99$; however, note that $\Pr(\beta_\alpha < 0) = 0.954$ for the per capita effect of *F. microstachys* on itself with alternative model 2, Table C.3). These competition coefficients varied by over 2–3 orders of magnitude across the entire water supply gradient. This relationship was uncertain for the per capita effect of *P. erecta* on *F. microstachys* (median $\beta_\alpha = -1.02$, $\Pr(\beta_\alpha < 0) = 0.702$, Table 3.1).

Intraspecific competition was generally stronger than interspecific competition for *F. microstachys*, whereas the opposite was true for *P. erecta* (Figure 3.3). We found evidence that intraspecific competition decreased more sharply than interspecific competition in response to increasing water supply for *P. erecta* (median $\Delta\beta_\alpha = -2.00$, $\Pr(\Delta\beta_\alpha < 0) = 0.953$, where $\Delta\beta_\alpha$ is the slope for the intraspecific competition coefficient minus the slope for the interspecific competition coefficient; note that $\Pr(\Delta\beta_\alpha < 0) > 0.98$ with alternative models 2–3). Such an interaction between water supply and type of competition was not clearly supported for *F. microstachys* (median $\Delta\beta_\alpha = -1.27$, $\Pr(\Delta\beta_\alpha < 0) = 0.811$).

3.4.3 Low-density population growth rates and total effects of competition

The distinct responses of species to water supply in terms of both intrinsic fecundity and per capita competitive effects resulted in variable low-density population growth rates (LDGRs) and coex-

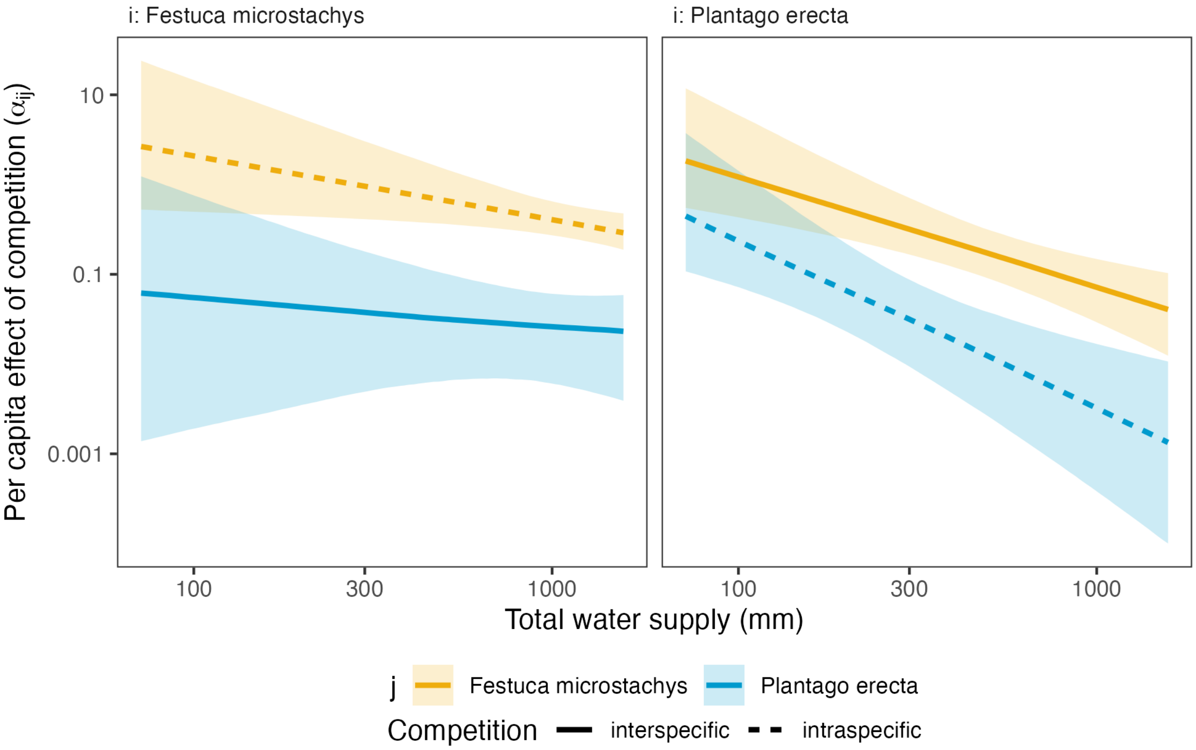

Figure 3.3: Variation in per capita competitive effects (α_{ij}) in response to total water supply. For each species (i), estimated relationships for both interspecific ($i \neq j$, solid lines) and intraspecific ($i = j$, dashed lines) competition coefficients are shown in the same panel. Solid lines represent posterior medians. Shaded areas represent 95% quantile credible intervals. Note that both x- and y-axes are shown on the $\log_{10}$ scale.

istence outcomes across the water supply gradient (Figure 3.4). As described for fecundity (Figure 3.2), LDGR peaked at intermediate water supply for *F. microstachys* and at low water supply for *P. erecta* in the absence of competitors. Both species were expected to persist under all water supply levels (in greenhouse conditions) as isolated populations (Figure 3.4a). However, competitors significantly altered these LDGRs, thereby impacting population persistence and species coexistence (Figure 3.4b). *F. microstachys* was able to increase from low density in the presence of a resident community of *P. erecta*. In contrast, *P. erecta* was unable to increase from low density with *F. microstachys* at resident state in all but the driest conditions (Pr$(r_1 < 0)$ > 0.975 from > ~125 mm). Taken together, invasion analyses showed that these species can coexist when water supply is limited, but that *F. microstachys* is expected to competitively exclude *P. erecta* as water supply increases. Interestingly, we also found that priority effects were plausible (up to nearly equally as likely as competitive exclusion) at the wettest end of the gradient, as signified by mutual noninvasibility of each species into a resident community of the other species (Mordecai 2011, Fukami 2015, Ke and Letten 2018, Grainger et al. 2019a).

Our invasion analyses allowed us to quantify the total effect of competition on population persistence as the reduction in LDGR due to the presence of competitors (Δr). This total effect of competition varied in response to water supply differently for each species (Figure 3.4c). The total effect of competition on LDGR of *F. microstachys* increased with increasing water supply. In contrast, the total effect of competition on LDGR of *P. erecta* peaked at ~350 mm, closely mirroring differences in density-independent fecundity (Figure C.5c) and resulting fitness differences between the focal species (Figure C.5b). The total effect of competition on *P. erecta* was similar at the driest and wettest ends of the water supply gradient.

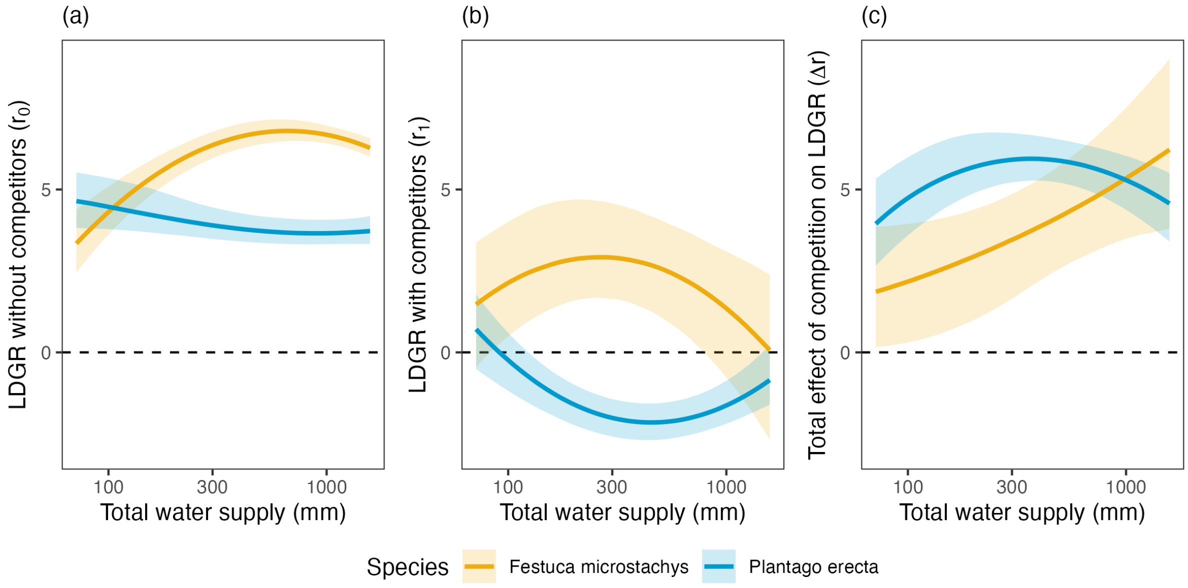

Figure 3.4: Variation in low-density population growth rates (LDGRs) in response to total water supply. LDGR was computed for each species (yellow = *F. microstachys*, blue = *P. erecta*) either in the absence of neighbors (r_0, a) or in the presence of a resident community of the other species (r_1, b). The total effect of competition on population persistence was computed as the difference between LDGRs in the absence versus presence of neighbors ($\Delta r = r_0 - r_1$, c). Solid lines represent posterior medians. Shaded areas represent 95% quantile credible intervals. Note that x-axes are shown on the $\log_{10}$ scale.

3.5 Discussion

Variation in the strength of competitive interactions along environmental gradients is a key ingredient of many fundamental theories in ecology and biogeography (Dobzhansky 1950, MacArthur 1972, Chesson 1994, 2000a, Bertness and Callaway 1994, Schemske et al. 2009). While the environmental context-dependence of competitive population dynamics has received much attention in recent years (e.g., Germain et al. 2018, Matías et al. 2018, Wainwright et al. 2019, Van Dyke et al. 2022, Cervantes-Loreto et al. 2023), motivated in large part by the ever-increasing risk of climate change (Gilman et al. 2010, HilleRisLambers et al. 2013, Alexander et al. 2016), a detailed understanding of when and how competition impacts population persistence and coexistence along geographic-scale abiotic gradients remains elusive (but see e.g., Armitage and Jones 2019, McGuire 2023, Sunday et al. 2024). In particular, dissecting how different sources of variation in competition contribute to population and range dynamics is crucial for forecasting the future of biodiversity (Louthan et al. 2015, Jones and Gilbert 2016). Here, we addressed this knowledge gap by experimentally quantifying the demography and competition of an annual grass and forb across a geographically relevant water supply gradient. Notably, we show that asymmetric demographic responses of species to water supply decouple the per capita effects of competition from the total effects of competition exerted by a resident community. This distinction between how species interact at the individual level and impact one another at the community level has important implications for our understanding of how competition shapes ecological communities, species distributions, and resulting patterns of biodiversity along abiotic gradients.

3.5.1 Contrasting per capita versus total effects of competition

We found strong support for the hypothesis that the per capita effect of competition is stronger when water supply is more limited, meaning that individual plants compete more strongly for this limiting resource in drier conditions. With the exception of the effect of *Plantago erecta* on *Festuca microstachys*, we observed a decrease in the per capita strength of intra- and interspecific competition with increasing water supply (Figure 3.3, Table 3.1). We also found that, at least for *P. erecta* as the focal species, the strength of intraspecific competition decreased more rapidly than interspecific competition in response to increasing water supply. In accordance with elevated self-limitation under low water supply, these species were most likely to coexist at the driest end of the water supply gradient (Figure 3.4b, Figure C.6), despite this being where the per capita competitive effect of *F. microstachys* on *P. erecta* was at its highest.

This work represents a novel empirical analysis of continuous variation in species-specific competition coefficients along a large-scale water supply gradient. Our finding that intraspecific competition is more sensitive to this abiotic gradient than interspecific competition supports the pursuit of variation in conspecific negative density dependence as a primary driver of biodiversity patterns (Schemske et al. 2009, LaManna et al. 2017, Hülsmann et al. 2021). However, given evidence that intra- and interspecific competition can respond differently to the same abiotic gradient, quantifying just one component of competition cannot fully reveal how competition shapes patterns of species coexistence and biodiversity. Emerging methods for estimating competition coefficients in species-rich communities may enable more widespread characterization of the differential responses of per capita competition to abiotic gradients (Weiss-Lehman et al. 2022). Note that in our model, slopes that describe the response of competition coefficients to water supply, β_α, are defined on a logarithmic scale (Equation 3.10). Therefore, the intraspecific competition coefficient for *F. microstachys* and the interspecific competition coefficient for *P. erecta* (top lines in Figure 3.3) exhibited larger absolute differences between the dry and wet ends of the water supply gradient than their respective counterparts for inter- and intraspecific competition. More work is needed to resolve potential functional forms of the relationship between competition coefficients and abiotic gradients and to explore their consequences for species coexistence in variable environments.

Asymmetries between species in density-independent demographic performance also play an important role in shaping coexistence outcomes (Chesson 2000b). These demographic asymmetries, coupled with per capita competitive effects, determine the total competitive effect of the resident community on population growth. Here, we found that the total effect of competition on low-density population growth rates (LDGRs; Figure 3.4c) did not simply mirror variation in the strength of per capita competition (Figure 3.3). Rather, the total effect of competition experienced by *P. erecta* was more closely aligned with interspecific differences in fecundity in the absence of neighbors (Figure 3.2, Figure C.5c). Strikingly, the total effect of competition exerted by a resident community of *P. erecta* on *F. microstachys* increased with increasing water supply, even in the absence of a corresponding increase in the per capita strength of interspecific competition. This relationship may be driven in part by priority effects at the wettest end of the water supply gradient, where a high density of resident *P. erecta* possibly preempts resources or modifies local abiotic conditions in ways that prevent the invasion of *F. microstachys* (Fukami 2015). Taken together, we found partial support for the hypothesis that the total effect of competition is stronger in environments that support higher intrinsic demographic performance of competitors. Our results exemplify how different mechanisms of competition (e.g., effect per interactor, effect of density, see also Louthan et al. 2015) interact to create complex patterns of total competition along abiotic gradients.

The stress-gradient hypothesis predicts that the frequency or intensity of competition decreases with increasing abiotic stress, in turn giving way to more facilitative interactions (Bertness and Callaway 1994, Louthan et al. 2015). Although this hypothesis has received mixed support over the years (Maestre et al. 2005, 2009, Lortie and Callaway 2006, Adams et al. 2022), it is nonetheless an important framework for studying variation in species interactions along abiotic gradients. The results of our study provide theoretically grounded insights into how an important abiotic gradient mediates such variation in competition. For example, we can identify aridity, and to a lesser extent an excess of water, as "stressful" conditions for *F. microstachys* on the basis that fecundity in the absence of neighbors is reduced toward either end of the water supply gradient (Figure 3.2). Water limitation in particular is often identified as a major source of abiotic stress in plant communities (e.g., Callaway et al. 2002, Maestre et al. 2005, Armas et al. 2011, Louthan et al. 2018). On one hand, that *F. microstachys* experiences stronger per capita intraspecific competition when water supply is more limited appears to be inconsistent with the stress-gradient hypothesis (Figure 3.3). On the other hand, this conclusion is reversed when considering that the total effect of competition experienced by *F. microstachys* is greater under increased water supply (Figure 3.4c). Thus, the stress-gradient hypothesis is simultaneously supported and contradicted by our results depending on how competition is quantified. This shows that distinguishing between the per capita versus total effects of competition is essential when considering how competition varies along abiotic gradients.

3.5.2 An alternative perspective: niche and fitness differences

Modern coexistence theory allows the determinants of species coexistence to be decomposed into niche differences that stabilize coexistence and fitness differences that drive competitive exclusion (Chesson 2000b). These quantities have been used to analyze how the abiotic environment alters plant species coexistence (e.g., Germain et al. 2018, Matías et al. 2018, Wainwright et al. 2019, Van Dyke et al. 2022) and can offer insights into the role of competition in shaping species distributions (Alexander et al. 2018). Computing niche and fitness differences for our focal species complemented our invasion analyses, most notably by revealing that fitness differences are greatest at intermediate water supply (~350 mm; Figure C.5b, Figure C.6) where the total effect of competition on *P. erecta* is largest. While fitness differences are the product of species' differences in demography and sensitivity to competition (see Appendix S2 for details), asymmetric fecundity of *F. microstachys* and *P. erecta* was especially strongly reflected in their fitness differences and total competitive effects along the water supply gradient (Figure C.5c). We also observed a trend toward reduced niche differences with increasing water supply (Figure C.5a; Figure C.6); this is qualitatively consistent with results of a previous field experiment that quantified niche and fitness differences for our focal species under ambient and reduced rainfall treatments (Van Dyke et al. 2022). Overall, these results highlight how fitness asymmetries can play a critical role in shaping competition and coexistence along environmental gradients.

3.5.3 Limitations and future directions

Our study reveals the complex interplay between intrinsic demography, per capita versus total competition, and coexistence of annual plants by emulating a geographic-scale rainfall gradient in a greenhouse setting. While this approach allowed us to feasibly track an entire generation of population dynamics across a wide range of abiotic conditions, there are important limitations to consider. Chief among these is that we are isolating a single axis of environmental variation in a controlled environment. In particular, water supply is expected to interact with temperature and soil properties to shape plant demography and competition in natural landscapes, especially in shallow serpentine soils with limited water holding capacity (Adams et al. 2009, Damschen et al. 2011, Fernandez-Going et al. 2012, Harrison et al. 2015, Butterfield et al. 2016, Midolo and Wellstein 2020). Moreover, the grasslands where our focal species occur not only host a diversity of native plant species but also are heavily invaded by Mediterranean grasses (e.g., *Avena* spp., *Bromus* spp.) (D'Antonio et al. 2007, Baldwin 2014). These abiotic and biotic factors unaccounted for in our experiment make it difficult to extrapolate from our competition model to predict species' distributions in geographic space. Future studies could look toward more mechanistic models of water competition to help bridge this gap (e.g., Levine et al. 2022).

In characterizing variation in demography and competition along a water supply gradient, we have focused here on understanding how competitive population dynamics differ under an array of fixed abiotic conditions. However, spatial and temporal fluctuations in the abiotic environment can also promote species coexistence (Chesson 1994, 2000a). Indeed, similar to how we found that *F. microstachys* is expected to competitively exclude *P. erecta* across much of our water supply gradient (Figure 3.4), many studies have found that any one abiotic context often fails to allow for the coexistence of naturally co-occurring species (e.g., Kraft et al. 2015b, Wainwright et al. 2019, Van Dyke et al. 2024). In California grasslands, annual rainfall variability has been shown to maintain coexistence of a dominant grass and forb (Hallett et al. 2019). Additionally, even species with broad-scale range overlap may occupy different habitats at finer spatial scales. Gram et al. (2004) identified *F. microstachys* (formerly *Vulpia microstachys*) as associated with serpentine hummocks and *P. erecta* as associated with transitional habitat between hummocks and grassland matrix. This suggests that fine-scale spatial environmental variation could contribute to the coexistence of our focal species. Quantifying these fluctuation-dependent coexistence mechanisms will provide a more complete picture of how competition shapes species coexistence and distributions in a dynamic world.

3.5.4 Conclusions

Understanding how the abiotic environment drives variation in the strength of competitive interactions is a fundamental challenge in ecology and biogeography. In this study, we leveraged an experimentally tractable California annual plant system to reveal contrasting effects of per capita (individual-level) and total (community-level) competition on population persistence along a large-scale water supply gradient. Whereas the per capita strength of competition was generally highest in arid conditions, fitness asymmetries between species contributed to a greater total effect of competition at intermediate to high water supply. Consequently, coexistence was most likely in arid conditions. This decoupling of per capita versus total competitive effects highlights the need to clearly distinguish between different mechanisms of competition in terms of their contributions to coexistence, species distributions, and resulting patterns of biodiversity. More broadly, our results provide theoretically grounded insights into how shifting rainfall regimes may have complex direct and indirect effects on plant populations and communities.

3.6 Acknowledgments

We acknowledge the Gabrielino/Tongva peoples as the traditional land caretakers of Tovaangar (Los Angeles basin, So. Channel Islands), where UCLA is located. We acknowledge the Chumash peoples as the traditional land caretakers of the area where we collected seeds for this study. We thank M. Van Dyke for seed collection. We thank S. Catella, S. Grimbert, R. McGuire, F. Negrete, M. Ochoa, and E. Purington for assistance with the greenhouse experiment. We thank UCLA Plant Growth Center staff, especially Weimin Deng, for support in the greenhouse. We are grateful to A. Angert, L. Glevanik, E. Ordway, and M. Tingley for insightful comments on the manuscript. We are also grateful to H. Carroll, A. Cisneros Carey, C. Kremer, M. Sagarin, K. Schneider, M. Van Dyke, and J. Yanowitz for discussions that helped improve the experiment and manuscript. This work was supported by National Science Foundation grants (DEB 1644641, DEB 2022810) and a UCLA EEB Departmental Research Grant.

Appendix A

Supplementary materials for Chapter 1

A.1 Appendix S1: Study landscape and soil environment

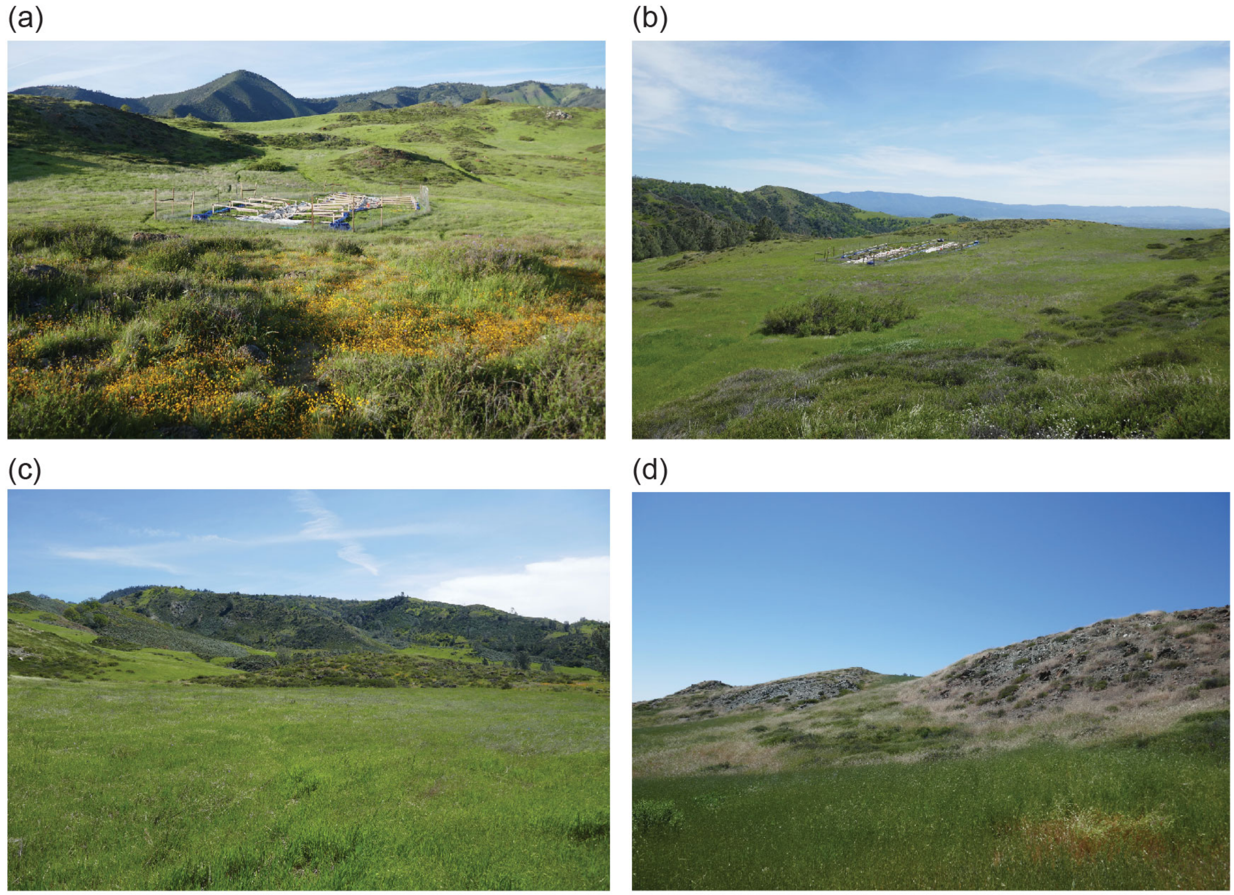

Figure A.1: Photographs of the study landscape taken facing (a) north, (b) south, (c) east, and (d) west in April 2019. Note that the enclosure visible in (a, b) is not part of this study. Photo credit: Kenji Hayashi.

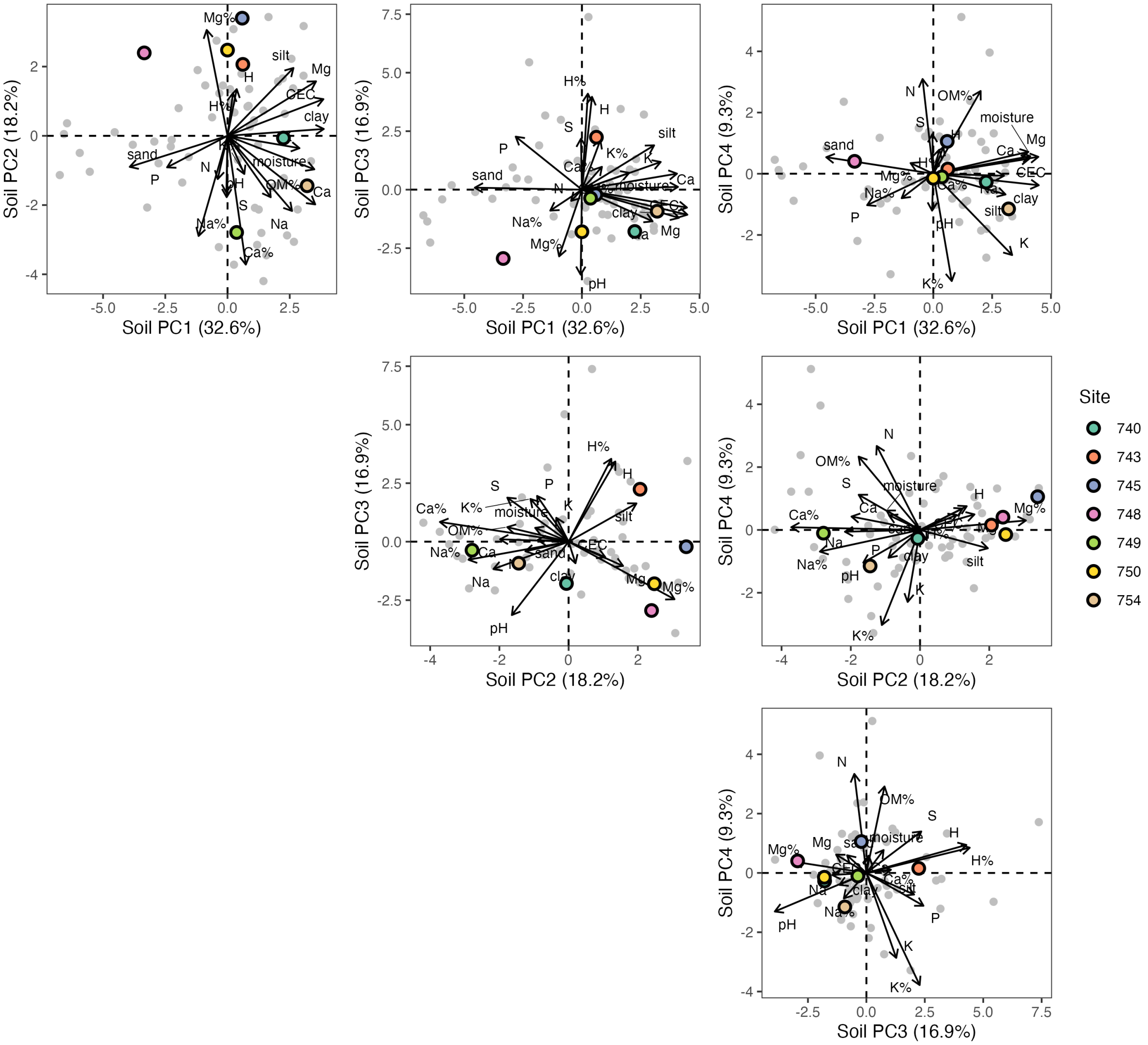

Figure A.2: Principal component analysis (PCA) of soil variables at study sites. The first four axes, corresponding to 77% of cumulative variance explained, are shown here. Colored points represent experimental sites. Gray points represent survey sites. Arrows represent the loadings of individual soil variables with respect to each axis. The percentage of variance explained by each axis is given in parentheses.

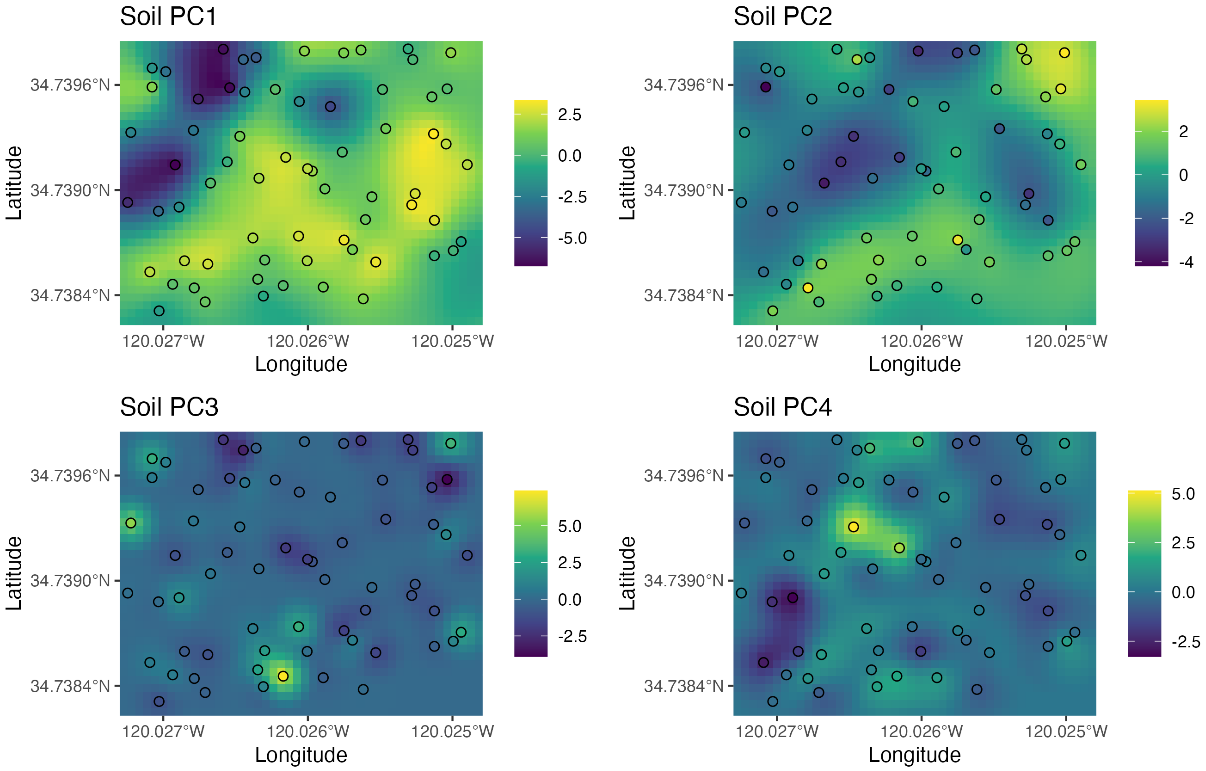

Figure A.3: Interpolated maps of soil principal component axes for the study landscape. Maps were generated by performing ordinary kriging with a spherical variogram model using `gstat` (Pebesma 2004, Gräler et al. 2016). Points represent the sites at which soil samples were collected and are colored according to their principal component scores.

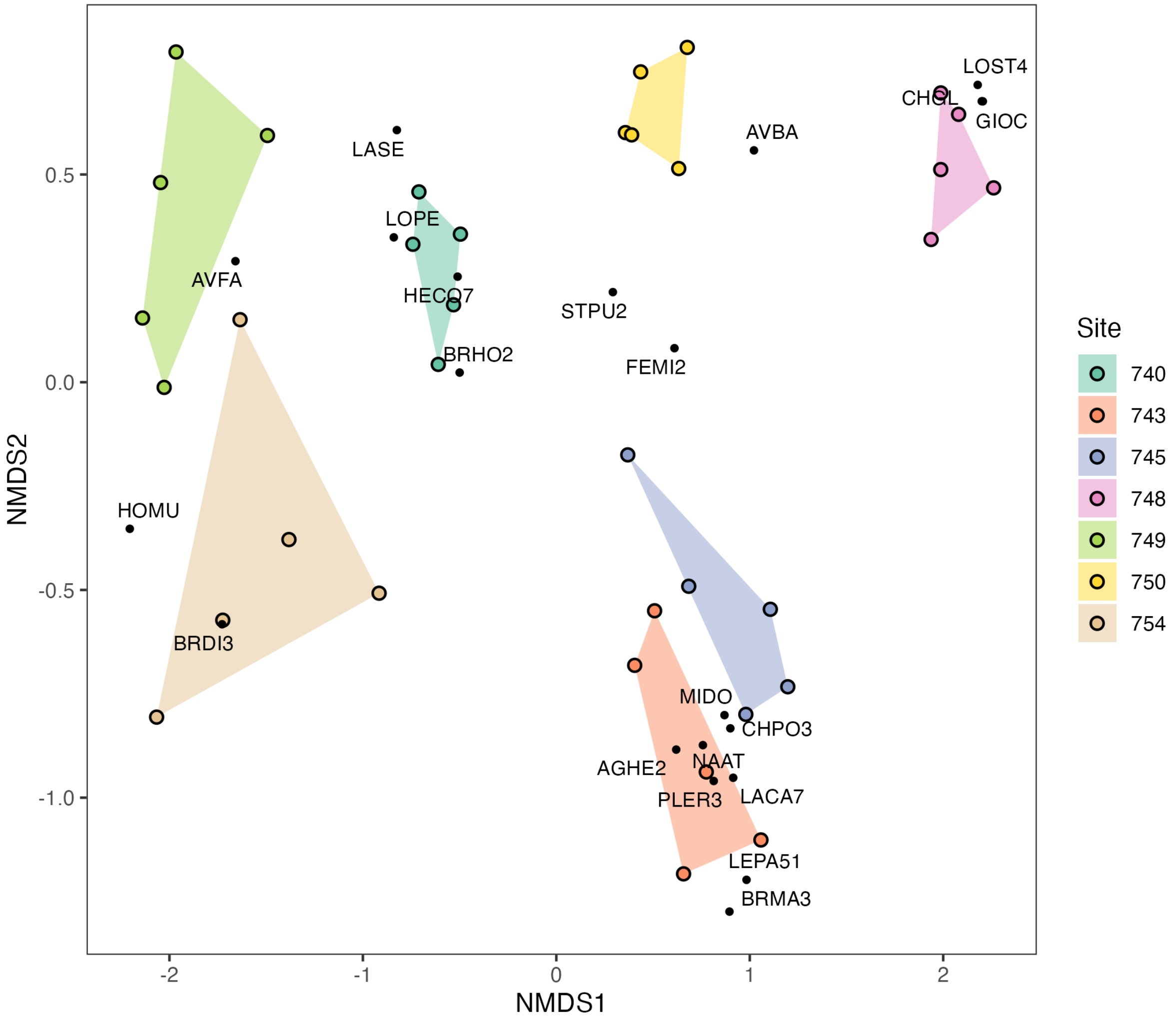

Figure A.4: Nonmetric multidimensional scaling (NMDS) for plant species cover at experimental sites. NMDS was performed using `vegan` (Oksanen et al. 2024) with Bray-Curtis dissimilarity and k (number of dimensions) = 2. Cover data were collected at our experimental sites in 2017 (data from Kandlikar 2021, Kandlikar et al. 2022). Colored points correspond to replicate plots at each site. Black points correspond to the (expanded) weighted average scores for species with over 5% cover in any plot. Species are labeled with their symbols in the U.S. Department of Agriculture PLANTS Database.

Table A.1: Soil variables used in principal component analysis.

Variable	**Description**	**Units**
OM%	Organic matter content	%
P	Phosphorus content	ppm
K	Potassium content	ppm
Mg	Magnesium content	ppm
Ca	Calcium content	ppm
Na	Sodium content	ppm
H	Hydrogen content	meq/100g
pH	pH	none
CEC	Cation exchange capacity	meq/100g
K%	Potassium saturation	%
Mg%	Magnesium saturation	%
Ca%	Calcium saturation	%
Na%	Sodium saturation	%
H%	Hydrogen saturation	%
N	Nitrate-nitrogen (NO_3-N) content	ppm
S	Sulfate-sulfer (SO_4-S) content	ppm
sand	Sand content	%
silt	Silt content	%
clay	Clay content	%
moisture	Gravimetric water content	%

A.2 Appendix S2: Methods for estimating fecundity

We estimated the lifetime fecundity of focal individuals in our demographic experiment by counting the number of seeds produced by each individual. However, direct seed counts in the field were impractical for some species. For ACWR, CHGL, HECO, LACA, and URLI, we first counted the number of reproductive structures on each focal individual. For ACWR, we counted the number of seed pods. For CHGL, HECO, LACA, and URLI, we counted the number of inflorescences. Next, we collected and dissected ~40 of these reproductive structures for each species and calculated the mean number of seeds per reproductive structure (Figure A.5). Finally, we estimated fecundity for each focal individual by multiplying the number of reproductive structures by the mean number of seeds per reproductive structure.

For SACO, we measured the radius of all seed heads (approximated as circles) on each focal individual. We collected and dissected ~40 of these seed heads and counted the number of seeds per seed head. We then fit a negative binomial generalized linear model with the number of seeds per seed head as the response and seed head radius as the predictor (Figure A.6). We implemented this model using the `glm.nb` function in `MASS` (Venables and Ripley 2002) with the formula `seeds ~ radius`, where `seeds` is the number of seeds per seed head and `radius` is seed head radius. We used a negative binomial likelihood in anticipation of overdispersion that could arise from collecting seed heads from across sites. We used this model to predict the expected number of seeds for each seed head, then estimated fecundity for each focal individual as the sum of the expected number of seeds for all of its seed heads.

We also considered a model in which seed head area was used as the predictor of the number of seeds per seed head for SACO (formula: `seeds ~ area`, where `area` is seed head area). In both models, the predictor was centered and scaled to unit variance. We used Akaike Information Criterion (AIC) to compare alternative models and found that the radius model was estimated to have better predictive performance (Table A.2). Therefore, we used the radius model to estimate fecundity for SACO as described above.

For PLER, we counted the number of flowers (or fruits), where each flower (or fruit) was observed to produce two seeds. For FEMI, we directly counted the number of seeds. All fecundity estimates were rounded down to integer values (where applicable). All counts of seeds and reproductive structures included those that were still emerging or developing and traces of those that were already lost at the time of fecundity estimation. Fecundity for marked focal individuals that were confirmed or inferred to have experienced mortality prior to seed production were recorded as zero. For subplots in which no focal individuals were marked (e.g., due to germination failure) or focal individuals were lost (e.g., due to disturbances such as gopher damage), fecundity was recorded as missing and excluded from analyses. Following estimation of fecundity, we removed focal individuals from plots to minimize seed set from these individuals.

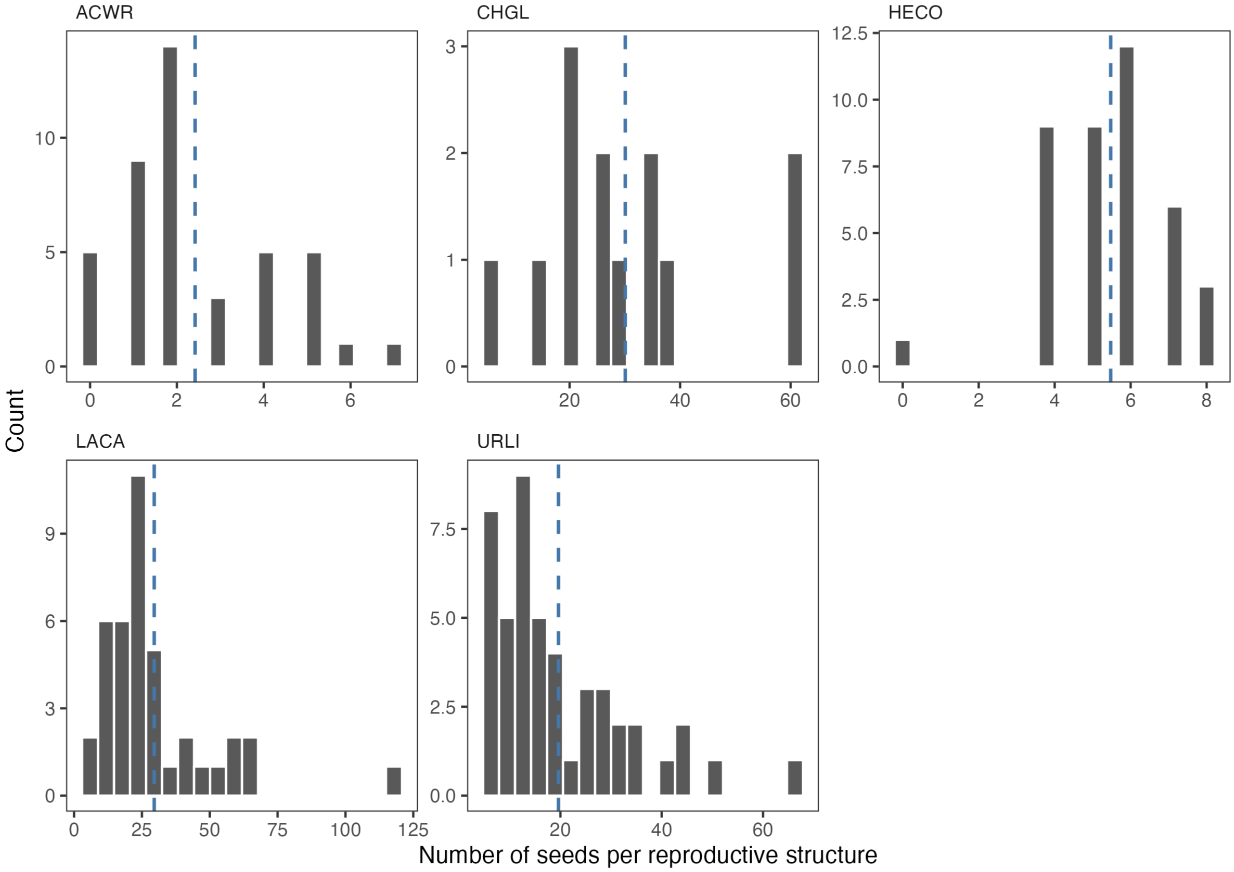

Figure A.5: Histograms of the number of seeds per reproductive structure for ACWR, CHGL, HECO, LACA, and URLI. Vertical dashed lines represent the mean value for each species.

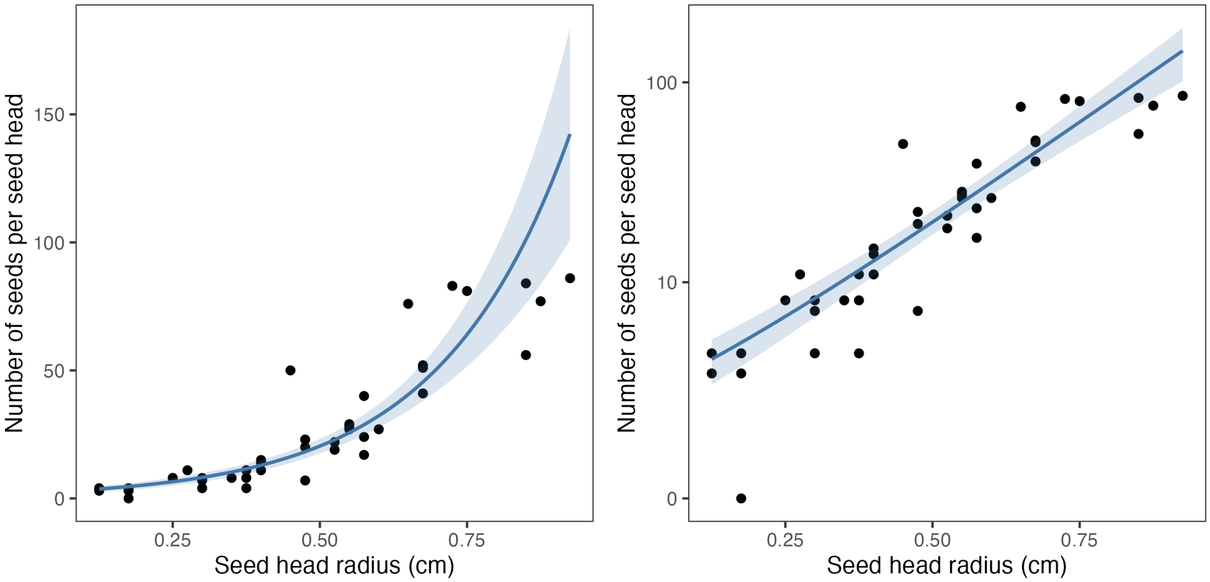

Figure A.6: Relationship between seed head radius and the number of seeds per seed head for SACO. The relationship is shown on both identity (left) and log (right) scales. Solid lines represent expected values. Shaded areas represent ± 1.96 SE around the expected values.

Table A.2: Comparison of models for the number of seeds per seed head for SACO. We used Akaike Information Criterion (AIC) to compare models with alternative predictors. The model selected for use in analyses is indicated with bold text.

Model	Predictor	AIC	ΔAIC
(2)	**Radius**	**285.89**	**0.00**
(1)	Area	302.60	16.71

A.3 Appendix S3: Analysis of demographic experiment

We used Bayesian hierarchical models to estimate the demographic responses of our focal species to the soil environment and competition. We started by fitting separate models for germination rate (g) and fecundity (F), which we then implemented jointly as a single model. We used this joint model, which we refer to as the *fitness model*, for all demographic analyses. We implemented all Bayesian models using Stan (Stan Development Team 2024) via `cmdstanr` (Gabry et al. 2024).

A.3.1 Germination model

We modeled the number of germinated seeds (n_i) for observation i = 1, …, 1,078 as following a beta-binomial distribution:

$$n_i \sim \text{Beta-Binomial}\left(N_i, \mu_i, \phi_i\right) \tag{A.1}$$

where N is the number of planted seeds, μ is the mean probability parameter, and ϕ is the precision parameter. This parameterization of the beta-binomial distribution follows that employed by `brms` (Bürkner 2017). Using a logit link function, we defined μ as:

$$\text{logit}\left(\mu_i\right) = \alpha_{\text{sp}_i,\text{trt}_i} + \sum_{j=1}^{4} \beta_{j,\text{sp}_i,\text{trt}_i} \times \text{PC}_{j,i} + \gamma_{\text{sp}_i,\text{trt}_i,\text{site}_i} \tag{A.2}$$

where α is an intercept and β_j is a slope for soil principal component axis j = 1, …, 4. α and β_j vary by species (sp = 1, …, 8) and neighborhood treatment (trt = 1, 2). That is, this linear model describes the response of expected germination rate (μ) to soil PC1–PC4 for each species in the presence (trt = 1) or absence (trt = 2) of neighbors. γ is a group-level (or "random") intercept that represents a site-specific deviation for each combination of species and treatment from the corresponding trend given by α and β_j. γ reflects our experimental design, wherein repeated measurements of $\{n, N\}$ were taken for each species and treatment at each site = 1, …, 7. γ was hierarchically modeled as:

$$\gamma_{\text{sp,trt,site}} \sim \text{Normal}\left(0, \sigma\right) \tag{A.3}$$

where σ is the standard deviation parameter that describes variation in γ. Finally, we allowed ϕ to vary by species as:

$$\phi_i = \alpha_{\phi,\text{sp}_i} \tag{A.4}$$

where α_ϕ is a species-specific intercept for ϕ.

We specified prior distributions for parameters as:

$$\alpha \sim \text{Normal}(0, 2) \tag{A.5}$$

$$\beta_j \sim \text{Normal}(0, 1) \tag{A.6}$$

$$\sigma \sim \text{Exponential}(1) \tag{A.7}$$

$$\alpha_\phi \sim \text{Exponential}(1) \tag{A.8}$$

Equation A.5, defined on the logit scale, translates to the probability scale as a roughly flat prior that assigns similar density to most values in $(0, 1)$. Equation A.6 was employed as a weakly regularizing prior that avoids assigning much density to strong relationships. Using (weakly) informative priors can be important for generalized linear (mixed) models with nonlinear (e.g., logit, log) link functions, where non-informative priors can imply nonsensical expectations (Wesner and Pomeranz 2021). Note that, for model fitting, raw values of soil PC1–PC4 (let these be x_j) were centered and scaled with respect to the mean ($\bar{x}_j$) and standard deviation (σ_{x_j}) of each axis across experimental sites: $\text{PC}_j = (x_j - \bar{x}_j)/\sigma_{x_j}$. For example, Equation A.6 implies that $\beta_j \approx -2$ and $\beta_j \approx 2$ correspond to around the 2.5% and 97.5% quantiles of this prior distribution, respectively. These slopes allow for nearly the entire possible range of expected germination rate (μ) to be traversed in response to four standard deviations of change along just a single axis (e.g., $\text{logit}^{-1}(-4) \approx 0.02$, $\text{logit}^{-1}(4) \approx 0.98$). Equation A.7 is a positive-constrained prior that implies variation in γ that is of similar magnitude as the expectations defined by Equations A.5 and A.6. Equation A.8 was chosen as a vague, positive-constrained prior for the species-specific precision parameter (ϕ). R code for conducting prior predictive simulations (Gabry et al. 2019, Wesner and Pomeranz 2021) is included as part of the archived data and code for this manuscript (Hayashi and Kraft 2024a).

We also considered a model in which a binomial likelihood function was employed. We used approximate leave-one-out cross-validation (LOO-CV) (Vehtari et al. 2017), implemented with `loo` (Vehtari et al. 2024a), to compare models based on their estimated out-of-sample predictive performance. We applied a moment matching correction as needed (specifically, if the Pareto k value for Pareto-smoothed importance sampling > 0.7) to improve the reliability of LOO-CV results (Paananen et al. 2021, Vehtari et al. 2024b). We considered models to differ in predictive performance if $|\Delta\text{ELPD}_{\text{LOO}}|/\text{SE}_{\Delta\text{ELPD}_{\text{LOO}}} > 2$, where $\Delta\text{ELPD}_{\text{LOO}}$ is the pairwise difference in the LOO estimate of expected log pointwise predictive density and $\text{SE}_{\Delta\text{ELPD}_{\text{LOO}}}$ is the standard error of this difference (see also Sivula et al. 2023). Here, we found that the beta-binomial model (described above) was estimated to have better predictive performance (Table A.13).

We fit all models using Stan's main Markov chain Monte Carlo sampling algorithm. For each model, we ran four Markov chains in parallel, each with 10,000 iterations (5,000 warmup, 5,000 sampling), yielding 20,000 posterior samples per model. This resulted in an effective sample size (ESS) of at least 10,000 for most parameters, which is the minimum ESS recommended by Kruschke (2015) for computing credible intervals at the 95% level. We used default options for the initial values and control parameters of the sampler. We assessed model convergence by first checking that the sampler produced no critical runtime warnings (e.g., divergent transitions after warmup). We then checked whether diagnostic quantities satisfied recommended criteria. In particular, we confirmed that the $\widehat{R}$ convergence diagnostic < 1.01 and the ratio of effective sample size to total sample size (N_{eff}/N) > 0.1 for all parameters (Vehtari et al. 2021, Stan Development Team 2022). Additionally, we inspected trace plots to confirm that Markov chains were well-mixed and stationary after warmup. We also conducted graphical posterior predictive checks (Gabry et al. 2019) to assess model fit.

A.3.2 Fecundity model

We modeled fecundity (F_i) for observation i = 1, …, 708 as following a zero-inflated negative binomial distribution:

If $F_i = 0$:

$$\text{Pr}\left(F_i \mid \theta_i, \mu_i, \phi_i\right) = \theta_i + (1 - \theta_i) \times \text{NegBinomial}\left(0 \mid \mu_i, \phi_i\right) \tag{A.9}$$

If $F_i > 0$:

$$\text{Pr}\left(F_i \mid \theta_i, \mu_i, \phi_i\right) = \left(1 - \theta_i\right) \times \text{NegBinomial}\left(F_i \mid \mu_i, \phi_i\right) \tag{A.10}$$

where θ is the probability of observing $F = 0$ from a zero-inflation process, and conversely, $(1-\theta)$ is the probability of observing $F \geq 0$ from a negative binomial process. μ is the mean parameter and ϕ is the shape parameter for the negative binomial distribution. Using a log link function, we defined μ as:

$$\log\left(\mu_i\right) = \alpha_{\text{sp}_i,\text{trt}_i} + \sum_{j=1}^{4} \beta_{j,\text{sp}_i,\text{trt}_i} \times \text{PC}_{j,i} + \gamma_{\text{sp}_i,\text{trt}_i,\text{site}_i} \tag{A.11}$$

$$\gamma_{\text{sp,trt,site}} \sim \text{Normal}\left(0, \sigma\right) \tag{A.12}$$

Similarly, using a logit link function, we defined θ as:

$$\text{logit}\left(\theta_i\right) = \alpha_{\theta,\text{sp}_i,\text{trt}_i} + \sum_{j=1}^{4} \beta_{\theta,j,\text{sp}_i,\text{trt}_i} \times \text{PC}_{j,i} + \gamma_{\theta,\text{sp}_i,\text{trt}_i,\text{site}_i} \tag{A.13}$$

$$\gamma_{\theta,\text{sp,trt,site}} \sim \text{Normal}\left(0, \sigma_\theta\right) \tag{A.14}$$

The right-hand sides of Equations A.11 and A.13 are specified identically to the right-hand side of Equation A.2, where the subscript θ denotes parameters for the zero-inflation component. That is, expected fecundity from the negative binomial process (μ) and the expected probability of zero-inflation (θ) are both allowed to vary for each species and treatment in response to soil PC1–PC4. We allowed ϕ to vary by species as:

$$\phi_i = \alpha_{\phi,\text{sp}_i} \tag{A.15}$$

where α_ϕ is a species-specific intercept for ϕ.

We specified prior distributions for parameters as:

$$\alpha \sim \text{Normal}(4, 2) \tag{A.16}$$

$$\alpha_\theta \sim \text{Normal}(0, 2) \tag{A.17}$$

$$\beta_j, \beta_{\theta,j} \sim \text{Normal}(0, 1) \tag{A.18}$$

$$\sigma, \sigma_\theta \sim \text{Exponential}(1) \tag{A.19}$$

$$\alpha_\phi \sim \text{Exponential}(1) \tag{A.20}$$

These priors were specified following a similar rationale as described for the germination model with the exception of Equation A.16, which is an informative prior based on previous fecundity estimates for our focal species in our study system (Godoy et al. 2014, Kraft et al. 2015b, Kandlikar et al. 2022, Van Dyke et al. 2022). Equation A.16 implies for example that, under average environmental conditions across experimental sites (i.e., $\text{PC}_j = 0$), an expected fecundity (μ) of $\exp(8) \approx$ 3,000 corresponds to around the 97.5% quantile of this prior distribution. From this intercept, μ can be further increased (or decreased) at each site according to β_j and γ. We also note that μ is the *expected* value of fecundity and thus *observed* values (i.e., draws from the prior predictive distribution) can be much larger (or smaller), especially as ϕ approaches 0.

We also considered a model in which (1) a negative binomial likelihood (without zero-inflation) was employed. Additionally, we considered models in which Equation A.13 was simplified as follows: (2) The expected probability of zero-inflation (θ) varies by species, including γ_θ that varies by species and site. (3) θ varies by species and treatment, including γ_θ that varies by species, treatment, and site. We used LOO-CV to compare alternative models and found that all zero-inflated models were estimated to have better predictive performance than model (1) (Table A.14), reflecting an excess of zeros in our fecundity data. All zero-inflated models were estimated to have similar predictive performance, especially model (3) and the maximal model (described above). This is unsurprising, as the former represents variation in θ across sites entirely with γ_θ, whereas the latter instead represents some of this variation with $\beta_{\theta,j}$. Therefore, we used the maximal model for our analyses, as it better aligns with our objective of quantifying demographic responses to environmental gradients. We followed the same procedure for fitting, checking, and comparing these models as described for the germination model.

A.3.3 Fitness model

We observed bimodalities in empirical estimates of fitness computed from paired measurements of germination rate and fecundity in each subplot, likely due to the excess of zeros in our fecundity data. Therefore, rather than modeling fitness directly, we implemented a joint model of the germination and fecundity models described above. This joint modeling approach allowed us to compute fitness (r) using the joint posterior distribution for the germination and fecundity sub-models. We followed the same procedure for fitting and checking this model as described for the individual models.

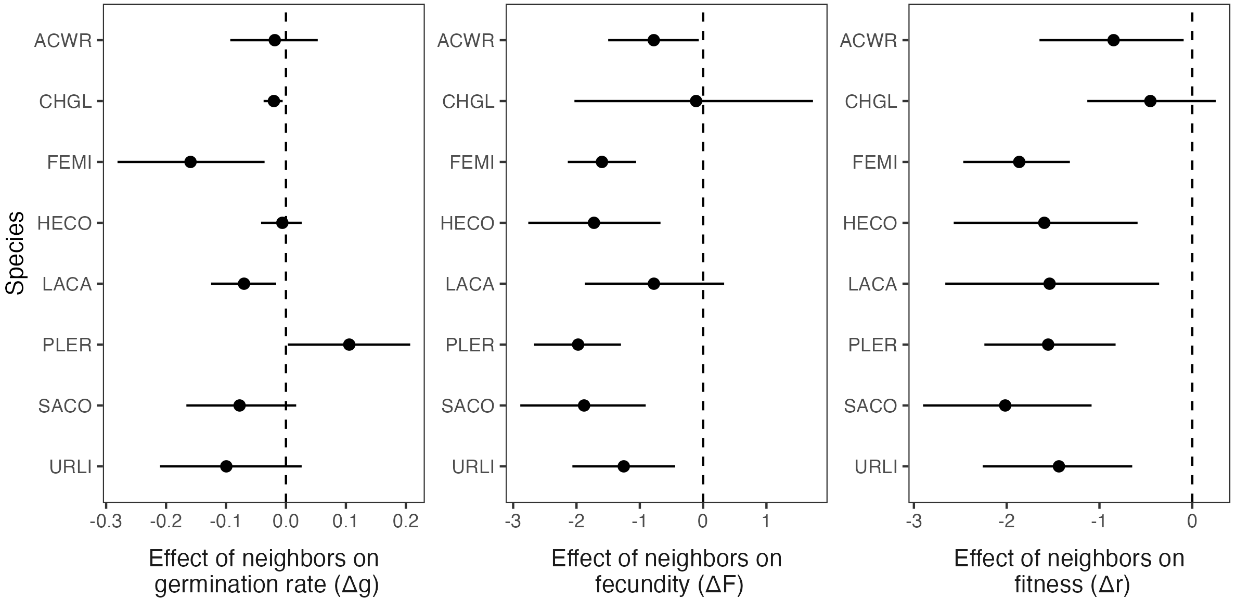

Figure A.7: Estimated effects of neighbors on germination rate (Δg), fecundity (ΔF), and fitness (Δr). For each demographic quantity (y), $\Delta y = y_{\text{trt}=1} - y_{\text{trt}=2}$ where trt $= 1$ is with neighbors present and trt $= 2$ is with neighbors absent. Thus, negative values of Δy correspond to negative effects of neighbors. For each species, effects are computed on the logit scale for germination rate, log scale for fecundity, and identity scale for fitness, with soil PC1–PC4 held at average conditions across experimental sites. Points represent posterior medians. Lines represent 95% highest-density continuous intervals.

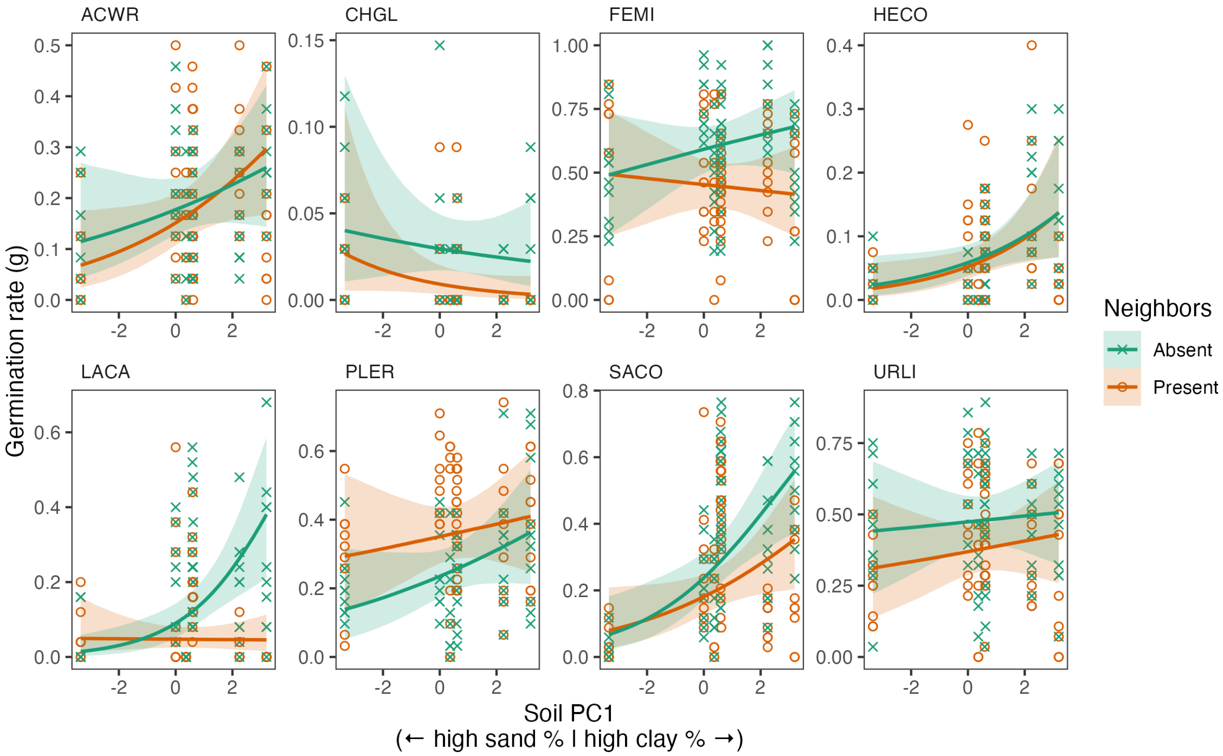

Figure A.8: Response of germination rate (g) to soil PC1 in the presence or absence of neighbors. Posterior expectations are shown for each species with soil PC2–PC4 held at average conditions across experimental sites. Solid lines represent medians. Shaded areas represent 95% quantile intervals.

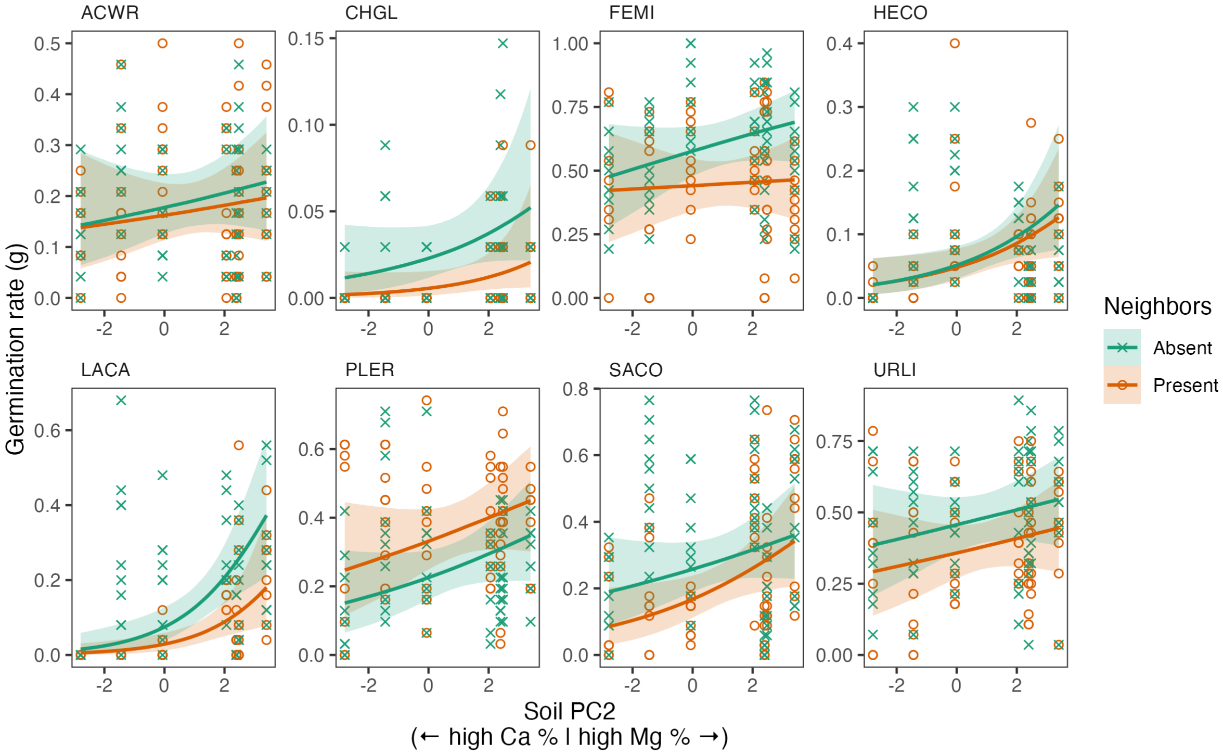

Figure A.9: Response of germination rate (g) to soil PC2 in the presence or absence of neighbors. Posterior expectations are shown for each species with soil PC1, PC3, and PC4 held at average conditions across experimental sites. Solid lines represent medians. Shaded areas represent 95% quantile intervals.

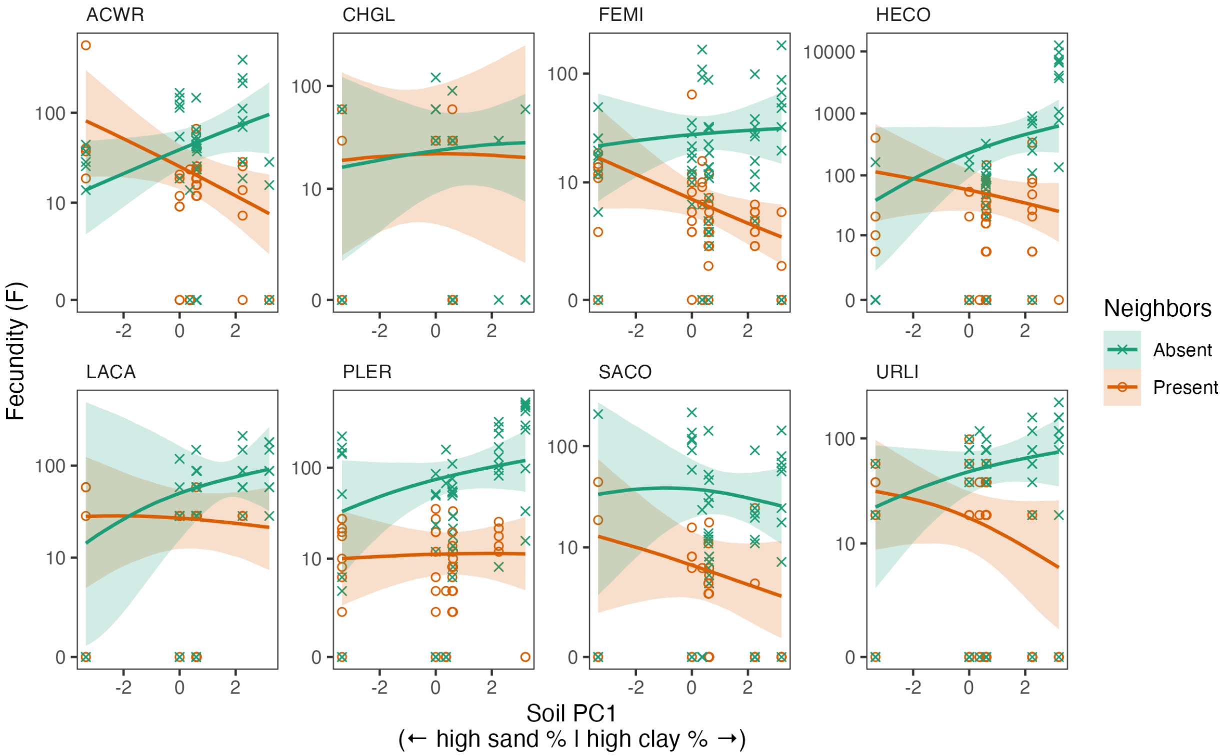

Figure A.10: Response of fecundity (F) to soil PC1 in the presence or absence of neighbors. Posterior expectations are shown for each species with soil PC2–PC4 held at average conditions across experimental sites. Solid lines represent medians. Shaded areas represent 95% quantile intervals.

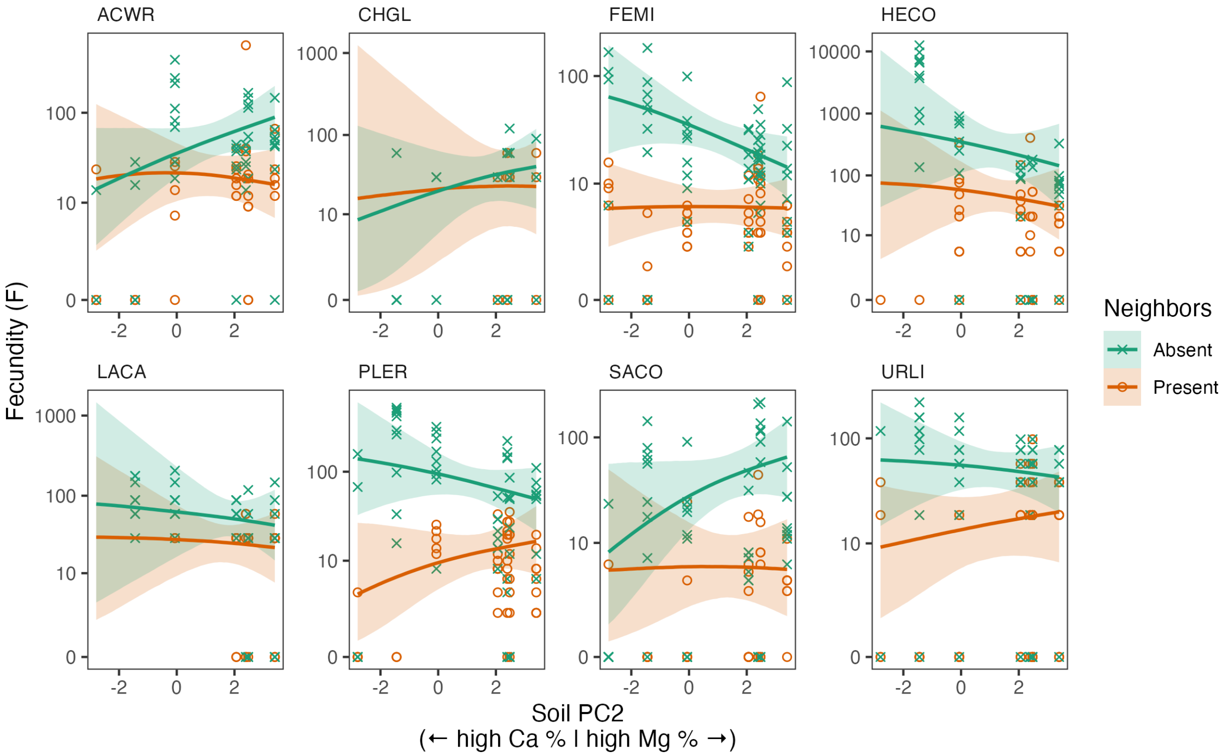

Figure A.11: Response of fecundity (F) to soil PC2 in the presence or absence of neighbors. Posterior expectations are shown for each species with soil PC1, PC3, and PC4 held at average conditions across experimental sites. Solid lines represent medians. Shaded areas represent 95% quantile intervals.

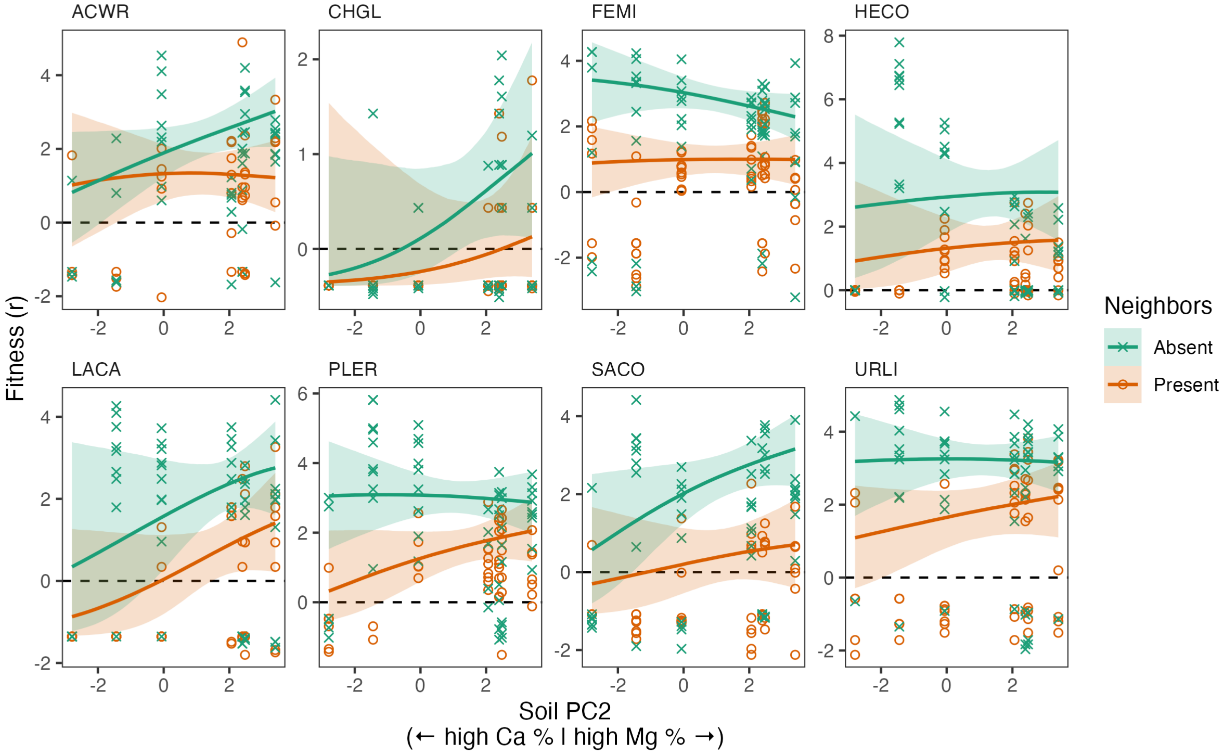

Figure A.12: Response of fitness (r) to soil PC2 in the presence or absence of neighbors. Posterior expectations are shown for each species with soil PC1, PC3, and PC4 held at average conditions across experimental sites. Solid lines represent medians. Shaded areas represent 95% quantile intervals.

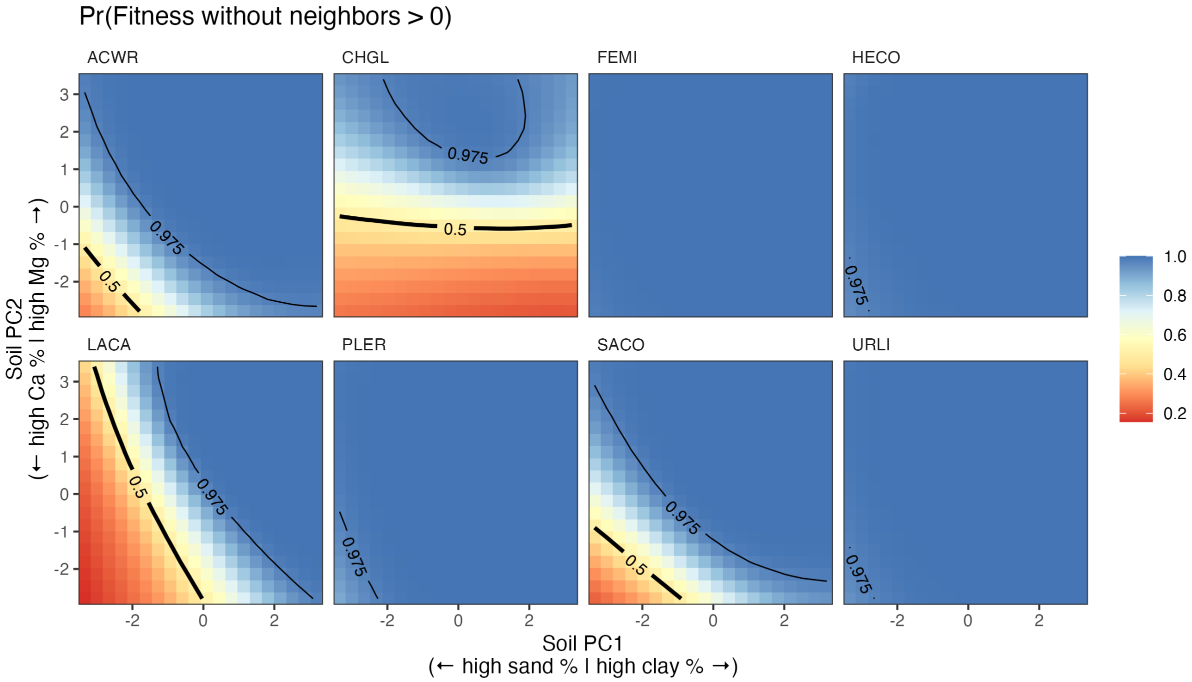

Figure A.13: Probability that fitness $(r) > 0$ in the absence of neighbors with respect to soil PC1 and PC2. Posterior probabilities are shown for each species with soil PC3 and PC4 held at average conditions across experimental sites.

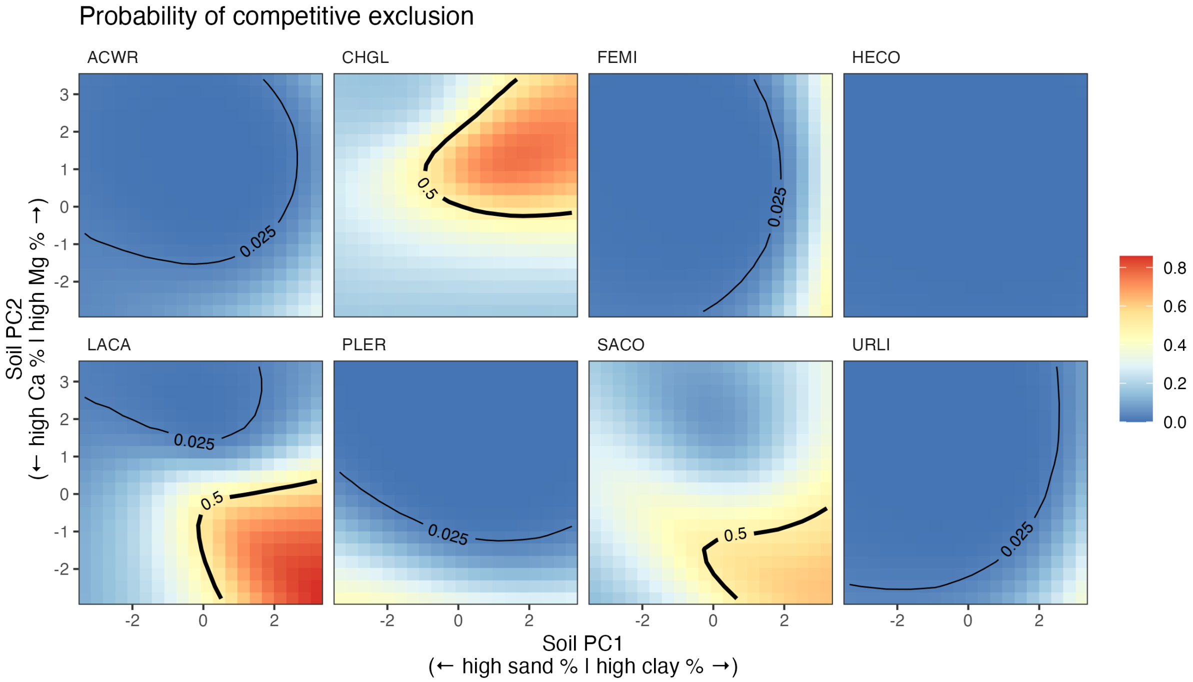

Figure A.14: Probability of competitive exclusion (i.e., fitness (r) is reduced from positive in the absence of neighbors to negative in the presence of neighbors) with respect to soil PC1 and PC2. Posterior probabilities are shown for each species with soil PC3 and PC4 held at average conditions across experimental sites.

Table A.3: Estimated effects of neighbors on germination rate (Δg), fecundity (ΔF), and fitness (Δr). For each demographic quantity (y), $\Delta y = y_{\text{trt}=1} - y_{\text{trt}=2}$ where trt $= 1$ is with neighbors present and trt $= 2$ is with neighbors absent. Thus, negative values of Δy correspond to negative effects of neighbors. For each species, effects are computed on the logit scale for germination rate, log scale for fecundity, and identity scale for fitness, with soil PC1–PC4 held at average conditions across experimental sites. Bold text indicates Pr(direction) ≥ 0.975.

Response	Species	Median	95% HDCI	Pr(direction)
Germination rate	ACWR	-0.019	[-0.093, 0.053]	0.702
	CHGL	**-0.020**	**[-0.037, -0.006]**	**0.998**
	FEMI	**-0.159**	**[-0.281, -0.036]**	**0.993**
	HECO	-0.006	[-0.041, 0.026]	0.640
	LACA	**-0.070**	**[-0.125, -0.016]**	**0.997**
	PLER	**0.106**	**[0.003, 0.207]**	**0.978**
	SACO	-0.077	[-0.166, 0.017]	0.951
	URLI	-0.100	[-0.210, 0.026]	0.949
Fecundity	**ACWR**	**-0.779**	**[-1.499, -0.069]**	**0.982**
	CHGL	-0.111	[-2.033, 1.735]	0.546
	FEMI	**-1.598**	**[-2.137, -1.058]**	**1.000**
	HECO	**-1.724**	**[-2.761, -0.673]**	**0.999**
	LACA	-0.777	[-1.868, 0.332]	0.920
	PLER	**-1.974**	**[-2.670, -1.298]**	**1.000**
	SACO	**-1.880**	**[-2.888, -0.907]**	**1.000**
	URLI	**-1.253**	**[-2.065, -0.441]**	**0.999**
Fitness	**ACWR**	**-0.848**	**[-1.647, -0.093]**	**0.982**
	CHGL	-0.451	[-1.131, 0.253]	0.910
	FEMI	**-1.865**	**[-2.468, -1.319]**	**1.000**
	HECO	**-1.595**	**[-2.571, -0.589]**	**0.999**
	LACA	**-1.537**	**[-2.662, -0.357]**	**0.995**
	PLER	**-1.553**	**[-2.240, -0.826]**	**1.000**
	SACO	**-2.016**	**[-2.901, -1.085]**	**1.000**
	URLI	**-1.437**	**[-2.258, -0.647]**	**1.000**

Table A.4: Estimated effects of soil PC1–PC4 on germination rate (g) with neighbors absent ($\beta_{\mathrm{trt}=2}$). Effects are computed on the logit scale. Bold text indicates Pr(direction) ≥ 0.975.

Variable	**Species**	**Median**	**95% HDCI**	**Pr(direction)**
PC1	ACWR	0.314	[-0.185, 0.840]	0.885
	CHGL	-0.189	[-0.871, 0.426]	0.717
	FEMI	0.248	[-0.275, 0.765]	0.827
	HECO	**0.598**	**[0.044, 1.164]**	**0.982**
	LACA	**1.172**	**[0.492, 1.871]**	**1.000**
	PLER	0.400	[-0.142, 0.894]	0.935
	SACO	**0.900**	**[0.369, 1.457]**	**0.999**
	URLI	0.081	[-0.414, 0.605]	0.626
PC2	ACWR	0.211	[-0.282, 0.741]	0.799
	CHGL	0.574	[-0.184, 1.376]	0.936
	FEMI	0.337	[-0.148, 0.858]	0.907
	HECO	**0.782**	**[0.128, 1.485]**	**0.992**
	LACA	**1.360**	**[0.574, 2.186]**	**1.000**
	PLER	0.410	[-0.113, 0.945]	0.940
	SACO	0.330	[-0.161, 0.827]	0.909
	URLI	0.244	[-0.260, 0.746]	0.836
PC3	ACWR	-0.056	[-0.485, 0.366]	0.606
	CHGL	-0.059	[-0.603, 0.478]	0.585
	FEMI	-0.102	[-0.540, 0.333]	0.679
	HECO	-0.057	[-0.513, 0.378]	0.603
	LACA	0.200	[-0.241, 0.650]	0.815
	PLER	-0.216	[-0.657, 0.203]	0.841
	SACO	**0.490**	**[0.079, 0.896]**	**0.990**
	URLI	-0.027	[-0.443, 0.398]	0.553
PC4	ACWR	-0.123	[-0.698, 0.443]	0.673
	CHGL	-0.356	[-1.104, 0.382]	0.832
	FEMI	-0.154	[-0.714, 0.469]	0.697
	HECO	-0.438	[-1.055, 0.181]	0.922
	LACA	-0.399	[-1.064, 0.245]	0.888
	PLER	-0.138	[-0.714, 0.440]	0.684
	SACO	-0.047	[-0.609, 0.497]	0.569
	URLI	-0.067	[-0.626, 0.521]	0.592

Table A.5: Estimated effects of soil PC1–PC4 on germination rate (g) with neighbors present ($\beta_{\text{trt}=1}$). Effects are computed on the logit scale. Bold text indicates Pr(direction) $\geq$ 0.975.

Variable	Species	Median	95% HDCI	Pr(direction)
PC1	**ACWR**	**0.553**	**[0.033, 1.082]**	**0.980**
	CHGL	-0.677	[-1.536, 0.137]	0.947
	FEMI	-0.101	[-0.628, 0.425]	0.650
	HECO	**0.681**	**[0.100, 1.257]**	**0.989**
	LACA	-0.027	[-0.676, 0.608]	0.535
	PLER	0.162	[-0.337, 0.685]	0.740
	SACO	**0.580**	**[0.047, 1.125]**	**0.981**
	URLI	0.160	[-0.358, 0.676]	0.731
PC2	ACWR	0.158	[-0.404, 0.672]	0.728
	CHGL	0.900	[-0.205, 2.160]	0.948
	FEMI	0.062	[-0.472, 0.595]	0.591
	HECO	**0.714**	**[0.063, 1.390]**	**0.987**
	LACA	**1.356**	**[0.443, 2.414]**	**0.999**
	PLER	0.342	[-0.160, 0.861]	0.908
	SACO	**0.645**	**[0.067, 1.234]**	**0.986**
	URLI	0.253	[-0.262, 0.806]	0.826
PC3	ACWR	-0.120	[-0.547, 0.309]	0.717
	CHGL	0.192	[-0.526, 0.872]	0.709
	FEMI	0.060	[-0.378, 0.486]	0.610
	HECO	-0.093	[-0.545, 0.347]	0.664
	LACA	0.420	[-0.058, 0.908]	0.955
	PLER	-0.016	[-0.419, 0.395]	0.530
	SACO	**0.440**	**[0.030, 0.859]**	**0.981**
	URLI	0.067	[-0.356, 0.489]	0.620
PC4	ACWR	0.184	[-0.386, 0.765]	0.738
	CHGL	0.019	[-0.939, 0.966]	0.515
	FEMI	-0.041	[-0.648, 0.534]	0.552
	HECO	0.133	[-0.496, 0.750]	0.664
	LACA	0.230	[-0.510, 0.981]	0.728
	PLER	-0.171	[-0.730, 0.419]	0.725
	SACO	0.085	[-0.493, 0.675]	0.621
	URLI	0.080	[-0.519, 0.655]	0.607

Table A.6: Estimated effects of neighbors on the response of germination rate (g) to soil PC1–PC4 ($\Delta\beta = \beta_{\text{trt}=1} - \beta_{\text{trt}=2}$). Effects are computed on the logit scale. Bold text indicates Pr(direction) $\geq$ 0.975.

Variable	Species	Median	95% HDCI	Pr(direction)
PC1	ACWR	0.239	[-0.497, 0.954]	0.740
	CHGL	-0.490	[-1.528, 0.585]	0.821
	FEMI	-0.344	[-1.078, 0.398]	0.825
	HECO	0.088	[-0.715, 0.884]	0.584
	LACA	**-1.207**	**[-2.168, -0.290]**	**0.994**
	PLER	-0.236	[-0.949, 0.499]	0.743
	SACO	-0.321	[-1.108, 0.427]	0.802
	URLI	0.077	[-0.698, 0.774]	0.583
PC2	ACWR	-0.050	[-0.792, 0.687]	0.557
	CHGL	0.330	[-1.094, 1.756]	0.678
	FEMI	-0.274	[-0.995, 0.465]	0.771
	HECO	-0.064	[-1.059, 0.874]	0.553
	LACA	0.004	[-1.229, 1.309]	0.502
	PLER	-0.071	[-0.802, 0.672]	0.575
	SACO	0.317	[-0.463, 1.067]	0.794
	URLI	0.005	[-0.700, 0.776]	0.506
PC3	ACWR	-0.065	[-0.672, 0.544]	0.586
	CHGL	0.248	[-0.634, 1.118]	0.714
	FEMI	0.163	[-0.474, 0.760]	0.700
	HECO	-0.038	[-0.674, 0.589]	0.550
	LACA	0.221	[-0.423, 0.886]	0.746
	PLER	0.201	[-0.407, 0.795]	0.751
	SACO	-0.051	[-0.623, 0.533]	0.572
	URLI	0.092	[-0.505, 0.694]	0.623
PC4	ACWR	0.307	[-0.500, 1.123]	0.779
	CHGL	0.375	[-0.788, 1.630]	0.728
	FEMI	0.114	[-0.723, 0.937]	0.606
	HECO	0.573	[-0.286, 1.470]	0.902
	LACA	0.624	[-0.353, 1.640]	0.896
	PLER	-0.029	[-0.876, 0.751]	0.529
	SACO	0.139	[-0.687, 0.919]	0.634
	URLI	0.149	[-0.680, 0.979]	0.639

Table A.7: Estimated effects of soil PC1–PC4 on fecundity (F) with neighbors absent ($\beta^*_{\text{trt}=2}$). Effects are computed on the log scale. Bold text indicates Pr(direction) $\geq$ 0.975.

Variable	**Species**	**Median**	**95% HDCI**	**Pr(direction)**
PC1	ACWR	0.604	[-0.022, 1.163]	0.972
	CHGL	0.174	[-0.766, 1.106]	0.650
	FEMI	0.119	[-0.414, 0.669]	0.677
	HECO	0.884	[-0.179, 2.002]	0.949
	LACA	0.583	[-0.809, 1.997]	0.801
	PLER	0.400	[-0.201, 1.040]	0.918
	SACO	-0.076	[-0.934, 0.836]	0.570
	URLI	0.382	[-0.242, 1.056]	0.894
PC2	ACWR	0.689	[-0.129, 1.484]	0.950
	CHGL	0.599	[-0.802, 2.102]	0.800
	FEMI	-0.560	[-1.129, 0.056]	0.966
	HECO	-0.548	[-2.131, 1.004]	0.753
	LACA	-0.234	[-1.655, 1.197]	0.628
	PLER	-0.377	[-1.166, 0.350]	0.840
	SACO	0.794	[-0.116, 1.801]	0.948
	URLI	-0.136	[-0.830, 0.545]	0.660
PC3	**ACWR**	**-0.528**	**[-1.036, -0.025]**	**0.981**
	CHGL	-0.316	[-1.249, 0.566]	0.771
	FEMI	-0.068	[-0.521, 0.379]	0.628
	HECO	-0.264	[-0.943, 0.452]	0.770
	LACA	0.120	[-0.351, 0.612]	0.708
	PLER	**-0.512**	**[-0.956, -0.049]**	**0.983**
	SACO	-0.398	[-0.939, 0.177]	0.913
	URLI	0.087	[-0.351, 0.532]	0.666
PC4	ACWR	-0.042	[-0.731, 0.633]	0.548
	CHGL	-0.040	[-1.049, 0.986]	0.532
	FEMI	0.157	[-0.444, 0.743]	0.704
	HECO	-0.590	[-1.608, 0.410]	0.876
	LACA	-0.029	[-0.780, 0.715]	0.532
	PLER	0.014	[-0.657, 0.645]	0.517
	SACO	-0.453	[-1.178, 0.297]	0.888
	URLI	-0.059	[-0.666, 0.579]	0.580

Table A.8: Estimated effects of soil PC1–PC4 on fecundity (F) with neighbors present ($\beta^{*}_{\text{trt}=1}$). Effects are computed on the log scale. Bold text indicates Pr(direction) $\geq$ 0.975.

Variable	**Species**	**Median**	**95% HDCI**	**Pr(direction)**
PC1	**ACWR**	**-0.760**	**[-1.429, -0.090]**	**0.985**
	CHGL	0.026	[-1.057, 1.199]	0.518
	FEMI	**-0.593**	**[-1.142, -0.035]**	**0.981**
	HECO	-0.472	[-1.257, 0.348]	0.883
	LACA	-0.080	[-0.755, 0.639]	0.596
	PLER	0.038	[-0.565, 0.658]	0.550
	SACO	-0.490	[-1.406, 0.446]	0.853
	URLI	-0.550	[-1.370, 0.250]	0.914
PC2	ACWR	-0.042	[-1.014, 0.894]	0.534
	CHGL	0.130	[-1.777, 2.104]	0.555
	FEMI	0.003	[-0.585, 0.557]	0.505
	HECO	-0.329	[-1.761, 1.216]	0.666
	LACA	-0.116	[-1.319, 1.174]	0.571
	PLER	0.564	[-0.439, 1.514]	0.874
	SACO	0.012	[-1.206, 1.218]	0.508
	URLI	0.304	[-0.504, 1.193]	0.773
PC3	ACWR	-0.059	[-0.588, 0.442]	0.593
	CHGL	-0.108	[-1.014, 0.870]	0.596
	FEMI	-0.036	[-0.465, 0.430]	0.564
	HECO	-0.102	[-0.688, 0.474]	0.641
	LACA	-0.051	[-0.533, 0.442]	0.590
	PLER	-0.159	[-0.642, 0.314]	0.757
	SACO	-0.202	[-0.916, 0.495]	0.726
	URLI	0.188	[-0.472, 0.846]	0.720
PC4	ACWR	0.759	[-0.119, 1.722]	0.957
	CHGL	0.190	[-0.958, 1.249]	0.640
	FEMI	-0.154	[-0.843, 0.539]	0.670
	HECO	-0.155	[-1.251, 0.928]	0.615
	LACA	0.124	[-0.666, 0.948]	0.626
	PLER	-0.248	[-1.085, 0.589]	0.725
	SACO	0.211	[-0.857, 1.316]	0.651
	URLI	0.056	[-0.866, 0.997]	0.547

Table A.9: Estimated effects of neighbors on the response of fecundity (F) to soil PC1–PC4 ($\Delta\beta^* = \beta^*_{\text{trt}=1} - \beta^*_{\text{trt}=2}$). Effects are computed on the log scale. Bold text indicates Pr(direction) $\geq$ 0.975.

Variable	Species	Median	95% HDCI	Pr(direction)
PC1	**ACWR**	**-1.362**	**[-2.262, -0.465]**	**0.997**
	CHGL	-0.157	[-1.709, 1.234]	0.584
	FEMI	-0.712	[-1.494, 0.065]	0.963
	HECO	**-1.360**	**[-2.725, -0.035]**	**0.976**
	LACA	-0.667	[-2.245, 0.903]	0.805
	PLER	-0.371	[-1.238, 0.497]	0.806
	SACO	-0.419	[-1.649, 0.899]	0.742
	URLI	-0.951	[-2.009, 0.091]	0.964
PC2	ACWR	-0.730	[-1.980, 0.523]	0.873
	CHGL	-0.485	[-2.889, 1.902]	0.652
	FEMI	0.562	[-0.261, 1.386]	0.911
	HECO	0.231	[-2.073, 2.270]	0.583
	LACA	0.125	[-1.770, 2.032]	0.554
	PLER	0.945	[-0.259, 2.204]	0.933
	SACO	-0.789	[-2.274, 0.789]	0.841
	URLI	0.449	[-0.615, 1.530]	0.798
PC3	ACWR	0.471	[-0.254, 1.198]	0.902
	CHGL	0.219	[-1.073, 1.526]	0.635
	FEMI	0.030	[-0.597, 0.668]	0.540
	HECO	0.158	[-0.768, 1.043]	0.635
	LACA	-0.173	[-0.848, 0.524]	0.713
	PLER	0.353	[-0.322, 1.010]	0.852
	SACO	0.183	[-0.707, 1.076]	0.657
	URLI	0.096	[-0.736, 0.853]	0.602
PC4	ACWR	0.795	[-0.334, 1.953]	0.917
	CHGL	0.239	[-1.217, 1.725]	0.625
	FEMI	-0.313	[-1.208, 0.626]	0.751
	HECO	0.440	[-1.017, 1.939]	0.723
	LACA	0.148	[-0.929, 1.250]	0.615
	PLER	-0.256	[-1.291, 0.824]	0.690
	SACO	0.664	[-0.635, 1.997]	0.842
	URLI	0.113	[-0.974, 1.274]	0.583

Table A.10: Estimated effects of soil PC1–PC4 on fitness (r) with neighbors absent ($\beta^{*}_{\text{trt}=2}$). Effects are computed on the identity scale. Bold text indicates Pr(direction) $\geq$ 0.975.

Variable	Species	Median	95% HDCI	Pr(direction)
PC1	**ACWR**	**0.817**	**[0.143, 1.430]**	**0.987**
	CHGL	-0.001	[-0.598, 0.465]	0.501
	FEMI	0.223	[-0.344, 0.816]	0.784
	HECO	**1.194**	**[0.347, 1.768]**	**0.991**
	LACA	**1.346**	**[0.292, 1.960]**	**0.984**
	PLER	**0.675**	**[0.031, 1.311]**	**0.977**
	SACO	0.550	[-0.266, 1.308]	0.889
	URLI	0.422	[-0.230, 1.103]	0.901
PC2	ACWR	0.828	[0.000, 1.625]	0.968
	CHGL	0.461	[-0.178, 0.986]	0.926
	FEMI	-0.416	[-1.034, 0.219]	0.905
	HECO	0.172	[-1.289, 1.596]	0.586
	LACA	0.894	[-0.432, 1.936]	0.887
	PLER	-0.065	[-0.899, 0.765]	0.563
	SACO	**0.976**	**[0.101, 1.776]**	**0.975**
	URLI	-0.004	[-0.714, 0.734]	0.504
PC3	ACWR	-0.554	[-1.114, 0.008]	0.972
	CHGL	-0.167	[-0.557, 0.342]	0.773
	FEMI	-0.109	[-0.596, 0.369]	0.684
	HECO	-0.298	[-1.002, 0.461]	0.781
	LACA	0.283	[-0.299, 0.866]	0.838
	PLER	**-0.650**	**[-1.149, -0.110]**	**0.991**
	SACO	-0.068	[-0.643, 0.536]	0.587
	URLI	0.069	[-0.416, 0.548]	0.619
PC4	ACWR	-0.134	[-0.898, 0.669]	0.631
	CHGL	-0.177	[-0.789, 0.409]	0.725
	FEMI	0.095	[-0.552, 0.709]	0.620
	HECO	-0.922	[-1.824, 0.105]	0.956
	LACA	-0.357	[-1.176, 0.492]	0.791
	PLER	-0.086	[-0.848, 0.648]	0.587
	SACO	-0.470	[-1.246, 0.332]	0.876
	URLI	-0.091	[-0.756, 0.583]	0.610

Table A.11: Estimated effects of soil PC1–PC4 on fitness (r) with neighbors present ($\beta^*_{\text{trt}=1}$). Effects are computed on the identity scale. Bold text indicates Pr(direction) $\geq$ 0.975.

Variable	Species	Median	95% HDCI	Pr(direction)
PC1	ACWR	-0.282	[-1.008, 0.438]	0.775
	CHGL	-0.121	[-0.669, 0.227]	0.809
	FEMI	**-0.610**	**[-1.184, -0.035]**	**0.978**
	HECO	0.112	[-0.590, 0.701]	0.630
	LACA	-0.086	[-0.808, 0.598]	0.591
	PLER	0.126	[-0.461, 0.702]	0.660
	SACO	-0.041	[-0.788, 0.665]	0.544
	URLI	-0.419	[-1.146, 0.354]	0.852
PC2	ACWR	0.087	[-0.874, 0.972]	0.570
	CHGL	0.152	[-0.432, 0.681]	0.815
	FEMI	0.039	[-0.569, 0.637]	0.551
	HECO	0.240	[-0.914, 1.097]	0.663
	LACA	0.839	[-0.144, 1.536]	0.939
	PLER	0.649	[-0.166, 1.299]	0.930
	SACO	0.366	[-0.563, 1.079]	0.779
	URLI	0.425	[-0.333, 1.177]	0.853
PC3	ACWR	-0.147	[-0.689, 0.447]	0.699
	CHGL	0.009	[-0.313, 0.374]	0.545
	FEMI	-0.006	[-0.461, 0.475]	0.510
	HECO	-0.140	[-0.611, 0.376]	0.706
	LACA	0.277	[-0.264, 0.797]	0.846
	PLER	-0.155	[-0.620, 0.308]	0.744
	SACO	0.081	[-0.504, 0.654]	0.604
	URLI	0.211	[-0.423, 0.836]	0.742
PC4	ACWR	0.810	[-0.016, 1.513]	0.966
	CHGL	0.026	[-0.361, 0.511]	0.614
	FEMI	-0.166	[-0.847, 0.552]	0.673
	HECO	-0.026	[-0.886, 0.715]	0.524
	LACA	0.273	[-0.546, 1.047]	0.738
	PLER	-0.306	[-1.023, 0.483]	0.778
	SACO	0.197	[-0.625, 0.877]	0.682
	URLI	0.096	[-0.742, 0.962]	0.583

Table A.12: Estimated effects of neighbors on the response of fitness (r) to soil PC1–PC4 ($\Delta\beta^* = \beta^*_{\text{trt}=1} - \beta^*_{\text{trt}=2}$). Effects are computed on the identity scale. Bold text indicates Pr(direction) $\geq$ 0.975.

Variable	Species	Median	95% HDCI	Pr(direction)
PC1	**ACWR**	**-1.097**	**[-2.060, -0.106]**	**0.983**
	CHGL	-0.138	[-0.805, 0.608]	0.664
	FEMI	-0.833	[-1.674, -0.030]	0.975
	HECO	-1.068	[-2.034, -0.038]	0.973
	LACA	**-1.387**	**[-2.432, -0.142]**	**0.978**
	PLER	-0.546	[-1.450, 0.288]	0.892
	SACO	-0.590	[-1.671, 0.545]	0.847
	URLI	-0.849	[-1.845, 0.205]	0.944
PC2	ACWR	-0.738	[-1.985, 0.512]	0.877
	CHGL	-0.301	[-1.076, 0.537]	0.808
	FEMI	0.457	[-0.421, 1.319]	0.846
	HECO	0.036	[-1.789, 1.816]	0.516
	LACA	-0.086	[-1.598, 1.453]	0.544
	PLER	0.693	[-0.425, 1.795]	0.883
	SACO	-0.619	[-1.861, 0.557]	0.848
	URLI	0.430	[-0.616, 1.467]	0.785
PC3	ACWR	0.408	[-0.388, 1.216]	0.845
	CHGL	0.175	[-0.395, 0.714]	0.750
	FEMI	0.103	[-0.564, 0.772]	0.622
	HECO	0.161	[-0.753, 1.021]	0.640
	LACA	-0.007	[-0.773, 0.789]	0.506
	PLER	0.496	[-0.220, 1.189]	0.911
	SACO	0.144	[-0.700, 0.963]	0.633
	URLI	0.138	[-0.665, 0.928]	0.636
PC4	ACWR	0.927	[-0.194, 2.029]	0.939
	CHGL	0.226	[-0.477, 0.960]	0.745
	FEMI	-0.266	[-1.189, 0.713]	0.703
	HECO	0.875	[-0.433, 2.117]	0.903
	LACA	0.622	[-0.554, 1.780]	0.847
	PLER	-0.216	[-1.318, 0.816]	0.656
	SACO	0.645	[-0.510, 1.694]	0.867
	URLI	0.184	[-0.902, 1.258]	0.630

Table A.13: Comparison of germination models. We used approximate leave-one-out cross-validation (LOO-CV) to compare models with alternative likelihood functions. The model selected for use in analyses is indicated with bold text.

Model	**Likelihood**	**$\mathrm{ELPD}_{\mathrm{LOO}}$**	**$\Delta\mathrm{ELPD}_{\mathrm{LOO}}$**
(2)	**Beta-binomial**	**-2656.74 ± 35.91**	**0.00 ± 0.00**
(1)	Binomial	-3361.97 ± 89.28	-705.23 ± 67.05

Table A.14: Comparison of fecundity models. We used approximate leave-one-out cross-validation (LOO-CV) to compare models with alternative likelihood functions (NB = negative binomial, ZINB = zero-inflated negative binomial) and predictors for the zero-inflation component (sp = species, trt = neighbor treatment, soil = soil PC1–PC4). The model selected for use in analyses is indicated with bold text.

Model	Likelihood	ZI predictors	$\mathbf{ELPD_{LOO}}$	$\mathbf{\Delta ELPD_{LOO}}$
(4)	**ZINB**	**sp, trt, soil**	**-2849.79 ± 57.80**	**0.00 ± 0.00**
(3)	ZINB	sp, trt	-2851.77 ± 57.46	-1.98 ± 3.90
(2)	ZINB	sp	-2862.11 ± 57.11	-12.32 ± 8.59
(1)	NB	N/A	-3048.14 ± 53.60	-198.35 ± 17.06

A.4 Appendix S4: Analysis of occurrence surveys

We used Bayesian generalized linear models to quantify the relationship between observed occurrence (presence vs. absence) of our focal species and the soil environment. We modeled the number of plots in which presence was recorded (n_i) for observation i = 1, ..., 248 as following a beta-binomial distribution:

$$n_i \sim \text{Beta-Binomial}\left(N_i, \mu_i, \phi_i\right) \tag{A.21}$$

where N is the number of surveyed plots per site, μ is the mean probability parameter, and ϕ is the precision parameter. To align the scope of this analysis with our demographic experiment, we only used occurrence data for sites within the range of soil PC1–PC4 across experimental sites, corresponding to 92 plots at 31 sites. Using a logit link function, we defined μ as:

$$\text{logit}\left(\mu_i\right) = \alpha_{\text{sp}_i} + \sum_{j=1}^{4} \beta_{j,\text{sp}_i} \times \text{PC}_{j,i} \tag{A.22}$$

where α is a species-specific intercept and β_j is a species-specific slope for soil principal component axis j. Soil PC1–PC4 were centered and scaled with respect to the mean and standard deviation of each axis across sites. We allowed ϕ to vary by species as:

$$\phi_i = \alpha_{\phi,\text{sp}_i} \tag{A.23}$$

where α_ϕ is a species-specific intercept for ϕ.

We specified prior distributions for parameters as:

$$\alpha \sim \text{Normal}(0, 2) \tag{A.24}$$

$$\beta_j \sim \text{Normal}(0, 1) \tag{A.25}$$

These priors were specified following a similar rationale as described for the germination model in Appendix S3.

We also considered a model in which a binomial likelihood was employed. We used LOO-CV to compare alternative models and found that both models were estimated to have similar predictive performance, although $|\Delta\text{ELPD}_{\text{LOO}}|/\text{SE}_{\Delta\text{ELPD}_{\text{LOO}}}$ was close to two in favor of the beta-binomial model (Table A.16). We therefore used the beta-binomial model (described above) for our analyses. We followed the same procedure for fitting, checking, and comparing these models as described for the germination model in Appendix S3.

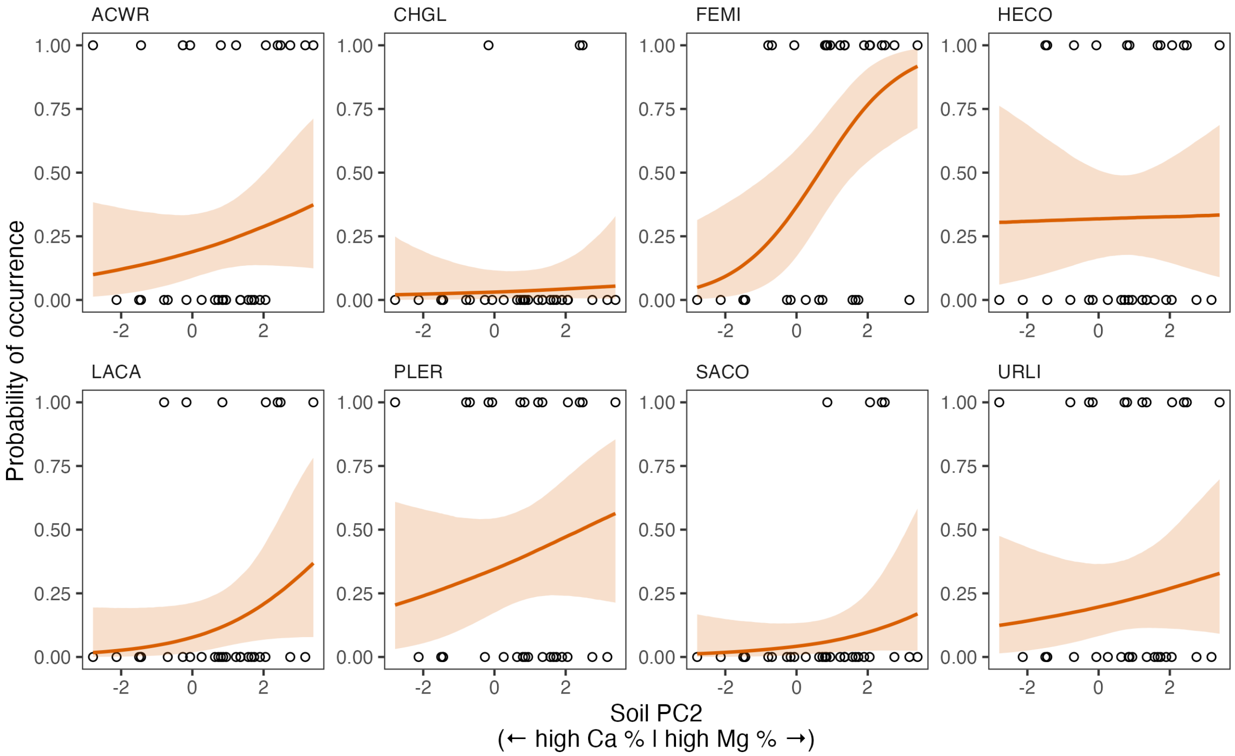

Figure A.15: Observed patterns of occurrence along soil PC2. Posterior expectations are shown for each species with soil PC1, PC3, and PC4 held at average conditions across sites. Solid lines represent medians. Shaded areas represent 95% quantile intervals.

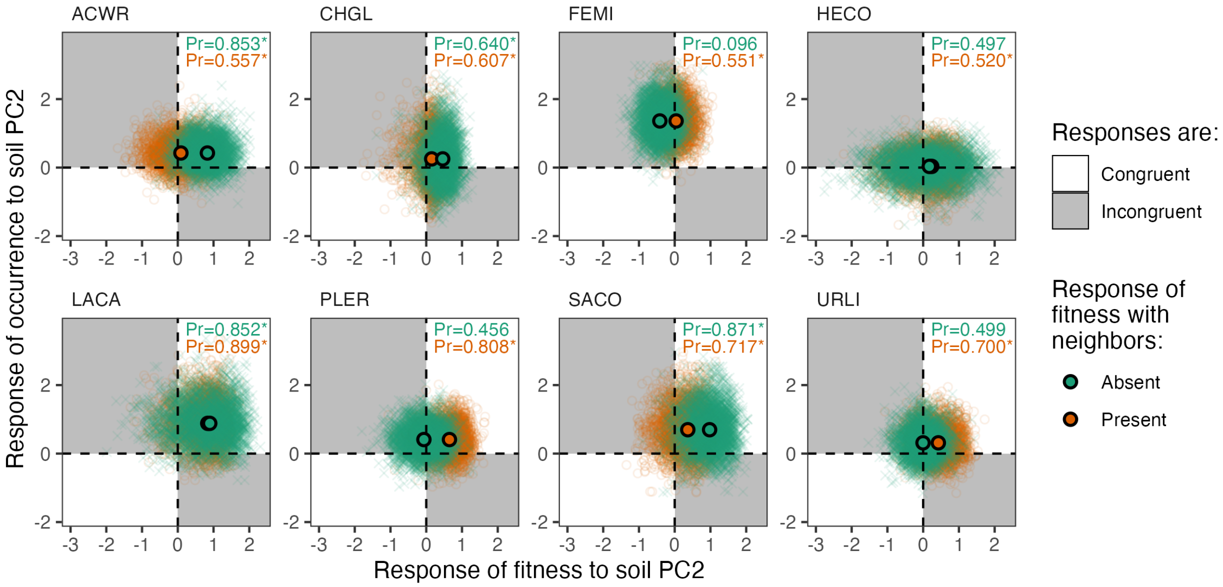

Figure A.16: Congruence between responses of occurrence and fitness to soil PC2. For each species, the slope of occurrence in response to soil PC2 ($\beta_{j=2}$ for the occurrence model) is plotted against the axis-wide slope of fitness in response to soil PC2 ($\beta^*_{j=2}$ for the fitness model), the latter of which is computed in the presence (orange) or absence (green) of neighbors. Point clouds are posterior samples (thinned to 4,000 samples for visualization) and center points are medians. White regions denote congruent responses (i.e., slopes are both positive or both negative) and gray regions denote incongruent responses (i.e., one slope is positive while the other slope is negative). The total probability of congruence (i.e., the proportion of posterior samples that fall in the white regions) is shown in the top-right corner of each panel. Asterisks indicate that responses are more likely to be congruent that not (i.e., Pr(congruence) > 0.5); note that these are not results of statistical significance tests.

Table A.15: Estimated effects of soil PC1–PC4 on occurrence. Effects are computed on the logit scale. Bold text indicates Pr(direction) ≥ 0.975.

Variable	Species	Median	95% HDCI	Pr(direction)
PC1	ACWR	-0.042	[-0.689, 0.622]	0.551
	CHGL	**-1.241**	**[-2.273, -0.250]**	**0.993**
	FEMI	**-0.855**	**[-1.697, -0.063]**	**0.988**
	HECO	0.036	[-0.673, 0.720]	0.541
	LACA	**-1.076**	**[-1.977, -0.209]**	**0.994**
	PLER	**-0.873**	**[-1.684, -0.122]**	**0.991**
	SACO	-0.339	[-1.225, 0.604]	0.767
	URLI	**-1.099**	**[-1.970, -0.275]**	**0.999**
PC2	ACWR	0.425	[-0.298, 1.229]	0.876
	CHGL	0.254	[-0.885, 1.506]	0.667
	FEMI	**1.362**	**[0.449, 2.369]**	**0.999**
	HECO	0.034	[-0.772, 0.829]	0.534
	LACA	0.883	[-0.191, 2.000]	0.954
	PLER	0.409	[-0.370, 1.194]	0.857
	SACO	0.697	[-0.427, 1.923]	0.890
	URLI	0.314	[-0.470, 1.152]	0.785
PC3	ACWR	0.253	[-0.373, 0.879]	0.780
	CHGL	-0.313	[-1.387, 0.681]	0.727
	FEMI	0.272	[-0.515, 1.017]	0.762
	HECO	-0.015	[-0.693, 0.629]	0.519
	LACA	**1.225**	**[0.376, 2.101]**	**0.997**
	PLER	**0.756**	**[0.050, 1.520]**	**0.983**
	SACO	0.075	[-0.731, 0.876]	0.572
	URLI	**0.767**	**[0.083, 1.485]**	**0.989**
PC4	ACWR	-0.208	[-0.962, 0.522]	0.713
	CHGL	-0.182	[-1.409, 0.971]	0.619
	FEMI	-0.385	[-1.259, 0.448]	0.818
	HECO	0.762	[-0.009, 1.586]	0.974
	LACA	0.183	[-0.727, 1.116]	0.650
	PLER	0.038	[-0.790, 0.815]	0.538
	SACO	-0.265	[-1.330, 0.805]	0.690
	URLI	-0.638	[-1.491, 0.196]	0.939

Table A.16: Comparison of occurrence models. We used approximate leave-one-out cross-validation (LOO-CV) to compare models with alternative likelihood functions. The model selected for use in analyses is indicated with bold text.

Model	**Likelihood**	**$\mathrm{ELPD}_{\mathrm{LOO}}$**	**$\Delta\mathrm{ELPD}_{\mathrm{LOO}}$**
(2)	**Beta-binomial**	**-192.62 ± 15.73**	**0.00 ± 0.00**
(1)	Binomial	-210.70 ± 20.02	-18.09 ± 10.76

Appendix B

Supplementary materials for Chapter 2

B.1 Supplementary figures

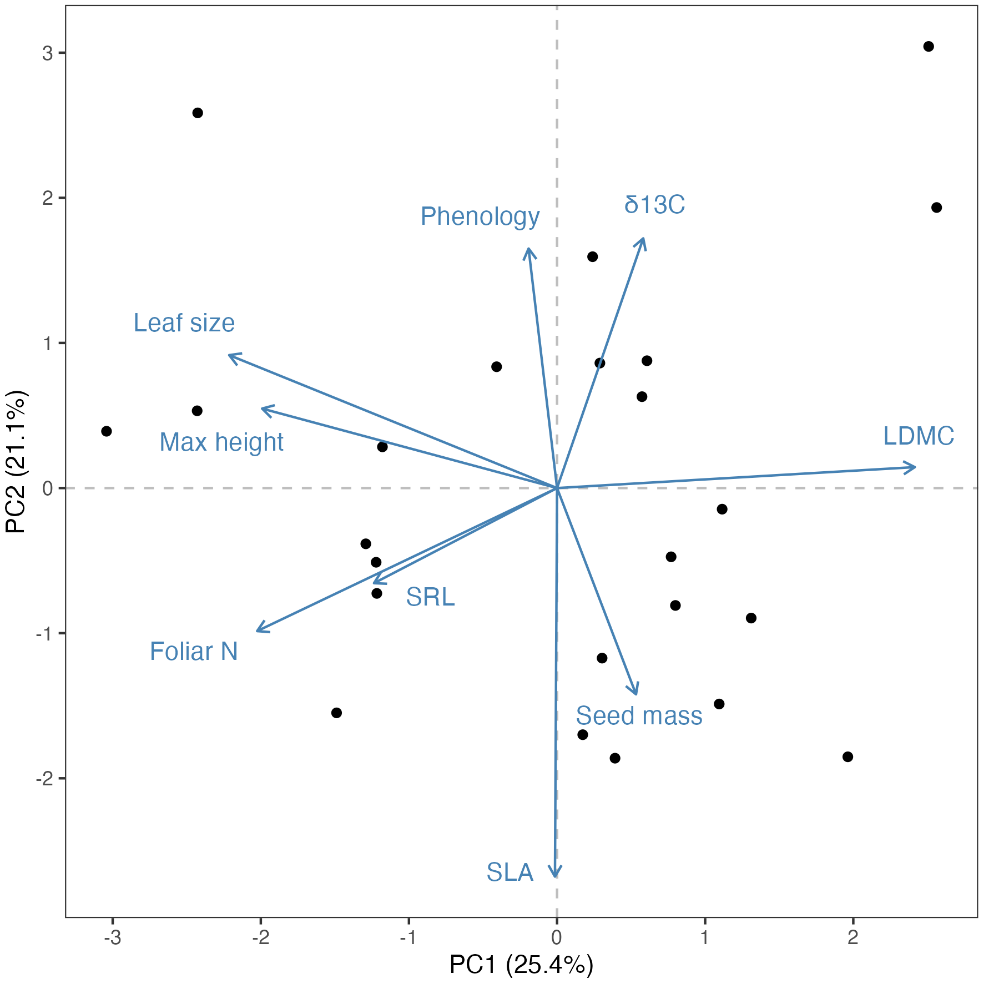

Figure B.1: Principal component analysis for functional traits of the species used in this study. Points represent species. Arrows represent the loadings of individual traits with respect to the primary (PC1) and secondary (PC2) principal component axes. The percentage of variance explained by the axes are given in axis labels.

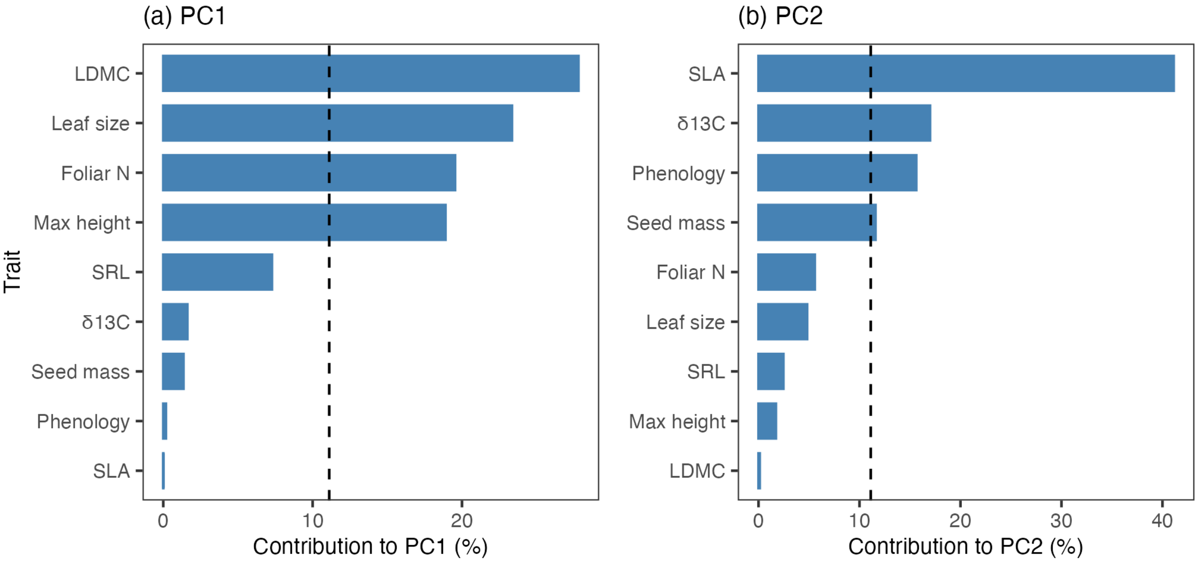

Figure B.2: Contributions of individual traits to the (a) primary (PC1) and (b) secondary (PC2) axes of the principal component analysis for functional traits. Vertical dashed lines represent the expected contributions if all traits contributed uniformly to each axis.

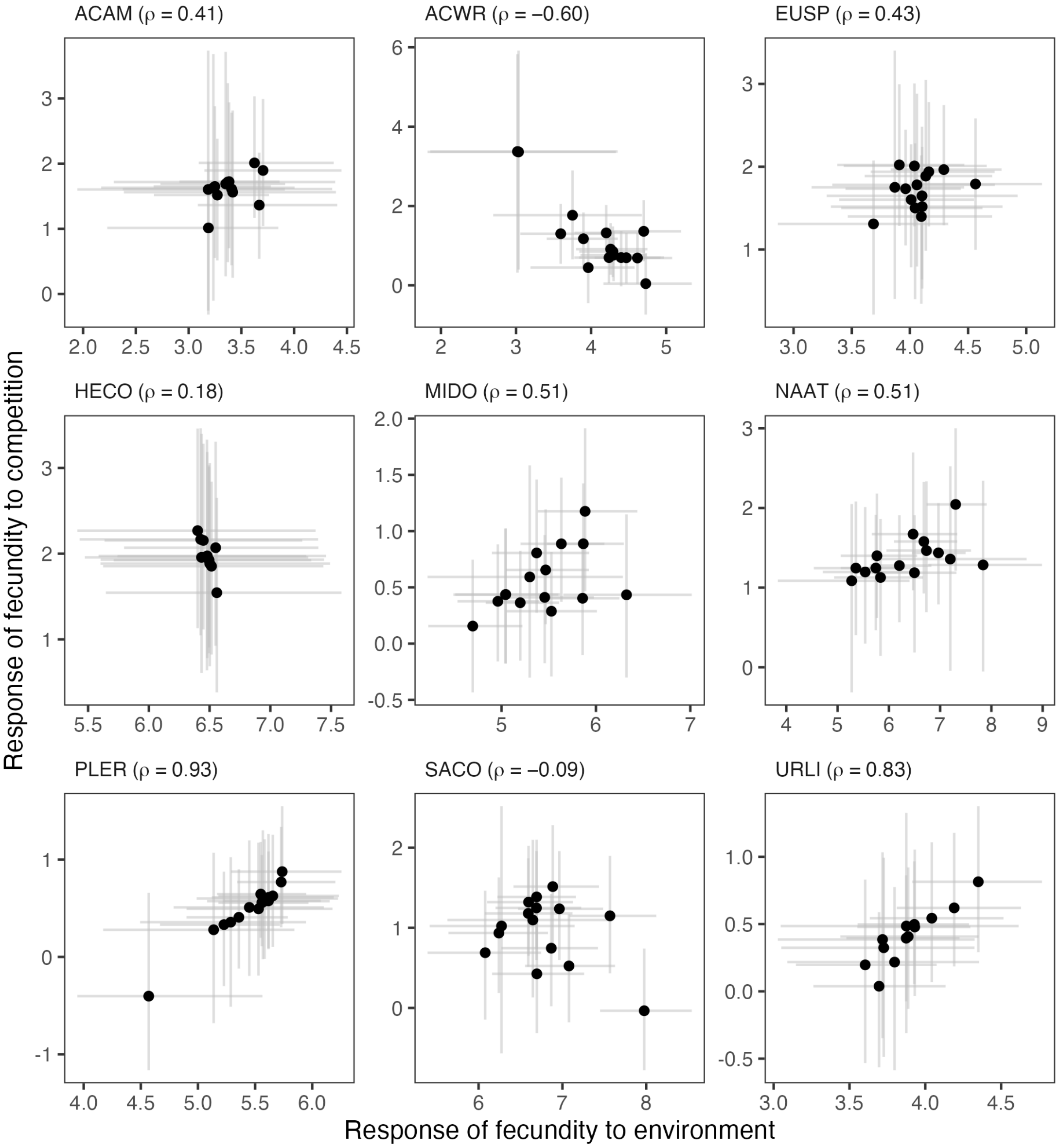

Figure B.3: Correlation (ρ) between responses of fecundity to environment and competition for each species in the 2013 experiment. See Figure 2.2 for a full description of this figure.

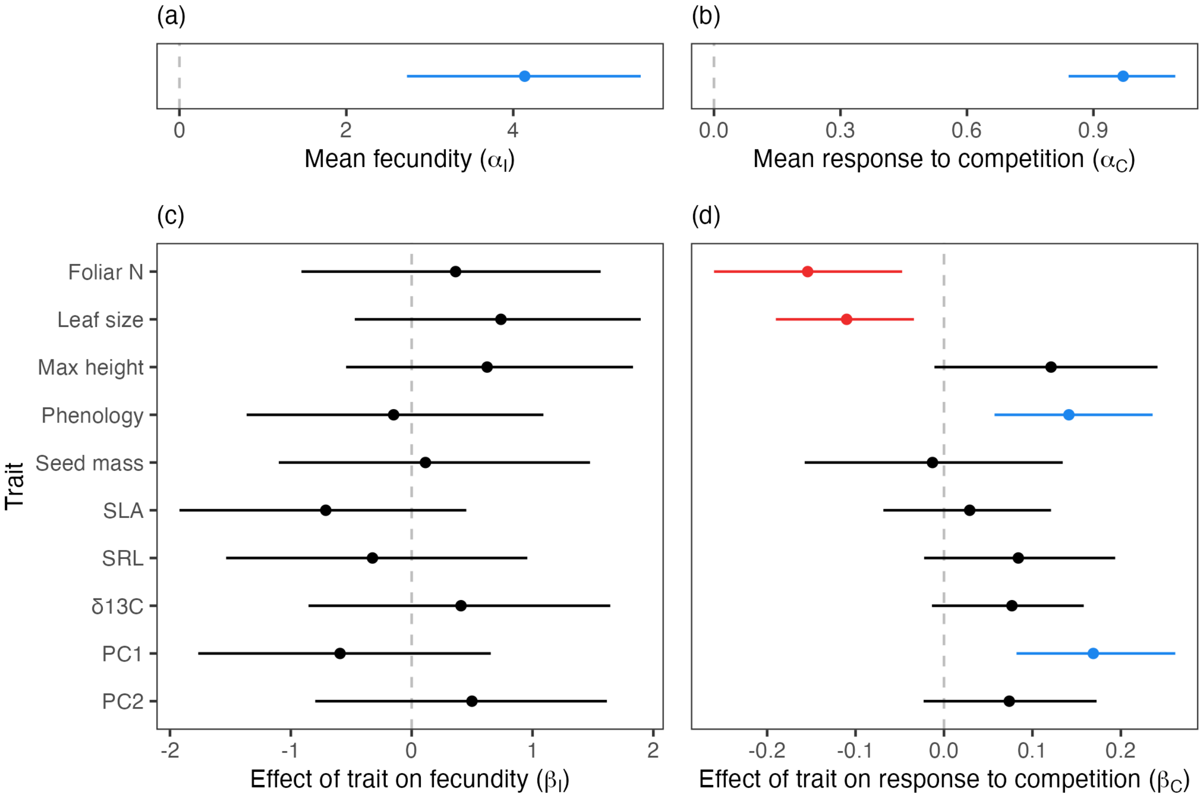

Figure B.4: Effects of functional traits on fecundity under mean environmental conditions in the 2013 experiment. See Figure 2.3 for a full description of this figure. Results for models that failed to satisfy diagnostic criteria are excluded here.

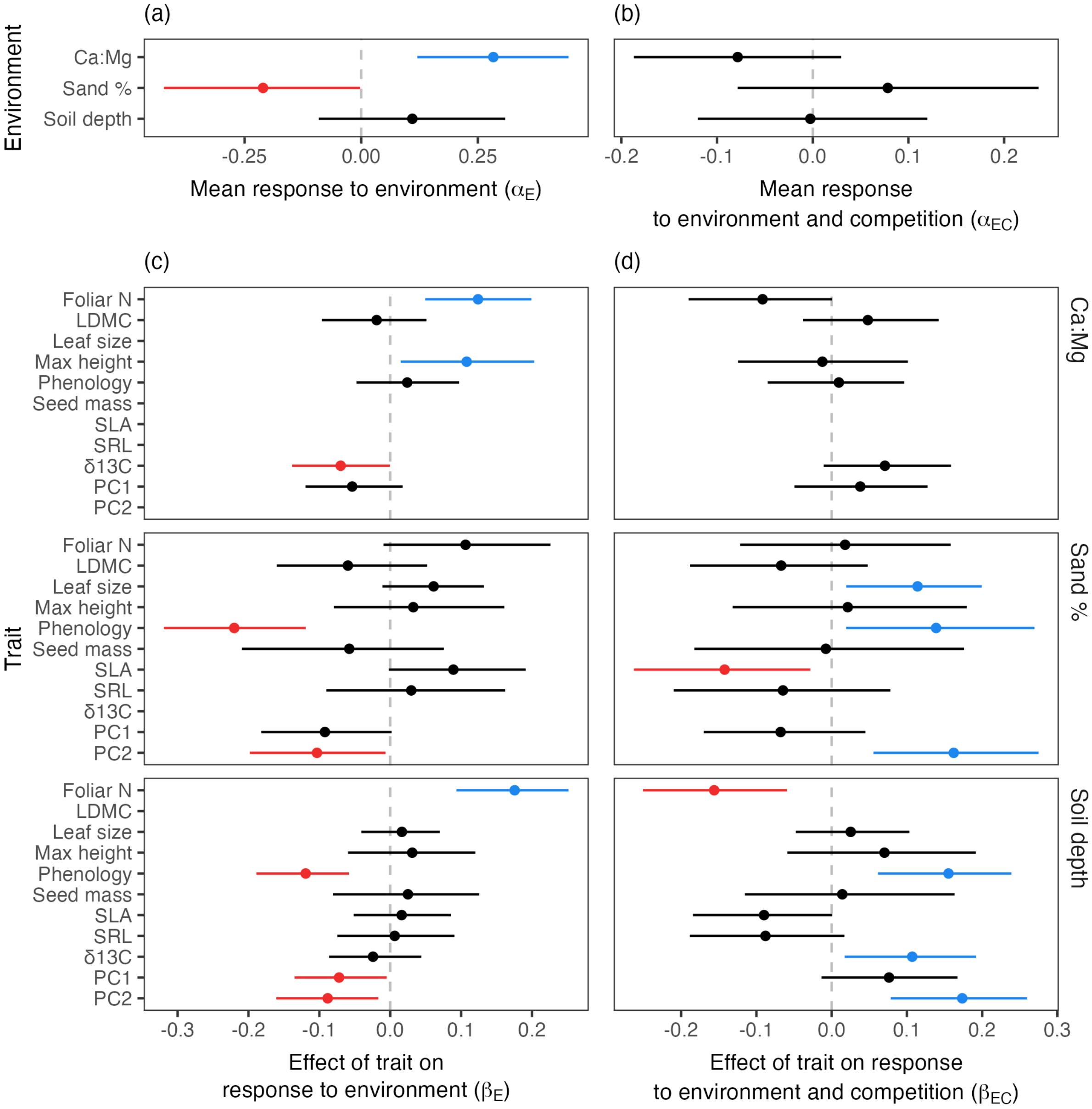

Figure B.5: Effects of functional traits on responses to environment and competition in the 2013 experiment. See Figure 2.4 for a full description of this figure. Results for models that failed to satisfy diagnostic criteria are excluded here.

B.2 Supplementary tables

Table B.1: Plant functional traits used in this study.

Trait	**Description**	**Units**
Foliar N	Leaf nitrogen content	%
LDMC	Leaf dry matter content	mg g^{-1}
Leaf size	Surface area of a single leaf (one side)	cm^2
Max height	95th percentile of typical plant height	cm
Phenology	First day of year (doy) with ~50% fruiting individuals	doy
Seed mass	Seed mass	g
SLA	Specific leaf area	cm^2 g^{-1}
SRL	Specific root length	m g^{-1}
$\delta^{13}C$	Carbon isotope discrimination	‰

Appendix C

Supplementary materials for Chapter 3

C.1 Supplementary figures

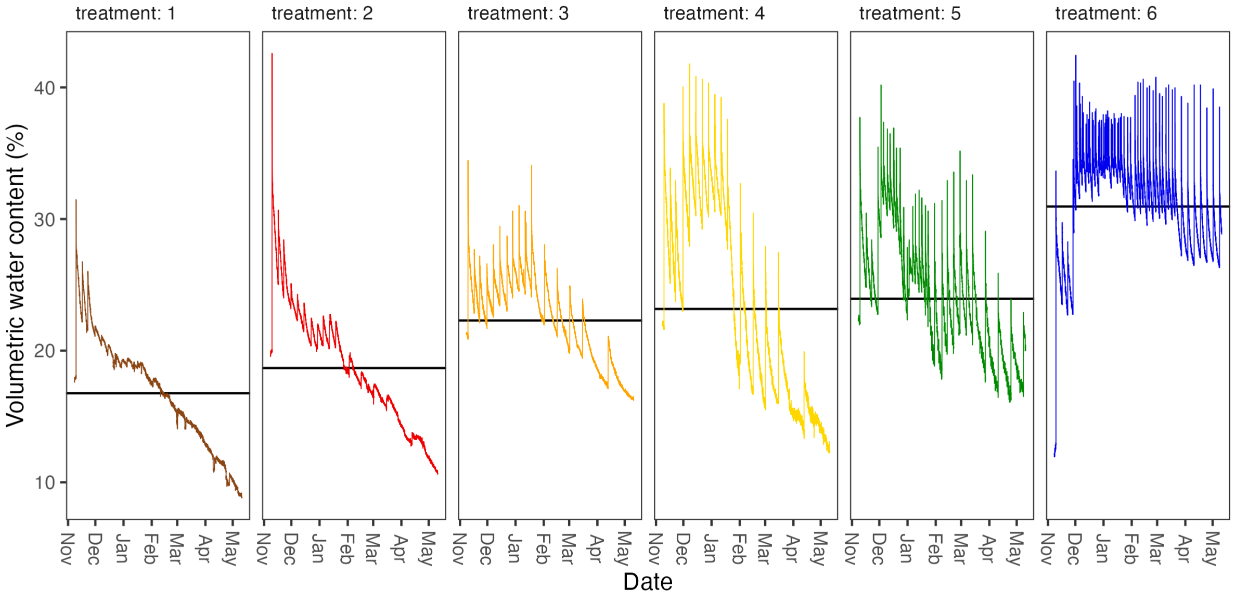

Figure C.1: Volumetric water content (VWC) under each watering treatment over the duration of the greenhouse experiment. VWC was measured at 10-minute intervals using EC5 Soil Moisture Smart Sensors (Onset Computer Corporation) in pots that contained only soil. Solid horizontal lines denote the mean VWC measured in each treatment.

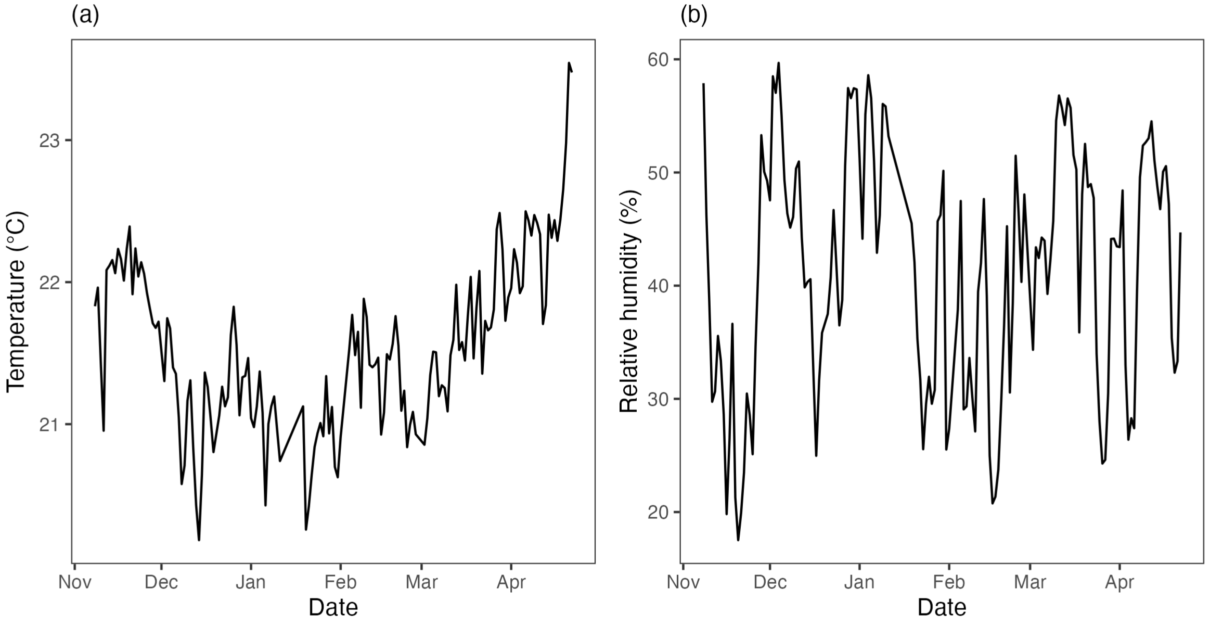

Figure C.2: Daily mean (a) temperature and (b) relative humidity in the greenhouse over the duration of the experiment. Measurements were taken at 10-minute intervals using a HOBO Temp/RH 2.5% Data Logger (Onset Computer Corporation). Note that measurements were terminated before the end of the experiment because the data logger was damaged in late April.

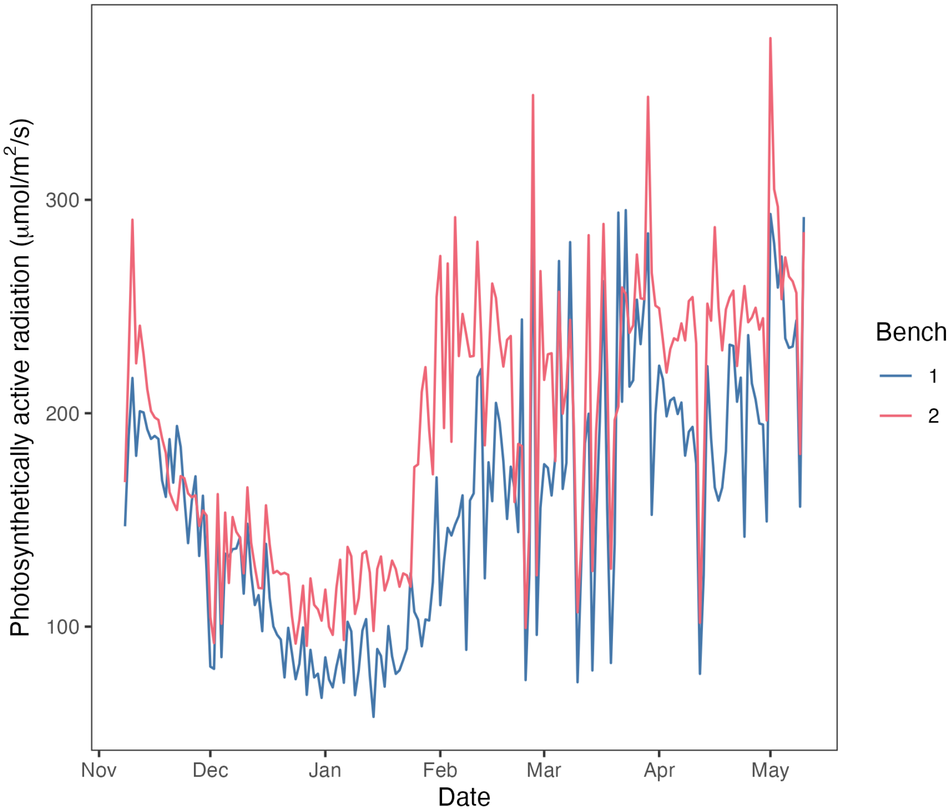

Figure C.3: Daily mean photosynthetically active radiation (PAR) during peak hours (10am–2pm) in the greenhouse over the duration of the experiment. PAR was measured at 10-minute intervals using Photosynthetic Light (PAR) Smart Sensors (Onset Computer Corporation) placed at the end of each bench.

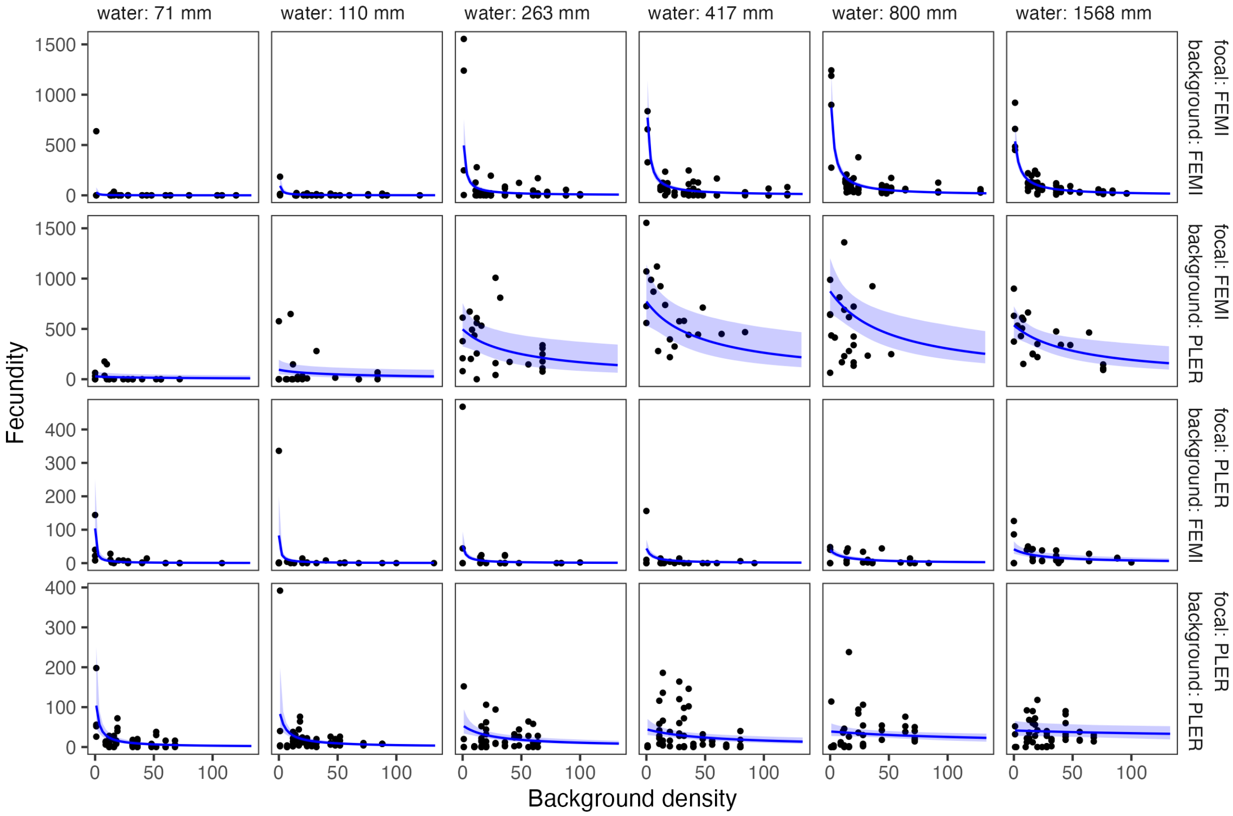

Figure C.4: Fecundity for each focal species (FEMI = *Festuca microstachys*, PLER = *Plantago erecta*) as a function of background competitor density and total water supply, characterized by fitting the competition model described in the main text to our experimental data. Data points are faceted by watering treatment (columns) and species identity (rows). Solid lines represent posterior medians computed at the total water supply level for each watering treatment. Shaded areas represent 95% quantile credible intervals.

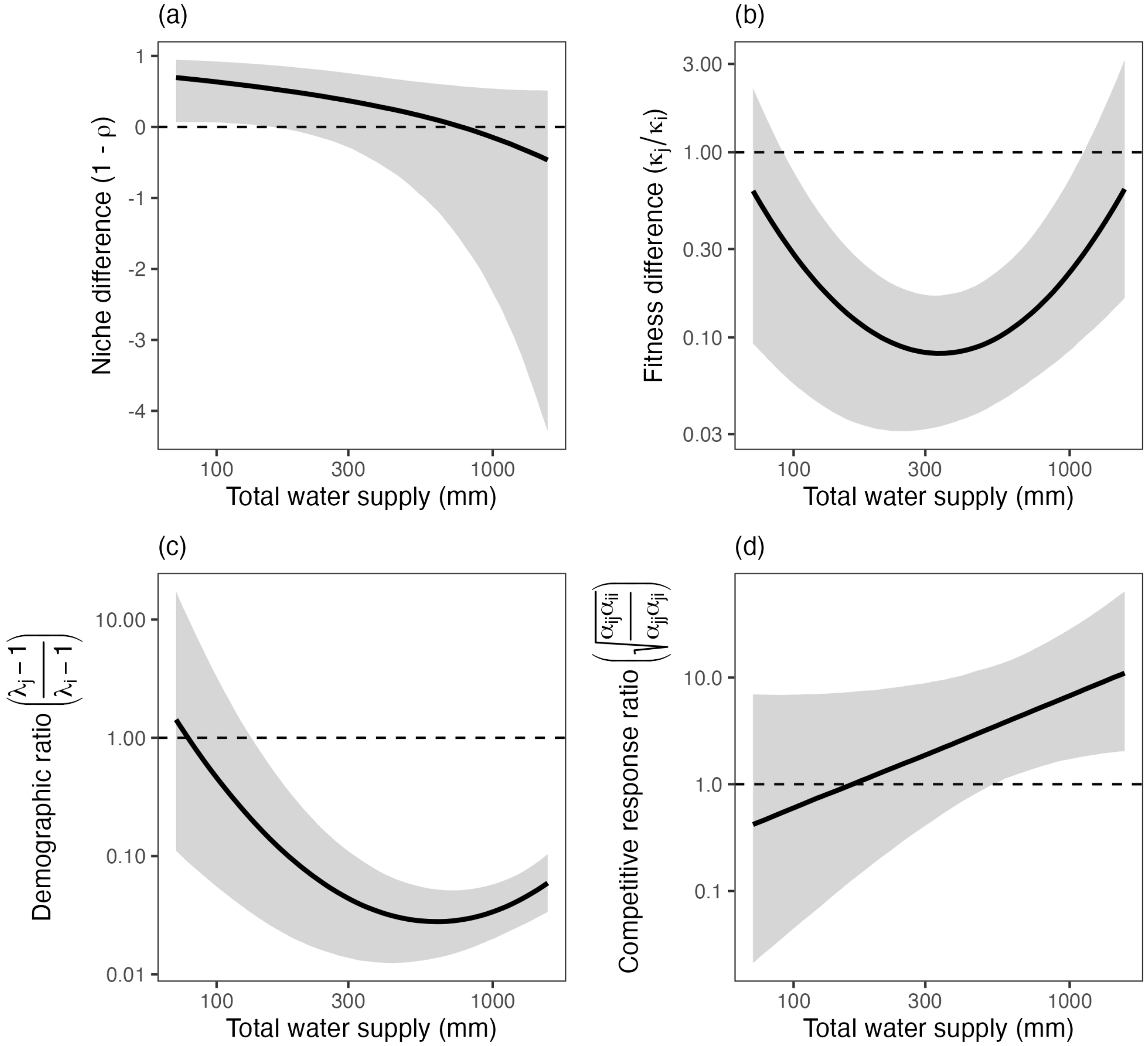

Figure C.5: Responses of the (a) niche difference, (b) fitness difference, (c) demographic ratio, and (d) competitive response ratio of the focal species (i = *Festuca microstachys*, j = *Plantago erecta*) to total water supply. Niche differences (ND) stabilize coexistence when $0 < \text{ND}$ and destabilize coexistence when $\text{ND} < 0$. Fitness differences (FD) are expressed as ratios, where *F. microstachys* has superior fitness when $\text{FD} < 1$. Fitness differences can be decomposed into the demographic ratio and competitive response ratio. See Appendix S2 for details. Solid lines represent posterior medians. Shaded areas represent 95% quantile credible intervals. Note that axes (except for niche differences) are shown on the $\log_{10}$ scale.

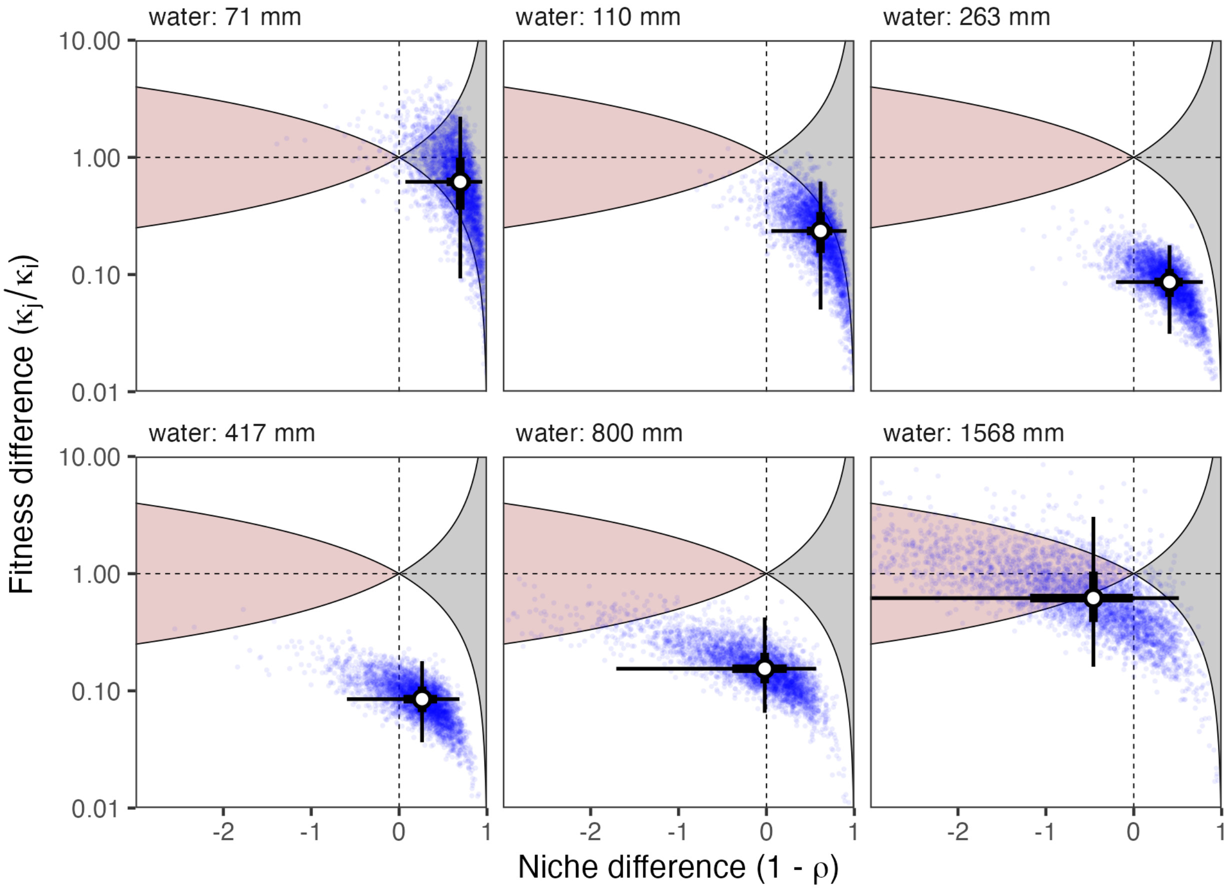

Figure C.6: Niche and fitness differences computed at the total water supply level for each watering treatment. Niche differences (ND) stabilize coexistence when $0 < ND$ and destabilize coexistence when $ND < 0$. Fitness differences (FD) are expressed as ratios, where *Festuca microstachys* has superior fitness when $FD < 1$. Species are expected to coexist in gray regions, whereas competitive exclusion is expected in white regions. Priority effects are expected in red regions. See Appendix S2 for details. Blue points are 4,000 posterior samples (thinned for visualization). White points represent posterior medians. Thick and thin lines represent 50% and 95% quantile credible intervals. Note that fitness differences are shown on the $\log_{10}$ scale and x-axes are truncated at -2.999 for visualization.

C.2 Supplementary tables

Table C.1: Total amount of water added per pot under each watering treatment in each phase of the experiment. Water addition was divided evenly over the number of weeks in each phase. Phase 0 = 11/13/22–11/26/22 (two weeks), phase 1 = 11/27/22–1/21/23 (eight weeks), phase 2 = 1/22/23–3/18/23 (eight weeks), and phase 4 = 3/19/23–5/13/23 (eight weeks).

Treatment	**Phase (mm)**				**Total (mm)**
	0	**1**	**2**	**3**	
1	33	22	11	5	71
2	33	44	22	11	110
3	33	132	66	33	263
4	33	219	110	55	417
5	33	439	219	110	800
6	33	877	439	219	1,568

Table C.2: Comparison of alternative models for fecundity (F_i). We used approximate leave-one-out cross-validation (LOO-CV) to compare the following models: the Beverton-Holt model described in the main text (BH) and five models with alternative functional forms for fecundity (1–5). ELPD_{LOO} is the LOO estimate of expected log pointwise predictive density and $\Delta\text{ELPD}_{\text{LOO}}$ is the difference in ELPD_{LOO} relative to the model in the first row, both reported with $\pm$ one standard error. With the exception of alternative model 1, these models are not clearly distinguishable from one another on the basis of estimated out-of-sample predictive performance, as one standard error of $\Delta\text{ELPD}_{\text{LOO}}$ > the mean estimate of $\Delta\text{ELPD}_{\text{LOO}}$ (Sivula et al. 2023, McLatchie et al. 2024).

Model	$\mathbf{F_i}$	$\mathbf{ELPD_{LOO}}$	$\mathbf{\Delta ELPD_{LOO}}$
4	$\lambda_i/[1+(\alpha_{ii}N_i+\alpha_{ij}N_j)^{b_i}]$	-3431.02 ± 72.99	0.00 ± 0.00
5	$\lambda_i/(1+\alpha_{ii}N_i+\alpha_{ij}N_j)^{b_i}$	-3431.15 ± 72.98	-0.13 ± 0.30
2	$\lambda_i e^{-\alpha_{ii}\log(N_i+1)-\alpha_{ij}\log(N_j+1)}$	-3432.54 ± 73.16	-1.51 ± 2.56
3	$\lambda_i/(1+N_i^{\alpha_{ii}}+N_j^{\alpha_{ij}})$	-3432.71 ± 73.25	-1.68 ± 3.23
BH	$\lambda_i/(1+\alpha_{ii}N_i+\alpha_{ij}N_j)$	-3433.24 ± 73.25	-2.22 ± 2.75
1	$\lambda_i e^{-\alpha_{ii}N_i-\alpha_{ij}N_j}$	-3470.17 ± 75.07	-39.15 ± 8.83

Table C.3: Estimated predictor terms for the parameters of alternative model 2 (Table C.2). See Table 3.1 for a full description of this table.

Species (*i*)	**Parameter**	**Term**	**Median**	**95% CI**	**Pr**
Festuca microstachys	λ_i	γ_λ	6.22	[5.72, 6.79]	1.000
		$\beta_{\lambda,1}$	2.87	[1.35, 4.26]	0.998
		$\beta_{\lambda,2}$	-1.74	[-2.28, -1.19]	1.000
	α_{ii}	γ_α	-0.06	[-0.24, 0.10]	0.780
		β_α	-0.39	[-0.82, 0.07]	0.954
	α_{ij}	γ_α	-2.54	[-4.37, -1.37]	1.000
		β_α	0.91	[-2.57, 4.97]	0.722
Plantago erecta	λ_i	γ_λ	4.14	[3.70, 4.62]	1.000
		$\beta_{\lambda,1}$	-0.81	[-1.89, 0.29]	0.935
		$\beta_{\lambda,2}$	0.54	[-0.10, 1.21]	0.953
	α_{ii}	γ_α	-1.60	[-2.60, -0.88]	1.000
		β_α	-2.57	[-4.69, -0.79]	0.999
	α_{ij}	γ_α	-0.52	[-0.77, -0.29]	1.000
		β_α	-1.05	[-1.64, -0.49]	1.000

Table C.4: Estimated predictor terms for the parameters of alternative model 3 (Table C.2). See Table 3.1 for a full description of this table.

Species (*i*)	**Parameter**	**Term**	**Median**	**95% CI**	**Pr**
Festuca microstachys	λ_i	γ_λ	6.42	[6.01, 6.86]	1.000
		$\beta_{\lambda,1}$	2.93	[1.63, 4.06]	1.000
		$\beta_{\lambda,2}$	-0.89	[-1.16, -0.61]	1.000
	α_{ii}	γ_α	-0.01	[-0.14, 0.12]	0.534
		β_α	-0.39	[-0.70, -0.06]	0.988
	α_{ij}	γ_α	-2.81	[-5.12, -1.05]	1.000
		β_α	-1.17	[-7.33, 4.99]	0.654
Plantago erecta	λ_i	γ_λ	4.65	[4.28, 5.05]	1.000
		$\beta_{\lambda,1}$	-0.47	[-1.41, 0.44]	0.848
		$\beta_{\lambda,2}$	0.24	[-0.06, 0.55]	0.943
	α_{ii}	γ_α	-1.36	[-2.31, -0.69]	1.000
		β_α	-2.36	[-4.50, -0.72]	1.000
	α_{ij}	γ_α	-0.27	[-0.52, -0.06]	0.997
		β_α	-0.98	[-1.54, -0.43]	1.000

C.3 Appendix S1: Details of statistical models

C.3.1 Main model

Here, we provide additional details about the statistical specification, fitting, and checking of our main competition model described in the main text. For Equations 3.5–3.11 in the main text, we defined prior distributions for parameters as:

$$\gamma_\lambda \sim \mathrm{Normal}(5, 2.5) \tag{C.1}$$

$$\beta_{\lambda,1},\ \beta_{\lambda,2} \sim \mathrm{Normal}(0, 10) \tag{C.2}$$

$$\sigma_{\text{block}},\ \sigma_{\text{pot}} \sim \mathrm{Exponential}(2) \tag{C.3}$$

$$\gamma_\alpha \sim \mathrm{Normal}(0, 2) \tag{C.4}$$

$$\beta_\alpha \sim \mathrm{Normal}(0, 8) \tag{C.5}$$

$$\gamma_\phi \sim \mathrm{Normal}(0, 1) \tag{C.6}$$

$$\beta_\phi \sim \mathrm{Normal}(0, 4) \tag{C.7}$$

Equations C.1–C.5 were informed by prior estimates of intrinsic fecundity (λ) and competition coefficients (α) for annual plants in our study system, including for our focal species (Godoy et al. 2014, Kraft et al. 2015b, Van Dyke et al. 2022). For example, the 95% quantile interval for γ_λ defined by Equation C.1 encompasses a larger range of λ than all estimates of this quantity given by Godoy et al. (2017). Equation C.2 allows this entire range (and more) of λ to be traversed across our experimental water supply gradient. Similar logic applies for Equations C.4 and C.5. Equations C.6 and C.7 were employed as uninformed priors that allow for a range of dispersion in observed fecundity as controlled by the precision parameter (ϕ).

For model fitting, we generally used default options for the initial values and control parameters of the CmdStan sampler via `cmdstanr` (Gabry et al. 2024). However, we increased the control parameter `adapt_delta` to 0.99 to avoid potential divergent transitions during sampling. We confirmed model convergence by validating that: (1) The sampler did not produce critical runtime warnings. (2) The $\hat{R}$ convergence diagnostic was < 1.01 for all parameters. (3) The ratio of effective sample size to total sample size (N_{eff}/N) was > 0.1 for all parameters. (4) Trace plots of post-warmup posterior samples were well-mixed and stationary for all parameters. Details of these model diagnostics are provided by Vehtari et al. (2021) and Stan Development Team (2022). We also conducted graphical posterior predictive checks to visually confirm that posterior predictions from the fitted model were able to adequately represent the distribution of our data (Gabry et al. 2019).

We note that some of the individual parameters of this model were only weakly identified. That is, given the nonlinear structure of the competition model (Equations 3.4 and 3.6 in the main text), some sets of parameters could take on different combinations of values with similar likelihoods. For instance, we observed a positive posterior correlation between the intercepts for intrinsic fecundity (γ_λ) and competition coefficients (γ_α) because an increase in one of these quantities could be coupled with an increase in the other to produce similar values of expected fecundity (μ). Importantly, we do not expect such identifiability issues to systematically bias our parameter estimates. Rather, this can inflate uncertainty in parameter estimates by creating “ridges” in likelihood space. In contrast, the nonlinear combination of model parameters (e.g., as employed when simulating population growth in invasion analyses) is well identified (Figure C.4). We understand this to be an inherent property of nonlinear models such as this one, be it for structural or practical reasons (Polansky et al. 2009, Boyko and O'Meara 2024). However, employing weakly informed priors (described above) allowed us to ameliorate the severity of nonidentifiability by avoiding regions of parameter space that are biologically nonsensical (see also Wesner and Pomeranz 2021). This was achieved without imposing hard constraints on upper bounds of parameter values, as is often done when parameterizing competition models using maximum likelihood methods (e.g., Van Dyke et al. 2022). We emphasize that, despite these challenges, our model converged without warnings and satisfied all diagnostic criteria.

C.3.2 Alternative models

We also considered models with alternative functional forms for fecundity (Equations 3.4 and 3.6 in the main text). In particular, we fit and compared a collection of models previously explored by Law and Watkinson (1987) (see also Levine and HilleRisLambers 2009) (Table C.2). Two of these models (4–5) contained an exponent, b, that modulates the curvature of the relationship between fecundity (F) and population density (N). For these models, we modeled this additional parameter for each species as a linear function of total water supply (w):

$$\log\left(b\right) = \gamma_b + \beta_b w \tag{C.8}$$

$$\gamma_b \sim \text{Normal}(0, 1) \tag{C.9}$$

$$\beta_b \sim \text{Normal}(0, 4) \tag{C.10}$$

where γ_b is an intercept and β_b is a slope coefficient.

Model fitting and checking followed the same general procedure as described for our main model. We found that alternative model 1, the Ricker model (Ricker 1954), had by far the worst fit to our data (Table C.2). All other models were effectively indistinguishable from one another in terms of estimated out-of-sample predictive performance (Table C.2). While all models suffered from some degree of nonidentifiability (discussed above), this was particularly severe for alternative models 4–5. Critically, these models resulted in nonidentifiability between biologically meaningful parameters of interest (terms for λ and α) and parameters with less clear biological meaning (terms for b). Therefore, we did not further pursue alternative models 4–5 in this study. For the remaining alternative models (2–3), we show that analyzing these models in place of our main model does not significantly alter our results (Table C.3, Table C.4). Note that competition coefficients are included as exponents in alternative models 2–3, and thus their magnitudes differ from those in our main model.

C.4 Appendix S2: Computing niche and fitness differences

We computed niche differences that stabilize coexistence, $1-\rho$, and fitness differences that drive competitive exclusion, κ_j/κ_i, following previous derivation of these quantities for our main competition model (Godoy and Levine 2014, see also Germain et al. 2018):

$$1-\rho = 1-\sqrt{\frac{\alpha_{ij}\alpha_{ji}}{\alpha_{jj}\alpha_{ii}}} \tag{C.11}$$

$$\frac{\kappa_j}{\kappa_i} = \left(\frac{\lambda_j-1}{\lambda_i-1}\right)\sqrt{\frac{\alpha_{ij}\alpha_{ii}}{\alpha_{jj}\alpha_{ji}}} \tag{C.12}$$

where ρ is niche overlap ($\rho \geq 0$). Niche differences stabilize coexistence when $1-\rho > 0$ (Chesson 2000b). Conversely, niche differences destabilize coexistence via positive frequency-dependent population growth when $1-\rho < 0$ (Mordecai 2011, Ke and Letten 2018, Grainger et al. 2019a). Fitness differences are expressed as fitness ratios, where the fitness superior is species i when $\kappa_j/\kappa_i < 1$ and species j when $\kappa_j/\kappa_i > 1$. Fitness differences can be decomposed into the demographic ratio, $(\lambda_j-1)/(\lambda_i-1)$, and competitive response ratio, $\sqrt{(\alpha_{ij}\alpha_{ii})/(\alpha_{jj}\alpha_{ji})}$ (Godoy and Levine 2014). The demographic ratio describes differences between species in fecundity, whereas the competitive response ratio describes differences in sensitivity to competition. Here, we computed niche and fitness differences with *Festuca microstachys* as species i and *Plantago erecta* as species j (Figure C.5, Figure C.6).

Long-term coexistence is predicted when niche differences are sufficiently large (i.e., niche overlap is sufficiently small) relative to fitness differences (Chesson and Kuang 2008):

$$\rho < \frac{\kappa_j}{\kappa_i} < \frac{1}{\rho} \tag{C.13}$$

Note that predicting coexistence outcomes by comparing niche and fitness differences in this way is comparable to predicting coexistence outcomes via analysis of mutual invasibility (Godoy and Levine 2014).

Bibliography

Adams, A. E., E. M. Besozzi, G. Shahrokhi, and M. A. Patten. 2022. A case for associational resistance: Apparent support for the stress gradient hypothesis varies with study system. Ecology Letters 25:202–217.

Adams, H. D., M. Guardiola-Claramonte, G. A. Barron-Gafford, J. C. Villegas, D. D. Breshears, C. B. Zou, P. A. Troch, and T. E. Huxman. 2009. Temperature sensitivity of drought-induced tree mortality portends increased regional die-off under global-change-type drought. Proceedings of the National Academy of Sciences 106:7063–7066.

Adams, W. T., and R. W. Allard. 1982. Mating system variation in *Festuca microstachys*. Evolution 36:591–595.

Adler, P. B., S. P. Ellner, and J. M. Levine. 2010. Coexistence of perennial plants: An embarrassment of niches. Ecology Letters 13:1019–1029.

Adler, P. B., A. Fajardo, A. R. Kleinhesselink, and N. J. B. Kraft. 2013. Trait-based tests of coexistence mechanisms. Ecology Letters 16:1294–1306.

Adler, P. B., J. HilleRisLambers, P. C. Kyriakidis, Q. Guan, and J. M. Levine. 2006. Climate variability has a stabilizing effect on the coexistence of prairie grasses. Proceedings of the National Academy of Sciences 103:12793–12798.

Alexander, J. M., J. M. Diez, S. P. Hart, and J. M. Levine. 2016. When climate reshuffles competitors: A call for experimental macroecology. Trends in Ecology & Evolution 31:831–841.

Alexander, J. M., J. M. Diez, and J. M. Levine. 2015. Novel competitors shape species' responses to climate change. Nature 525:515–518.

Alexander, J. M., J. M. Diez, J. Usinowicz, and S. P. Hart. 2018. Species' distributions as a coexistence problem: A response to Godsoe *et al.* Trends in Ecology & Evolution 33:143–144.

Amarasekare, P. 2003. Competitive coexistence in spatially structured environments: A synthesis. Ecology Letters 6:1109–1122.

Anderegg, L. D. L., and J. HilleRisLambers. 2019. Local range boundaries vs. large-scale trade-offs: Climatic and competitive constraints on tree growth. Ecology Letters 22:787–796.

Angert, A. L., T. E. Huxman, P. Chesson, and D. L. Venable. 2009. Functional tradeoffs determine species coexistence via the storage effect. Proceedings of the National Academy of Sciences 106:11641–11645.

Armas, C., S. Rodríguez-Echeverría, and F. I. Pugnaire. 2011. A field test of the stress-gradient hypothesis along an aridity gradient. Journal of Vegetation Science 22:818–827.

Armitage, D. W., and S. E. Jones. 2019. Negative frequency-dependent growth underlies the stable coexistence of two cosmopolitan aquatic plants. Ecology 100:e02657.

Armitage, D. W., and S. E. Jones. 2020. Coexistence barriers confine the poleward range of a globally distributed plant. Ecology Letters 23:1838–1848.

Aschehoug, E. T., R. Brooker, D. Z. Atwater, J. L. Maron, and R. M. Callaway. 2016. The mechanisms and consequences of interspecific competition among plants. Annual Review of Ecology, Evolution, and Systematics 47:263–281.

Austin, M. P., and K. P. Van Niel. 2011. Improving species distribution models for climate change studies: Variable selection and scale. Journal of Biogeography 38:1–8.

Baldwin, B. G. 2014. Origins of plant diversity in the California Floristic Province. Annual Review of Ecology, Evolution, and Systematics 45:347–369.

Baldwin, B. G., D. Goldman, D. J. Keil, R. Patterson, T. J. Rosatti, and D. H. Wilken, editors. 2012. The Jepson Manual: Vascular Plants of California. Second edition. University of California Press, Berkeley and Los Angeles, CA, USA.

Banner, K. M., K. M. Irvine, and T. J. Rodhouse. 2020. The use of Bayesian priors in Ecology: The good, the bad and the not great. Methods in Ecology and Evolution 11:882–889.

Bassett, I. J., and C. W. Crompton. 1968. Pollen morphology and chromosome numbers of the family Plantaginaceae in North America. Canadian Journal of Botany 46:349–361.

Beck, H. E., N. E. Zimmermann, T. R. McVicar, N. Vergopolan, A. Berg, and E. F. Wood. 2018. Present and future Köppen-Geiger climate classification maps at 1-km resolution. Scientific Data 5:180214.

Benito Garzón, M., T. M. Robson, and A. Hampe. 2019. ΔTraitSDMs: Species distribution models that account for local adaptation and phenotypic plasticity. New Phytologist 222:1757–1765.

Bertness, M. D., and R. Callaway. 1994. Positive interactions in communities. Trends in Ecology & Evolution 9:191–193.

Bertness, M. D., and A. M. Ellison. 1987. Determinants of pattern in a New England salt marsh plant community. Ecological Monographs 57:129–147.

Beverton, R. J. H., and S. J. Holt. 1957. On the Dynamics of Exploited Fish Populations. H. M. Stationery Office, London, UK.

Blois, J. L., P. L. Zarnetske, M. C. Fitzpatrick, and S. Finnegan. 2013. Climate change and the past, present, and future of biotic interactions. Science 341:499–504.

Blumenthal, D. M., K. E. Mueller, J. A. Kray, T. W. Ocheltree, D. J. Augustine, and K. R. Wilcox. 2020. Traits link drought resistance with herbivore defence and plant economics in semi-arid grasslands: The central roles of phenology and leaf dry matter content. Journal of Ecology 108:2336–2351.

Bontrager, M., T. Usui, J. A. Lee-Yaw, D. N. Anstett, H. A. Branch, A. L. Hargreaves, C. D. Muir, and A. L. Angert. 2021. Adaptation across geographic ranges is consistent with strong selection in marginal climates and legacies of range expansion. Evolution 75:1316–1333.

Boult, V. L., and L. C. Evans. 2021. Mechanisms matter: Predicting the ecological impacts of global change. Global Change Biology 27:1689–1691.

Bowler, D. E., C. Hof, P. Haase, I. Kröncke, O. Schweiger, R. Adrian, L. Baert, H.-G. Bauer, T. Blick, R. W. Brooker, W. Dekoninck, S. Domisch, R. Eckmann, F. Hendrickx, T. Hickler, S. Klotz, A. Kraberg, I. Kühn, S. Matesanz, A. Meschede, H. Neumann, R. O'Hara, D. J. Russell, A. F. Sell, M. Sonnewald, S. Stoll, A. Sundermann, O. Tackenberg, M. Türkay, F. Valladares, K. van Herk, R. van Klink, R. Vermeulen, K. Voigtländer, R. Wagner, E. Welk, M. Wiemers, K. H. Wiltshire, and K. Böhning-Gaese. 2017. Cross-realm assessment of climate change impacts on species' abundance trends. Nature Ecology & Evolution 1:0067.

Boyko, J. D., and B. C. O'Meara. 2024. dentist: Quantifying uncertainty by sampling points around maximum likelihood estimates. Methods in Ecology and Evolution 15:628–638.

Brady, K. U., A. R. Kruckeberg, and H. D. Bradshaw Jr. 2005. Evolutionary ecology of plant adaptation to serpentine soils. Annual Review of Ecology, Evolution, and Systematics 36:243–

266.

Bullock, J. M., R. J. Edwards, P. D. Carey, and R. J. Rose. 2000. Geographical separation of two *Ulex* species at three spatial scales: Does competition limit species' ranges? Ecography 23:257–271.

Bürkner, P.-C. 2017. brms: An R package for Bayesian multilevel models using Stan. Journal of Statistical Software 80:1–28.

Butterfield, B. J., J. B. Bradford, C. Armas, I. Prieto, and F. I. Pugnaire. 2016. Does the stress-gradient hypothesis hold water? Disentangling spatial and temporal variation in plant effects on soil moisture in dryland systems. Functional Ecology 30:10–19.

Callaway, R. M., R. W. Brooker, P. Choler, Z. Kikvidze, C. J. Lortie, R. Michalet, L. Paolini, F. I. Pugnaire, B. Newingham, E. T. Aschehoug, C. Armas, D. Kikodze, and B. J. Cook. 2002. Positive interactions among alpine plants increase with stress. Nature 417:844–848.

Cervantes-Loreto, A., A. I. Pastore, C. R. P. Brown, M. L. Marraffini, C. Aldebert, M. M. Mayfield, and D. B. Stouffer. 2023. Environmental context, parameter sensitivity, and structural sensitivity impact predictions of annual-plant coexistence. Ecological Monographs 93:e1592.

Chalmandrier, L., F. Hartig, D. C. Laughlin, H. Lischke, M. Pichler, D. B. Stouffer, and L. Pellissier. 2021. Linking functional traits and demography to model species-rich communities. Nature Communications 12:2724.

Chen, B.-M., C. M. D'Antonio, N. Molinari, and S.-L. Peng. 2018. Mechanisms of influence of invasive grass litter on germination and growth of coexisting species in California. Biological Invasions 20:1881–1897.

Chen, I.-C., J. K. Hill, R. Ohlemuller, D. B. Roy, and C. D. Thomas. 2011. Rapid range shifts of species associated with high levels of climate warming. Science 333:1024–1026.

Chesson, P. 1994. Multispecies competition in variable environments. Theoretical Population Biology 45:227–276.

Chesson, P. 2000a. General theory of competitive coexistence in spatially-varying environments. Theoretical Population Biology 58:211–237.

Chesson, P. 2000b. Mechanisms of maintenance of species diversity. Annual Review of Ecology and Systematics 31:343–366.

Chesson, P. 2018. Updates on mechanisms of maintenance of species diversity. Journal of Ecology 106:1773–1794.

Chesson, P. L. 1990. Geometry, heterogeneity and competition in variable environments. Philosophical Transactions of the Royal Society of London. Series B: Biological Sciences 330:165–173.

Chesson, P., and J. J. Kuang. 2008. The interaction between predation and competition. Nature 456:235–238.

Choat, B., S. Jansen, T. J. Brodribb, H. Cochard, S. Delzon, R. Bhaskar, S. J. Bucci, T. S. Feild, S. M. Gleason, U. G. Hacke, A. L. Jacobsen, F. Lens, H. Maherali, J. Martínez-Vilalta, S. Mayr, M. Mencuccini, P. J. Mitchell, A. Nardini, J. Pittermann, R. B. Pratt, J. S. Sperry, M. Westoby, I. J. Wright, and A. E. Zanne. 2012. Global convergence in the vulnerability of forests to drought. Nature 491:752–755.

Cohen, D. 1966. Optimizing reproduction in a randomly varying environment. Journal of Theoretical Biology 12:119–129.

Connell, J. H. 1961. The influence of interspecific competition and other factors on the distribution of the barnacle *Chthamalus stellatus*. Ecology 42:710–723.

County of Santa Barbara. 2025a. Daily rainfall data (XLS). Available at: https://www.countyofsb.org/2328/Daily-Rainfall-Data-XLS. Last accessed 23 January 2025.

County of Santa Barbara. 2025b. Monthly & yearly rainfall. Available at: https://www.countyofsb.org/2322/Monthly-Yearly-Rainfall. Last accessed 13 January 2025.

Craig, E., M. Szojka, R. Germain, and L. Shoemaker. 2023. Sink populations decouple species occupancy and persistence across a productivity gradient. Authorea 28 September 2023.

Craine, J. M., and R. Dybzinski. 2013. Mechanisms of plant competition for nutrients, water and light. Functional Ecology 27:833–840.

D'Antonio, C. M., C. Malmstrom, S. A. Reynolds, and J. Gerlach. 2007. Ecology of invasive non-native species in California grassland. Pages 67–84 *in* M. Stromberg, J. Corbin, and C. D'Antonio, editors. California Grasslands: Ecology and Management. University of California Press, Berkeley and Los Angeles, CA, USA.

Dai, A. 2013. Increasing drought under global warming in observations and models. Nature Climate Change 3:52–58.

Damschen, E. I., S. Harrison, B. M. Going, and B. L. Anacker. 2011. Climate change and plant communities on unusual soils. Pages 359–381 *in* S. Harrison and N. Rajakaruna, editors. Serpentine: The Evolution and Ecology of a Model System. University of California Press, Berkeley and Los Angeles, CA, USA.

Davis, A. J., L. S. Jenkinson, J. H. Lawton, B. Shorrocks, and S. Wood. 1998. Making mistakes when predicting shifts in species range in response to global warming. Nature 391:783–786.

DeMarche, M. L., D. F. Doak, and W. F. Morris. 2019. Incorporating local adaptation into forecasts of species' distribution and abundance under climate change. Global Change Biology 25:775–793.

Díaz, S., J. Kattge, J. H. C. Cornelissen, I. J. Wright, S. Lavorel, S. Dray, B. Reu, M. Kleyer, C. Wirth, I. Colin Prentice, E. Garnier, G. Bönisch, M. Westoby, H. Poorter, P. B. Reich, A. T. Moles, J. Dickie, A. N. Gillison, A. E. Zanne, J. Chave, S. Joseph Wright, S. N. Sheremet'ev, H. Jactel, C. Baraloto, B. Cerabolini, S. Pierce, B. Shipley, D. Kirkup, F. Casanoves, J. S. Joswig, A. Günther, V. Falczuk, N. Rüger, M. D. Mahecha, and L. D. Gorné. 2016. The global spectrum of plant form and function. Nature 529:167–171.

Dinno, A. 2024. paran: Horn's test of principal components/factors. R package version 1.5.3.

Dobzhansky, T. 1950. Evolution in the tropics. American Scientist 38:208–221.

Ehrlén, J., and W. F. Morris. 2015. Predicting changes in the distribution and abundance of species under environmental change. Ecology Letters 18:303–314.

Elith, J., and J. R. Leathwick. 2009. Species distribution models: Ecological explanation and prediction across space and time. Annual Review of Ecology, Evolution, and Systematics 40:677–697.

Engelbrecht, B. M. J., L. S. Comita, R. Condit, T. A. Kursar, M. T. Tyree, B. L. Turner, and S. P. Hubbell. 2007. Drought sensitivity shapes species distribution patterns in tropical forests. Nature 447:80–82.

Enquist, B. J., R. Condit, R. K. Peet, M. Schildhauer, and B. M. Thiers. 2016. Cyberinfrastructure for an integrated botanical information network to investigate the ecological impacts of global climate change on plant biodiversity. PeerJ Preprints 4:e2615v2.

Esch, E. H., A. C. Ashbacher, C. W. Kopp, and E. E. Cleland. 2018. Competition reverses the response of shrub seedling mortality and growth along a soil moisture gradient. Journal of Ecology 106:2096–2108.

Espeland, E. K., and K. J. Rice. 2007. Facilitation across stress gradients: The importance of local adaptation. Ecology 88:2404–2409.

Ettinger, A. K., and J. HilleRisLambers. 2013. Climate isn't everything: Competitive interactions and variation by life stage will also affect range shifts in a warming world. American Journal of Botany 100:1344–1355.

Feeley, K. J., C. Bravo-Avila, B. Fadrique, T. M. Perez, and D. Zuleta. 2020. Climate-driven changes in the composition of New World plant communities. Nature Climate Change 10:965–970.

Fernandez-Going, B. M., B. L. Anacker, and S. P. Harrison. 2012. Temporal variability in California grasslands: Soil type and species functional traits mediate response to precipitation. Ecology 93:2104–2114.

Fick, S. E., and R. J. Hijmans. 2017. WorldClim 2: New 1-km spatial resolution climate surfaces for global land areas. International Journal of Climatology 37:4302–4315.

Freschet, G. T., J. H. C. Cornelissen, R. S. P. Van Logtestijn, and R. Aerts. 2010. Evidence of the "plant economics spectrum" in a subarctic flora. Journal of Ecology 98:362–373.

Fukami, T. 2015. Historical contingency in community assembly: Integrating niches, species pools, and priority effects. Annual Review of Ecology, Evolution, and Systematics 46:1–23.

Funk, J. L., J. E. Larson, G. M. Ames, B. J. Butterfield, J. Cavender-Bares, J. Firn, D. C. Laughlin,

A. E. Sutton-Grier, L. Williams, and J. Wright. 2017. Revisiting the Holy Grail: Using plant functional traits to understand ecological processes. Biological Reviews 92:1156–1173.

Gabry, J., R. Češnovar, and A. Johnson. 2024. cmdstanr: R interface to “CmdStan”. R package version 0.8.1.

Gabry, J., D. Simpson, A. Vehtari, M. Betancourt, and A. Gelman. 2019. Visualization in Bayesian workflow. Journal of the Royal Statistical Society Series A: Statistics in Society 182:389–402.

Galmés, J., J. Flexas, R. Savé, and H. Medrano. 2007. Water relations and stomatal characteristics of Mediterranean plants with different growth forms and leaf habits: Responses to water stress and recovery. Plant and Soil 290:139–155.

Germain, R. M., M. M. Mayfield, and B. Gilbert. 2018. The “filtering” metaphor revisited: Competition and environment jointly structure invasibility and coexistence. Biology Letters 14:20180460.

Germain, R. M., S. Y. Strauss, and B. Gilbert. 2017. Experimental dispersal reveals characteristic scales of biodiversity in a natural landscape. Proceedings of the National Academy of Sciences 114:4447–4452.

Germain, R. M., J. T. Weir, and B. Gilbert. 2016. Species coexistence: Macroevolutionary relationships and the contingency of historical interactions. Proceedings of the Royal Society B: Biological Sciences 283:20160047.

Gilman, S. E., M. C. Urban, J. Tewksbury, G. W. Gilchrist, and R. D. Holt. 2010. A framework for community interactions under climate change. Trends in Ecology & Evolution 25:325–331.

Godoy, O. 2019. Coexistence theory as a tool to understand biological invasions in species interaction networks: Implications for the study of novel ecosystems. Functional Ecology 33:1190–

1201.

Godoy, O., N. J. B. Kraft, and J. M. Levine. 2014. Phylogenetic relatedness and the determinants of competitive outcomes. Ecology Letters 17:836–844.

Godoy, O., N. J. B. Kraft, and J. M. Levine. 2017. Dataset Godoy et al. 2014 Ecology Letters. figshare. https://doi.org/10.6084/m9.figshare.4793488.v3.

Godoy, O., and J. M. Levine. 2014. Phenology effects on invasion success: Insights from coupling field experiments to coexistence theory. Ecology 95:726–736.

Godsoe, W., J. Jankowski, R. D. Holt, and D. Gravel. 2017. Integrating biogeography with contemporary niche theory. Trends in Ecology & Evolution 32:488–499.

Goldberg, D. E., and A. M. Barton. 1992. Patterns and consequences of interspecific competition in natural communities: A review of field experiments with plants. The American Naturalist 139:771–801.

Grainger, T. N., A. D. Letten, B. Gilbert, and T. Fukami. 2019a. Applying modern coexistence theory to priority effects. Proceedings of the National Academy of Sciences 116:6205–6210.

Grainger, T. N., J. M. Levine, and B. Gilbert. 2019b. The invasion criterion: A common currency for ecological research. Trends in Ecology & Evolution 34:925–935.

Gräler, B., E. Pebesma, and G. Heuvelink. 2016. Spatio-temporal interpolation using gstat. The R Journal 8:204–218.

Gram, W. K., E. T. Borer, K. L. Cottingham, E. W. Seabloom, V. L. Boucher, L. Goldwasser, F. Micheli, B. E. Kendall, and R. S. Burton. 2004. Distribution of plants in a California serpentine grassland: Are rocky hummocks spatial refuges for native species? Plant Ecology 172:159–171.

Grime, J. P. 1977. Evidence for the existence of three primary strategies in plants and its relevance to ecological and evolutionary theory. The American Naturalist 111:1169–1194.

Hallett, L. M., L. Aoyama, G. Barabás, B. Gilbert, L. Larios, N. Shackelford, C. M. Werner, O. Godoy, E. R. Ladouceur, J. E. Lucero, C. P. Weiss-Lehman, J. M. Chase, C. Chu, W. S. Harpole, M. M. Mayfield, A. M. Faist, and L. G. Shoemaker. 2023. Restoration ecology through the lens of coexistence theory. Trends in Ecology & Evolution 38:1085–1096.

Hallett, L. M., L. G. Shoemaker, C. T. White, and K. N. Suding. 2019. Rainfall variability maintains grass-forb species coexistence. Ecology Letters 22:1658–1667.

Hamilton, J. G., C. Holzapfel, and B. E. Mahall. 1999. Coexistence and interference between a native perennial grass and non-native annual grasses in California. Oecologia 121:518–526.

Harrison, S., H. Cornell, and K. A. Moore. 2010. Spatial niches and coexistence: Testing theory with tarweeds. Ecology 91:2141–2150.

Harrison, S., E. Damschen, B. Fernandez-Going, A. Eskelinen, and S. Copeland. 2015. Plant communities on infertile soils are less sensitive to climate change. Annals of Botany 116:1017–1022.

Harrison, S., M. J. Spasojevic, and D. Li. 2020. Climate and plant community diversity in space and time. Proceedings of the National Academy of Sciences 117:4464–4470.

Harsch, M. A., and J. HilleRisLambers. 2016. Climate warming and seasonal precipitation change interact to limit species distribution shifts across western North America. PLoS ONE 11:e0159184.

Hart, S. P., R. P. Freckleton, and J. M. Levine. 2018. How to quantify competitive ability. Journal of Ecology 106:1902–1909.

Hart, S. P., J. Usinowicz, and J. M. Levine. 2017. The spatial scales of species coexistence. Nature Ecology & Evolution 1:1066–1073.

Haston, L., and J. Michaelsen. 1997. Spatial and temporal variability of southern California precipitation over the last 400 yr and relationships to atmospheric circulation patterns. Journal of Climate 10:1836–1852.

Hayashi, K. T., and N. J. B. Kraft. 2024a. Data and code for "Spatially variable competition contributes to mismatched responses of plant fitness and occurrence to environmental gradients." Zenodo. https://doi.org/10.5281/zenodo.12978683.

Hayashi, K. T., and N. J. B. Kraft. 2024b. Spatially variable competition contributes to mismatched responses of plant fitness and occurrence to environmental gradients. bioRxiv 14 November, 2024.

HilleRisLambers, J., M. A. Harsch, A. K. Ettinger, K. R. Ford, and E. J. Theobald. 2013. How will biotic interactions influence climate change-induced range shifts? Annals of the New York Academy of Sciences 1297:112–125.

HilleRisLambers, J., S. G. Yelenik, B. P. Colman, and J. M. Levine. 2010. California annual grass invaders: The drivers or passengers of change? Journal of Ecology 98:1147–1156.

Hobbs, R. J., S. Yates, and H. A. Mooney. 2007. Long-term data reveal complex dynamics in grassland in relation to climate and disturbance. Ecological Monographs 77:545–568.

Holt, R. D. 2009. Bringing the Hutchinsonian niche into the 21st century: Ecological and evolutionary perspectives. Proceedings of the National Academy of Sciences 106:19659–19665.

Horn, J. L. 1965. A rationale and test for the number of factors in factor analysis. Psychometrika 30:179–185.

Hulshof, C. M., C. Violle, M. J. Spasojevic, B. McGill, E. Damschen, S. Harrison, and B. J. Enquist. 2013. Intra-specific and inter-specific variation in specific leaf area reveal the importance of abiotic and biotic drivers of species diversity across elevation and latitude. Journal of Vegetation Science 24:921–931.

Hülsmann, L., R. A. Chisholm, and F. Hartig. 2021. Is variation in conspecific negative density dependence driving tree diversity patterns at large scales? Trends in Ecology & Evolution 36:151–163.

von Humboldt, A., and A. Bonpland. 1805. Essai sur la Géographie des Plantes: Accompagné d'un Tableau Physique des Régions Équinoxiales. Levrault, Schoell et Compagnie, Paris, France.

Hutchinson, G. E. 1961. The paradox of the plankton. The American Naturalist 95:137–145.

Hutchinson, G. E. 1978. An Introduction to Population Ecology. Yale University Press, New Haven, CT, USA.

Johnson, E. C., O. Godoy, and A. Hastings. 2023. The storage effect is not about bet-hedging or population stage-structure. arXiv 12 January, 2023.

Johnson, E. C., and A. Hastings. 2022. Towards a heuristic understanding of the storage effect. Ecology Letters 25:2347–2358.

Jones, N. T., and B. Gilbert. 2016. Biotic forcing: The push–pull of plant ranges. Plant Ecology 217:1331–1344.

Kandlikar, G. 2021. gauravsk/sedgwick-CWM-demography: Archived version of code and data. Zenodo. https://doi.org/10.5281/zenodo.5796738.

Kandlikar, G. S., A. R. Kleinhesselink, and N. J. B. Kraft. 2022. Functional traits predict species responses to environmental variation in a California grassland annual plant community. Journal of Ecology 110:833–844.

Kandlikar, G. S., X. Yan, J. M. Levine, and N. J. B. Kraft. 2020. Soil microbes generate stronger fitness differences than stabilization among California annual plants. The American Naturalist 197:E30–E39.

Kannenberg, L. W., and R. W. Allard. 1967. Population studies in predominantly self-pollinated species. VIII. Genetic variability in the *Festuca microstachys* complex. Evolution 21:227–240.

Kay, M. 2024a. ggdist: Visualizations of distributions and uncertainty. R package version 3.3.2.

Kay, M. 2024b. ggdist: Visualizations of distributions and uncertainty in the grammar of graphics. IEEE Transactions on Visualization and Computer Graphics 30:414–424.

Ke, P.-J., and A. D. Letten. 2018. Coexistence theory and the frequency-dependence of priority effects. Nature Ecology & Evolution 2:1691–1695.

Kearney, M., and W. Porter. 2009. Mechanistic niche modelling: Combining physiological and spatial data to predict species' ranges. Ecology Letters 12:334–350.

Kelly, A. E., and M. L. Goulden. 2008. Rapid shifts in plant distribution with recent climate change. Proceedings of the National Academy of Sciences 105:11823–11826.

Körner, C. 2003. Limitation and stress – always or never? Journal of Vegetation Science 14:141–143.

Kraft, N. J. B., P. B. Adler, O. Godoy, E. C. James, S. Fuller, and J. M. Levine. 2015a. Community assembly, coexistence and the environmental filtering metaphor. Functional Ecology 29:592–599.

Kraft, N. J. B., O. Godoy, and J. M. Levine. 2015b. Plant functional traits and the multidimensional nature of species coexistence. Proceedings of the National Academy of Sciences 112:797–802.

Kramer-Walter, K. R., P. J. Bellingham, T. R. Millar, R. D. Smissen, S. J. Richardson, and D. C. Laughlin. 2016. Root traits are multidimensional: Specific root length is independent from root tissue density and the plant economic spectrum. Journal of Ecology 104:1299–1310.

Kruschke, J. K. 2015. Doing Bayesian Data Analysis: A Tutorial with R, JAGS, and Stan. Second edition. Academic Press, Burlington, MA, USA.

Kuang, J. J., and P. Chesson. 2009. Coexistence of annual plants: Generalist seed predation weakens the storage effect. Ecology 90:170–182.

Kunstler, G., D. Falster, D. A. Coomes, F. Hui, R. M. Kooyman, D. C. Laughlin, L. Poorter, M. Vanderwel, G. Vieilledent, S. J. Wright, M. Aiba, C. Baraloto, J. Caspersen, J. H. C. Cornelissen, S. Gourlet-Fleury, M. Hanewinkel, B. Herault, J. Kattge, H. Kurokawa, Y. Onoda, J. Peñuelas, H. Poorter, M. Uriarte, S. Richardson, P. Ruiz-Benito, I.-F. Sun, G. Ståhl, N. G. Swenson, J. Thompson, B. Westerlund, C. Wirth, M. A. Zavala, H. Zeng, J. K. Zimmerman, N. E. Zimmermann, and M. Westoby. 2016. Plant functional traits have globally consistent effects on competition. Nature 529:204–207.

LaForgia, M. L. 2021. Impacts of invasive annual grasses and their litter vary by native functional strategy. Biological Invasions 23:2621–2633.

LaManna, J. A., S. A. Mangan, A. Alonso, N. A. Bourg, W. Y. Brockelman, S. Bunyavejchewin, L.-W. Chang, J.-M. Chiang, G. B. Chuyong, K. Clay, R. Condit, S. Cordell, S. J. Davies, T. J. Furniss, C. P. Giardina, I. A. U. N. Gunatilleke, C. V. S. Gunatilleke, F. He, R. W. Howe, S. P. Hubbell, C.-F. Hsieh, F. M. Inman-Narahari, D. Janík, D. J. Johnson, D. Kenfack, L. Korte, K. Král, A. J. Larson, J. A. Lutz, S. M. McMahon, W. J. McShea, H. R. Memiaghe, A. Nathalang, V. Novotny, P. S. Ong, D. A. Orwig, R. Ostertag, G. G. Parker, R. P. Phillips, L. Sack, I.-F. Sun,

J. S. Tello, D. W. Thomas, B. L. Turner, D. M. Vela Díaz, T. Vrška, G. D. Weiblen, A. Wolf, S. Yap, and J. A. Myers. 2017. Plant diversity increases with the strength of negative density dependence at the global scale. Science 356:1389–1392.

Laughlin, D. C., R. T. Strahan, P. B. Adler, and M. M. Moore. 2018. Survival rates indicate that correlations between community-weighted mean traits and environments can be unreliable estimates of the adaptive value of traits. Ecology Letters 21:411–421.

Law, R., and A. R. Watkinson. 1987. Response-surface analysis of two-species competition: An experiment on *Phleum arenarium* and *Vulpia fasciculata*. Journal of Ecology 75:871–886.

Legault, G., M. E. Bitters, A. Hastings, and B. A. Melbourne. 2020. Interspecific competition slows range expansion and shapes range boundaries. Proceedings of the National Academy of Sciences 117:26854–26860.

Leibold, M. A., M. Holyoak, N. Mouquet, P. Amarasekare, J. M. Chase, M. F. Hoopes, R. D. Holt, J. B. Shurin, R. Law, D. Tilman, M. Loreau, and A. Gonzalez. 2004. The metacommunity concept: A framework for multi-scale community ecology. Ecology Letters 7:601–613.

Lemoine, N. P. 2019. Moving beyond noninformative priors: Why and how to choose weakly informative priors in Bayesian analyses. Oikos 128:912–928.

Letten, A. D., M. K. Dhami, P.-J. Ke, and T. Fukami. 2018. Species coexistence through simultaneous fluctuation-dependent mechanisms. Proceedings of the National Academy of Sciences 115:6745–6750.

Levine, J. I., J. M. Levine, T. Gibbs, and S. W. Pacala. 2022. Competition for water and species coexistence in phenologically structured annual plant communities. Ecology Letters 25:1110–1125.

Levine, J. M. 2016. A trail map for trait-based studies. Nature 529:163–164.

Levine, J. M., J. Bascompte, P. B. Adler, and S. Allesina. 2017. Beyond pairwise mechanisms of species coexistence in complex communities. Nature 546:56–64.

Levine, J. M., and J. HilleRisLambers. 2009. The importance of niches for the maintenance of species diversity. Nature 461:254–257.

Levine, J. M., and M. Rees. 2004. Effects of temporal variability on rare plant persistence in annual systems. The American Naturalist 164:350–363.

Liancourt, P., L. A. Spence, D. S. Song, A. Lkhagva, A. Sharkhuu, B. Boldgiv, B. R. Helliker, P. S. Petraitis, and B. B. Casper. 2013. Plant response to climate change varies with topography, interactions with neighbors, and ecotype. Ecology 94:444–453.

Lortie, C. J., R. W. Brooker, Z. Kikvidze, and R. M. Callaway. 2004. The value of stress and limitation in an imperfect world: A reply to Körner. Journal of Vegetation Science 15:577–580.

Lortie, C. J., and R. M. Callaway. 2006. Re-analysis of meta-analysis: Support for the stress-gradient hypothesis. Journal of Ecology 94:7–16.

Louthan, A. M., D. F. Doak, and A. L. Angert. 2015. Where and when do species interactions set range limits? Trends in Ecology & Evolution 30:780–792.

Louthan, A. M., R. M. Pringle, J. R. Goheen, T. M. Palmer, W. F. Morris, and D. F. Doak. 2018. Aridity weakens population-level effects of multiple species interactions on *Hibiscus meyeri*. Proceedings of the National Academy of Sciences 115:543–548.

Ludwig, F., T. E. Dawson, H. H. T. Prins, F. Berendse, and H. de Kroon. 2004. Below-ground competition between trees and grasses may overwhelm the facilitative effects of hydraulic lift.

Ecology Letters 7:623–631.

Lyu, S., and J. M. Alexander. 2022. Competition contributes to both warm and cool range edges. Nature Communications 13:2502.

MacArthur, R. H. 1972. Geographical Ecology: Patterns in the Distribution of Species. Princeton University Press, Princeton, NJ, USA.

MacArthur, R., and R. Levins. 1967. The limiting similarity, convergence, and divergence of coexisting species. The American Naturalist 101:377–385.

MacDonald, N., and A. R. Watkinson. 1981. Models of an annual plant population with a seedbank. Journal of Theoretical Biology 93:643–653.

Maestre, F. T., R. M. Callaway, F. Valladares, and C. J. Lortie. 2009. Refining the stress-gradient hypothesis for competition and facilitation in plant communities. Journal of Ecology 97:199–205.

Maestre, F. T., F. Valladares, and J. F. Reynolds. 2005. Is the change of plant–plant interactions with abiotic stress predictable? A meta-analysis of field results in arid environments. Journal of Ecology 93:748–757.

Maitner, B. S., B. Boyle, N. Casler, R. Condit, J. Donoghue, S. M. Durán, D. Guaderrama, C. E. Hinchliff, P. M. Jørgensen, N. J. B. Kraft, B. McGill, C. Merow, N. Morueta-Holme, R. K. Peet, B. Sandel, M. Schildhauer, S. A. Smith, J.-C. Svenning, B. Thiers, C. Violle, S. Wiser, and B. J. Enquist. 2018. The BIEN R package: A tool to access the Botanical Information and Ecology Network (BIEN) database. Methods in Ecology and Evolution 9:373–379.

Makowski, D., M. S. Ben-Shachar, and D. Lüdecke. 2019. bayestestR: Describing effects and their uncertainty, existence and significance within the Bayesian framework. Journal of Open

Source Software 4:1541.

Marks, C. O., and M. J. Lechowicz. 2006. Alternative designs and the evolution of functional diversity. The American Naturalist 167:55–66.

Matías, L., O. Godoy, L. Gómez-Aparicio, and I. M. Pérez-Ramos. 2018. An experimental extreme drought reduces the likelihood of species to coexist despite increasing intransitivity in competitive networks. Journal of Ecology 106:826–837.

Mayfield, M. M., and J. M. Levine. 2010. Opposing effects of competitive exclusion on the phylogenetic structure of communities. Ecology Letters 13:1085–1093.

McGill, B. J., B. J. Enquist, E. Weiher, and M. Westoby. 2006. Rebuilding community ecology from functional traits. Trends in Ecology & Evolution 21:178–185.

McGuire, R. M. 2023. Elucidating the effects of warming on ectotherms through a trait-based approach: Experimental studies on a pest of stored products. PhD thesis, University of California, Los Angeles, Los Angeles, CA, USA.

McLatchie, Y., S. Rögnvaldsson, F. Weber, and A. Vehtari. 2024. Advances in projection predictive inference. arXiv 6 August 2024.

Merow, C., A. M. Latimer, A. M. Wilson, S. M. McMahon, A. G. Rebelo, and J. A. Silander. 2014. On using integral projection models to generate demographically driven predictions of species' distributions: Development and validation using sparse data. Ecography 37:1167–1183.

Midolo, G., and C. Wellstein. 2020. Plant performance and survival across transplant experiments depend upon temperature and precipitation change along elevation. Journal of Ecology 108:2107–2120.

Mod, H. K., D. Scherrer, M. Luoto, and A. Guisan. 2016. What we use is not what we know:

Environmental predictors in plant distribution models. Journal of Vegetation Science 27:1308–1322.

Monroe, J. G., H. Cai, and D. L. Des Marais. 2021. Diversity in nonlinear responses to soil moisture shapes evolutionary constraints in *Brachypodium*. G3 Genes|Genomes|Genetics 11:jkab334.

Moore, K. A., and S. C. Elmendorf. 2011. Plant competition and facilitation in systems with strong environmental gradients. Pages 223–236 *in* S. Harrison and N. Rajakaruna, editors. Serpentine: The Evolution and Ecology of a Model System. University of California Press, Berkeley and Los Angeles, CA, USA.

Mordecai, E. A. 2011. Pathogen impacts on plant communities: Unifying theory, concepts, and empirical work. Ecological Monographs 81:429–441.

Morin, X., and I. Chuine. 2006. Niche breadth, competitive strength and range size of tree species: A trade-off based framework to understand species distribution. Ecology Letters 9:185–195.

Muthukrishnan, R., L. L. Sullivan, A. K. Shaw, and J. D. Forester. 2020. Trait plasticity alters the range of possible coexistence conditions in a competition-colonisation trade-off. Ecology Letters 23:791–799.

Oksanen, J., G. L. Simpson, F. G. Blanchet, R. Kindt, P. Legendre, P. R. Minchin, R. B. O'Hara, P. Solymos, M. H. H. Stevens, E. Szoecs, H. Wagner, M. Barbour, M. Bedward, B. Bolker, D. Borcard, G. Carvalho, M. Chirico, M. De Caceres, S. Durand, H. B. A. Evangelista, R. FitzJohn, M. Friendly, B. Furneaux, G. Hannigan, M. O. Hill, L. Lahti, D. McGlinn, M.-H. Ouellette, E. Ribeiro Cunha, T. Smith, A. Stier, C. J. F. Ter Braak, and J. Weedon. 2024. vegan: Community ecology package. R package version 2.6-8.

Paananen, T., J. Piironen, P.-C. Bürkner, and A. Vehtari. 2021. Implicitly adaptive importance sampling. Statistics and Computing 31:16.

Parkhurst, D. F., and O. L. Loucks. 1972. Optimal leaf size in relation to environment. Journal of Ecology 60:505–537.

Parmesan, C., and G. Yohe. 2003. A globally coherent fingerprint of climate change impacts across natural systems. Nature 421:37–42.

Pearse, I. S., J. M. Aguilar, and S. Y. Strauss. 2020. Life-history plasticity and water-use tradeoffs associated with drought resistance in a clade of California jewelflowers. The American Naturalist 195:691–704.

Pearson, R. G., and T. P. Dawson. 2003. Predicting the impacts of climate change on the distribution of species: Are bioclimate envelope models useful? Global Ecology and Biogeography 12:361–371.

Pebesma, E. J. 2004. Multivariable geostatistics in S: The gstat package. Computers & Geosciences 30:683–691.

Pérez-Ramos, I. M., L. Matías, L. Gómez-Aparicio, and Ó. Godoy. 2019. Functional traits and phenotypic plasticity modulate species coexistence across contrasting climatic conditions. Nature Communications 10:2555.

Piedallu, C., J.-C. Gégout, V. Perez, and F. Lebourgeois. 2013. Soil water balance performs better than climatic water variables in tree species distribution modelling. Global Ecology and Biogeography 22:470–482.

Pitt, M. D., and H. F. Heady. 1978. Responses of annual vegetation to temperature and rainfall patterns in northern California. Ecology 59:336–350.

Polansky, L., P. de Valpine, J. O. Lloyd-Smith, and W. M. Getz. 2009. Likelihood ridges and multimodality in population growth rate models. Ecology 90:2313–2320.

Price, T. D., and M. Kirkpatrick. 2009. Evolutionarily stable range limits set by interspecific competition. Proceedings of the Royal Society B: Biological Sciences 276:1429–1434.

Pulliam, H. R. 2000. On the relationship between niche and distribution. Ecology Letters 3:349–361.

QGIS Development Team. 2020. QGIS Geographic Information System. Version 3.16. QGIS Association.

R Core Team. 2024. R: A language and environment for statistical computing. Version 4.4.1. R Foundation for Statistical Computing, Vienna, Austria.

Rees, M. 2013. Competition on productivity gradients – what do we expect? Ecology Letters 16:291–298.

Ricker, W. E. 1954. Stock and recruitment. Journal of the Fisheries Research Board of Canada 11:559–623.

Rosenblad, K. C., K. C. Baer, and D. D. Ackerly. 2023. Climate change, tree demography, and thermophilization in western US forests. Proceedings of the National Academy of Sciences 120:e2301754120.

Ryser, P. 1996. The importance of tissue density for growth and life span of leaves and roots: A comparison of five ecologically contrasting grasses. Functional Ecology 10:717–723.

Schemske, D. W., G. G. Mittelbach, H. V. Cornell, J. M. Sobel, and K. Roy. 2009. Is there a latitudinal gradient in the importance of biotic interactions? Annual Review of Ecology, Evolution, and Systematics 40:245–269.

Schimper, A. F. W. 1903. Plant-Geography upon a Physiological Basis. (W. R. Fisher, Tran.).

Clarendon Press, Oxford, UK.

Schurr, F. M., J. Pagel, J. S. Cabral, J. Groeneveld, O. Bykova, R. B. O'Hara, F. Hartig, W. D. Kissling, H. P. Linder, G. F. Midgley, B. Schröder, A. Singer, and N. E. Zimmermann. 2012. How to understand species' niches and range dynamics: A demographic research agenda for biogeography. Journal of Biogeography 39:2146–2162.

Seabloom, E. W., E. T. Borer, V. L. Boucher, R. S. Burton, K. L. Cottingham, L. Goldwasser, W. K. Gram, B. E. Kendall, and F. Micheli. 2003a. Competition, seed limitation, disturbance, and reestablishment of California native annual forbs. Ecological Applications 13:575–592.

Seabloom, E. W., W. S. Harpole, O. J. Reichman, and D. Tilman. 2003b. Invasion, competitive dominance, and resource use by exotic and native California grassland species. Proceedings of the National Academy of Sciences 100:13384–13389.

Sears, A. L. W., and P. Chesson. 2007. New methods for quantifying the spatial storage effect: An illustration with desert annuals. Ecology 88:2240–2247.

Sehler, R., J. Li, J. Reager, and H. Ye. 2019. Investigating relationship between soil moisture and precipitation globally using remote sensing observations. Journal of Contemporary Water Research & Education 168:106–118.

Seibt, U., A. Rajabi, H. Griffiths, and J. A. Berry. 2008. Carbon isotopes and water use efficiency: Sense and sensitivity. Oecologia 155:441–454.

Sexton, J. P., P. J. McIntyre, A. L. Angert, and K. J. Rice. 2009. Evolution and ecology of species range limits. Annual Review of Ecology, Evolution, and Systematics 40:415–436.

Siefert, A., and D. C. Laughlin. 2023. Estimating the net effect of functional traits on fitness across species and environments. Methods in Ecology and Evolution 14:1035–1048.

Siepielski, A. M., and M. A. McPeek. 2010. On the evidence for species coexistence: A critique of the coexistence program. Ecology 91:3153–3164.

Simha, A., C. J. Pardo-De La Hoz, and L. N. Carley. 2022. Moving beyond the "diversity paradox": The limitations of competition-based frameworks in understanding species diversity. The American Naturalist 200:89–100.

Singh, D., M. Ting, A. A. Scaife, and N. Martin. 2018. California winter precipitation predictability: Insights from the anomalous 2015–2016 and 2016–2017 seasons. Geophysical Research Letters 45:9972–9980.

Sivula, T., M. Magnusson, A. A. Matamoros, and A. Vehtari. 2023. Uncertainty in Bayesian leave-one-out cross-validation based model comparison. arXiv 21 October 2023.

Snyder, R. E. 2008. When does environmental variation most influence species coexistence? Theoretical Ecology 1:129–139.

Stan Development Team. 2022, March 10. Runtime warnings and convergence problems. Available at: https://mc-stan.org/misc/warnings.html. Last accessed 8 April 2024.

Stan Development Team. 2024. Stan modeling language users guide and reference manual, version 2.35. Available at: https://mc-stan.org. Last accessed 6 October 2024.

Stanton-Geddes, J., P. Tiffin, and R. G. Shaw. 2012. Role of climate and competitors in limiting fitness across range edges of an annual plant. Ecology 93:1604–1613.

Stomp, M., M. A. van Dijk, H. M. J. van Overzee, M. T. Wortel, C. A. M. Sigon, M. Egas, H. Hoogveld, H. J. Gons, and J. Huisman. 2008. The timescale of phenotypic plasticity and its impact on competition in fluctuating environments. The American Naturalist 172:E169–E185.

Stouffer, D. B. 2022. A critical examination of models of annual-plant population dynamics and density-dependent fecundity. Methods in Ecology and Evolution 13:2516–2530.

Stump, S. M., and D. A. Vasseur. 2023. Reexamining the storage effect: Why temporal variation in abiotic factors seems unlikely to cause coexistence. Ecological Monographs 93:e1585.

Sunday, J. M., J. R. Bernhardt, C. D. G. Harley, and M. I. O'Connor. 2024. Temperature dependence of competitive ability is cold-shifted compared to that of growth rate in marine phytoplankton. Ecology Letters 27:e14337.

Svenning, J.-C., D. Gravel, R. D. Holt, F. M. Schurr, W. Thuiller, T. Münkemüller, K. H. Schiffers, S. Dullinger, T. C. Edwards, T. Hickler, S. I. Higgins, J. E. M. S. Nabel, J. Pagel, and S. Normand. 2014. The influence of interspecific interactions on species range expansion rates. Ecography 37:1198–1209.

Swain, D. L., B. Langenbrunner, J. D. Neelin, and A. Hall. 2018. Increasing precipitation volatility in twenty-first-century California. Nature Climate Change 8:427–433.

Taniguchi, Y., and S. Nakano. 2000. Condition-specific competition: Implications for the altitudinal distribution of stream fishes. Ecology 81:2027–2039.

Thuiller, W., T. Münkemüller, K. H. Schiffers, D. Georges, S. Dullinger, V. M. Eckhart, T. C. Edwards, D. Gravel, G. Kunstler, C. Merow, K. Moore, C. Piedallu, S. Vissault, N. E. Zimmermann, D. Zurell, and F. M. Schurr. 2014. Does probability of occurrence relate to population dynamics? Ecography 37:1155–1166.

Tittes, S. B., J. F. Walker, L. Torres-Martínez, and N. C. Emery. 2019. Grow where you thrive, or where only you can survive? An analysis of performance curve evolution in a clade with diverse habitat affinities. The American Naturalist 193:530–544.

Towers, I. R., C. H. Bowler, M. M. Mayfield, and J. M. Dwyer. 2020. Requirements for the spatial storage effect are weakly evident for common species in natural annual plant assemblages. Ecology 101:e03185.

Treurnicht, M., J. Pagel, K. J. Esler, A. Schutte-Vlok, H. Nottebrock, T. Kraaij, A. G. Rebelo, and F. M. Schurr. 2016. Environmental drivers of demographic variation across the global geographical range of 26 plant species. Journal of Ecology 104:331–342.

Turcotte, M. M., and J. M. Levine. 2016. Phenotypic plasticity and species coexistence. Trends in Ecology & Evolution 31:803–813.

Turelli, M. 1978. Does environmental variability limit niche overlap? Proceedings of the National Academy of Sciences 75:5085–5089.

Uricchio, L. H., S. C. Daws, E. R. Spear, and E. A. Mordecai. 2019. Priority effects and nonhierarchical competition shape species composition in a complex grassland community. The American Naturalist 193:213–226.

Usinowicz, J., and J. M. Levine. 2018. Species persistence under climate change: A geographical scale coexistence problem. Ecology Letters 21:1589–1603.

Usinowicz, J., and J. M. Levine. 2021. Climate-driven range shifts reduce persistence of competitors in a perennial plant community. Global Change Biology 27:1890–1903.

Valladares, F., C. C. Bastias, O. Godoy, E. Granda, and A. Escudero. 2015. Species coexistence in a changing world. Frontiers in Plant Science 6:866.

Valladares, F., S. Matesanz, F. Guilhaumon, M. B. Araújo, L. Balaguer, M. Benito-Garzón, W. Cornwell, E. Gianoli, M. van Kleunen, D. E. Naya, A. B. Nicotra, H. Poorter, and M. A. Zavala. 2014. The effects of phenotypic plasticity and local adaptation on forecasts of species range shifts under climate change. Ecology Letters 17:1351–1364.

Van Dyke, M. N., J. M. Levine, and N. J. B. Kraft. 2022. Small rainfall changes drive substantial changes in plant coexistence. Nature 611:507–511.

Van Dyke, M. N., J. M. Levine, and N. J. B. Kraft. 2024. M. N. Van Dyke et al. reply. Nature 632:E21–E29.

Vehtari, A., J. Gabry, M. Magnusson, Y. Yao, P.-C. Bürkner, T. Paananen, and A. Gelman. 2024a. loo: Efficient leave-one-out cross-validation and WAIC for Bayesian models. R package version 2.8.0.9000.

Vehtari, A., A. Gelman, and J. Gabry. 2017. Practical Bayesian model evaluation using leave-one-out cross-validation and WAIC. Statistics and Computing 27:1413–1432.

Vehtari, A., A. Gelman, D. Simpson, B. Carpenter, and P.-C. Bürkner. 2021. Rank-normalization, folding, and localization: An improved $\widehat{R}$ for assessing convergence of MCMC (with discussion). Bayesian Analysis 16:667–718.

Vehtari, A., D. Simpson, A. Gelman, Y. Yao, and J. Gabry. 2024b. Pareto smoothed importance sampling. arXiv 13 March 2024.

Venables, W. N., and B. D. Ripley. 2002. Modern Applied Statistics with S. Fourth edition. Springer New York, New York, NY, USA.

Violle, C., M.-L. Navas, D. Vile, E. Kazakou, C. Fortunel, I. Hummel, and E. Garnier. 2007. Let the concept of trait be functional! Oikos 116:882–892.

Wainwright, C. E., J. HilleRisLambers, H. R. Lai, X. Loy, and M. M. Mayfield. 2019. Distinct responses of niche and fitness differences to water availability underlie variable coexistence outcomes in semi-arid annual plant communities. Journal of Ecology 107:293–306.

Walker, R. B. 1954. The ecology of serpentine soils II. Factors affecting plant growth on serpentine soils. Ecology 35:259–266.

Weiss-Lehman, C. P., C. M. Werner, C. H. Bowler, L. M. Hallett, M. M. Mayfield, O. Godoy, L. Aoyama, G. Barabás, C. Chu, E. Ladouceur, L. Larios, and L. G. Shoemaker. 2022. Disentangling key species interactions in diverse and heterogeneous communities: A Bayesian sparse modelling approach. Ecology Letters 25:1263–1276.

Wesner, J. S., and J. P. F. Pomeranz. 2021. Choosing priors in Bayesian ecological models by simulating from the prior predictive distribution. Ecosphere 12:e03739.

Westoby, M. 1998. A leaf-height-seed (LHS) plant ecology strategy scheme. Plant and Soil 199:213–227.

Whittaker, R. H. 1954. The ecology of serpentine soils. Ecology 35:258–288.

Whittaker, R. H. 1975. Communities and Ecosystems. Second edition. MacMillan Publishing Company, New York, NY, USA.

Wieczynski, D. J., B. Boyle, V. Buzzard, S. M. Duran, A. N. Henderson, C. M. Hulshof, A. J. Kerkhoff, M. C. McCarthy, S. T. Michaletz, N. G. Swenson, G. P. Asner, L. P. Bentley, B. J. Enquist, and V. M. Savage. 2019. Climate shapes and shifts functional biodiversity in forests worldwide. Proceedings of the National Academy of Sciences 116:587–592.

Wilson, P. J., K. Thompson, and J. G. Hodgson. 1999. Specific leaf area and leaf dry matter content as alternative predictors of plant strategies. New Phytologist 143:155–162.

Wisz, M. S., J. Pottier, W. D. Kissling, L. Pellissier, J. Lenoir, C. F. Damgaard, C. F. Dormann, M. C. Forchhammer, J.-A. Grytnes, A. Guisan, R. K. Heikkinen, T. T. Høye, I. Kühn, M. Luoto, L. Maiorano, M.-C. Nilsson, S. Normand, E. Öckinger, N. M. Schmidt, M. Termansen, A. Timmermann, D. A. Wardle, P. Aastrup, and J.-C. Svenning. 2013. The role of biotic interactions in shaping distributions and realised assemblages of species: Implications for species distribution modelling. Biological Reviews 88:15–30.

Wright, I. J., N. Dong, V. Maire, I. C. Prentice, M. Westoby, S. Díaz, R. V. Gallagher, B. F. Jacobs, R. Kooyman, E. A. Law, M. R. Leishman, Ü. Niinemets, P. B. Reich, L. Sack, R. Villar, H. Wang, and P. Wilf. 2017. Global climatic drivers of leaf size. Science 357:917–921.

Wright, I. J., P. B. Reich, J. H. C. Cornelissen, D. S. Falster, P. K. Groom, K. Hikosaka, W. Lee, C. H. Lusk, Ü. Niinemets, J. Oleksyn, N. Osada, H. Poorter, D. I. Warton, and M. Westoby. 2005. Modulation of leaf economic traits and trait relationships by climate. Global Ecology and Biogeography 14:411–421.

Wright, I. J., P. B. Reich, M. Westoby, D. D. Ackerly, Z. Baruch, F. Bongers, J. Cavender-Bares, T. Chapin, J. H. C. Cornelissen, M. Diemer, J. Flexas, E. Garnier, P. K. Groom, J. Gulias, K. Hikosaka, B. B. Lamont, T. Lee, W. Lee, C. Lusk, J. J. Midgley, M.-L. Navas, Ü. Niinemets, J. Oleksyn, N. Osada, H. Poorter, P. Poot, L. Prior, V. I. Pyankov, C. Roumet, S. C. Thomas, M. G. Tjoelker, E. J. Veneklaas, and R. Villar. 2004. The worldwide leaf economics spectrum. Nature 428:821–827.

Yoon, J.-H., S.-Y. S. Wang, R. R. Gillies, B. Kravitz, L. Hipps, and P. J. Rasch. 2015. Increasing water cycle extremes in California and in relation to ENSO cycle under global warming. Nature Communications 6:8657.

Zepeda, V., and C. Martorell. 2019. Fluctuation-independent niche differentiation and relative non-linearity drive coexistence in a species-rich grassland. Ecology 100:e02726.